Supramolecular chemistry of a series of organic zwitterions

By

Jean Lombard

Thesis presented in partial fulfilment of the requirements for the degree of Master of Science in the Faculty of Science

at

Stellenbosch University

Supervisor: Dr Tanya le Roex

Co-supervisor: Prof. Delia Haynes

Faculty of Science

Department of Chemistry & Polymer Science

December 2017

Declaration

By submitting this thesis electronically, I declare that the entirety of the work contained therein is my own, original work, that I am the sole author thereof (save to the extent explicitly otherwise stated), that reproduction and publication thereof by Stellenbosch University will not infringe any third party rights and that I have not previously in its entirety or in part submitted it for obtaining any qualification.

December 2017

ABSTRACT

The aim of the work presented in this thesis was to investigate the various solid-state forms that can be adopted by a series of organic zwitterionic molecules, formed from reaction of acetylenedicarboxylic acid with pyridine derivatives. By carrying out a thorough and systematic study we were able to determine the usefulness of these molecules as supramolecular building blocks.

The following zwitterions have been investigated:

- (Z)-3-carboxy-2-(4-cyanopyridin-1-ium-1-yl)-acrylate
- (Z)-1-(3-carboxy-1,1-dihydroxyprop-2-en-1-ide-2-yl)-pyridin-1-ium
- (Z)-2-(3-carbamoylpyridin-1-ium-1-yl)-3-carboxyacrylate
- (Z)-3-carboxy-2-(4-carboxypyridin-1-ium-1-yl)acrylate

The first two zwitterions are formed from the reaction of acetylenedicarboxylic acid with 4-cyanopyridine and pyridine, respectively. Two conformational polymorphs of the first were identified: a kinetic and thermodynamic form. Three polymorphs of the second zwitterion were identified, their formation depending purely on the solvent choice. In each case the relationship between the polymorphs has been extensively studied – no interconversion between polymorphs is observed, which is unusual and rarely reported.

The reaction between acetylenedicarboxylic acid and nicotinamide or isonicotinamide produces two new zwitterionic molecules (the third and fourth zwitterions in the list above), as well as a salt by-product. These zwitterions, as well as the 4-cyanopyridine zwitterion, were subsequently combined with various small organic co-formers in an attempt to form multi-component crystals. The structures of three new hydrated zwitterion-melamine salts have been identified, as well as the existence of six other salts which were identified based on NMR and IR data – all of which dissolve more easily compared to the zwitterions themselves. Considering the number of co-formers used, the discovery of so few salts is unusual – a search of the Cambridge Structural Database indicates that this may be due to a high propensity of charge-assisted hydrogen bonds that hold the zwitterions together to form homomeric molecular crystals.

In addition, the structure-property relationships of a series of isostructural solvates have been investigated in order to gain further insight into the solid-state behaviour of organic molecules. The host framework, consisting of 1,10-phenanthrolinium and pamoate ions, is shown to selectivity include DMA and DMSO above DMF. This selectivity has additionally been demonstrated mechanochemically, which has not been reported before.

Overall, the compounds investigated all show very interesting behaviour. Insight gained with respect to crystal packing, hydrogen- and charge-assisted hydrogen bonding, molecular shape, the inclusion of solvent into structures, the effect of temperature and solubility on crystallisation, and the usefulness of mechanochemistry, are discussed.

OPSOMMING

Die doel van die werk uiteengesit in hierdie tesis was om die verskeie vastestof vorms, wat 'n reeks organiese zwitterioniese molekules kan aanneem, te ondersoek. Hierdie zwitterione word gevorm deur die reaksie van asetileendikarboksielsuur (ADC) met verskeie piridien-afgeleides. Dit was moontlik om die bruikbaarheid van hierdie molekules as supramolekulêre "boustene" te bepaal deur 'n deeglike en sistematiese studie uit te voer.

Die volgende zwitterione is ondersoek:

- (Z)-3-karboksie-2-(4-sianopiridien-1-ium-1-iel)-akrilaat
- (Z)-1-(3-karboksie-1,1-dihidroksieprop-2-en-1-ied-2-yl)-piridien-1-ium
- (Z)-2-(3-karbamoielpiridien-1-ium-1-yl)-3-karboksiakrilaat
- (Z)-3-karboksie-2-(4-karboksiepiridien-1-ium-1-yl)akrilaat

Die eerste twee zwitterione word gevorm deur die reaksie van ADC met onderskeidelik 4-sianopiridien, en piridien. Twee konformasionele polimorfs van die eersgenoemde zwitterioon is geïdentifiseer: 'n kinetiese en termodinamiese vorm. Drie polimorfs van die tweede zwitterioon is geïdentifiseer, met die vorming van elk slegs afhanklik van die keuse van oplosmiddel. In elke geval is die verhouding tussen die verskillende vorms breedvoerig bestudeer – geen omskakeling tussen polimorfs is waargeneem nie, wat buitengewoon is.

Die reaksie tussen ADC en nikotienamied of isonikotienamied produseer twee nuwe zwitterioniese molekules (die derde en vierde zwitterione in die lys hierbo), sowel as 'n sout neweproduk. Hierdie molekules, sowel as die 4-sianopiridien zwitterioon, is daarna gekombineer met verskeie klein organiese molekules (ko-vormers) in ’n poging om multi-komponent kristalle te vorm. Drie nuwe gehidreerde zwitterioon-melamien soute is geïdentifiseer, sowel as 'n verdere ses potensiële soute – waarvan almal makliker oplos as die zwitterione self. In vergelyking met die groot aantal ko-vormers wat gebruik is, is die ontdekking van so min soute merkwaardig – 'n ondersoek van die 'Cambridge Structural Database' dui aan dat dit moontlik te doen het met die hoë geneigdheid van die lading-versterkte waterstofbindings wat die zwitterione verbind om molekulêre kristalle te vorm.

Bykomend tot hierdie is die struktuur-eienskap verhouding van 'n reeks isostrukturele solvate ook ondersoek om verdere insig te kry oor die gedrag van organiese molekules in

die vaste stof vorm. Die gasheer raamwerk, wat bestaan uit 1,10-phenanthrolinium en pamoaat ione, neem DMA en DMSO selektief bo DMF op. Hierdie selektiwiteit word boonop getoon selfs wanneer die eksperimente meganies uitgevoer word – iets wat nog nooit voorheen gerapporteer is nie.

Oor die algemeen toon die bestudeerde molekules baie interessante gedrag. Insig is verkry (en bespreek) oor die rangskikking van organiese molekules in kristalle, waterstofbindings en lading-versterkte waterstofbindings, molekulêre vorm, die insluiting van oplosmiddels binne strukture, die effek van temperatuur en oplosbaarheid op kristallisasie, en die bruikbaarheid van meganiese chemie.

ACKNOWLEDGEMENTS

Firstly I would like to thank my supervisors, Dr Tanya le Roex and Prof. Delia Haynes. Thank you both for always having kind words and being excited and optimistic about my work – it was contagious and I was always the most productive after talking to you. Thank you for asking the difficult questions and making me think about things that I did not want to at the time – I probably didn't answer many of them, but as they say, it's the thought that counts (hopefully). Most of all, thank you for teaching me to call weird results 'interesting' instead of 'wrong', and for believing in me when I did not.

I would also like to thank all the other students in the supramolecular research group. To Bella, Kerry and Natasha who started this journey with me – we made it guys! A special thanks to Monica, for our organic crystallisation brainstorming sessions in a group full of MOF students, and Dewald, who was always there for some comic relief and kind words when needed. Thanks also to Thalia Carstens and Bernard Dippenaar, for carrying out calculations to help us make sense of things.

And, of course, I would also like to thank my family for listening to me rant without understanding a word of what I'm saying – I have to remember to reimburse you one day for all the airtime.

Most of all I want to thank my heavenly Father for getting me to the end of the road and for placing these angels on my path.

Lastly, I would like to thank Stellenbosch University and the Wilhelm Frank Trust for financial support.

CONFERENCES

ICCOSSXXIII – *23rd International Conference on the Chemistry of the Organic Solid State*

Stellenbosch University, Stellenbosch, 2 – 7 April 2017

Poster presentation – *Solid-state supramolecular chemistry of a series of organic zwitterions*

IUCr 2017 – *24th Congress & General Assembly of the International Union of Crystallography*

Hyderabad, India, 21 – 28 August 2017

Poster presentation – *Solid-state supramolecular chemistry of a series of organic zwitterions*

IMPORTANT NOTE

Chapter 3 is presented as a draft of a paper that has been published in *Crystal Growth and Design* (DOI 10.1021/acs.cgd.7b01271). The version that was submitted is included as Appendix C. All the experimental work in this chapter was carried out by myself, unless otherwise stated. The draft included here was written by me.

Chapter 4 is presented as a draft of a paper that is about to be submitted to *CrystEngComm* All the experimental work in this chapter was carried out by myself. The draft included here was written by me.

LIST OF ABBREVIATIONS

A	-	Hydrogen bond acceptor atom
ADC	-	Acetylenedicarboxylic acid
ASU	-	Asymmetric unit
CAHB	-	Charge-Assisted Hydrogen Bond
CCDC	-	Cambridge Crystallographic Data Centre
$CHCl_3$	-	Chloroform
CIF	-	Crystallographic Information File
CSD	-	Cambridge Structural Database
DCM	-	Dichloromethane
DMA	-	Dimethylacetamide
DMF	-	Dimethylformamide
DMSO	-	Dimethyl sulfoxide
DSC	-	Differential Scanning Calorimetry
EtOAc	-	Ethyl acetate
Et_2O	-	Diethyl ether
EtOH	-	Ethanol
FTIR	-	Fourier Transfer Infrared spectroscopy
GRAS	-	Generally Recognised As Safe
HOF	-	Hydrogen-bonded Organic Framework
LAG	-	Liquid-Assisted Grinding
MeCN	-	Acetonitrile
MeOH	-	Methanol

NMR	-	Nuclear Magnetic Resonance
PXRD	-	Powder X-ray diffraction
SCD	-	Single-crystal X-ray diffraction
SOF	-	Supramolecular Organic Framework
TGA	-	Thermogravimetric Analysis
THF	-	Tetrahydrofuran
X−H	-	Hydrogen bond donor atom
1D	-	One-dimensional
2D	-	Two-dimensional
3D	-	Three-dimensional

ATOM COLOURS

Carbon

Oxygen

Nitrogen

Hydrogen

TABLE OF CONTENTS

Chapter 2 – Experimental and Analytical Techniques

Chapter 3 – Polymorphic behaviour of two organic zwitterions: a rare case of no observable conversion between polymorphs

CHAPTER 1

GENERAL INTRODUCTION

As we start our journey into the microscopic world of crystals and the molecules beneath the surface, some terms and concepts need to be introduced. The field of supramolecular chemistry will be introduced, and how this leads up to the relatively new research area of crystal engineering. The crystal engineering process will be further elaborated on by looking at synthons and intermolecular interactions and how their study leads to a better understanding, and therefore possible control, of crystal structures. This groundwork will be followed by a more in-depth discussion on polymorphism and multi-component crystals – phenomena which allow us to gain even more insight into the complexity of crystal structures and their structure-property relationships. Specifically, the molecules investigated in this study are based on a series of organic zwitterions; their history will be reported as this led to the research described in this thesis. Finally, the aims and objectives of the project will be stated, along with a brief overview of the chapters to follow.

1.1 From supramolecular chemistry to crystal engineering

"Supermolecules are to molecules and the intermolecular bond what molecules are to atoms and the covalent bond." [1]

J.-M. Lehn (1988)

Like children play with Lego® blocks, supramolecular chemists play with molecules. Instead of blocks interlocking, molecules are held together by intermolecular interactions to form supramolecular materials. These interactions, or non-covalent bonds, are reversible and include things like electrostatic interactions, π-π interactions, dispersion interactions, and hydrogen- and halogen bonding.[2] Broadly speaking, molecules can either combine to form host-guest systems where larger molecules (hosts) envelop smaller guests (usually small molecules like solvents or ions), or equally sized molecules can self-assemble.[2] Although supramolecular materials can form in solution, we are particularly interested in

cases where their formation leads to solid materials, i.e. in solid-state supramolecular chemistry.

When the solid materials formed by supramolecular interactions are crystalline (i.e. when the molecules have three-dimensional long-range periodic ordering),[3] it enables us to use a range of powerful X-ray diffraction-based techniques to analyse these materials and investigate their exact molecular structure and periodic arrangement in 3D space (i.e. their crystal structure). It is no wonder J. D. Dunitz called a crystal a "*supramolecule par excellence*".[4] By systematically examining the crystal structures of known supramolecular materials, we can try and deduce recurring patterns and 'rules' in an attempt to rationalise how molecules combine and how this relates to their properties, so that we can utilise this knowledge and understanding gained to design novel materials with potentially useful properties.[2] This sub-discipline within supramolecular chemistry is called 'crystal engineering'. Crystal engineering should not be confused with crystal structure prediction, which is purely theoretical and a field of study on its own.[5] Rather, crystal engineering is the design and creation of crystals, based on acquired knowledge, with desired properties for a particular purpose.

1.2 Synthons

To classify the motifs that we see in crystal structures, we use the concept of supramolecular synthons.[6] Synthons are recurring intermolecular interactions between specific functional groups (Figure 1.1).[7] For example, when we look at crystal structures we often see that two carboxylic acid groups dimerise *via* hydrogen bonding. Therefore, when we make a new material and our molecules have carboxylic acid groups, it would be reasonable to expect them to dimerise in the same way – and so begins the first step in crystal engineering.[2,8] However, it must be said that though this might seem a simple feat, chemistry is not usually as predictable as we would like,[6] at least not until we have a better comprehension of the complex and even delicate interplay between the relative strengths, directionalities, and distance dependencies of the various intermolecular interactions at work in the crystal structure.[6]

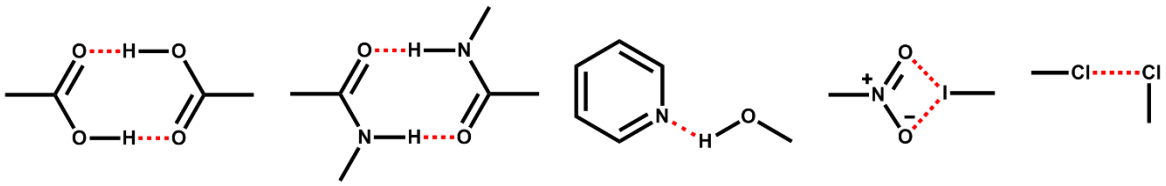

Figure 1.1 Selected examples of supramolecular synthons.[9]

1.3 Intermolecular interactions

For crystals to form the molecules need to have a net attractive force that holds them together[10] – these need not be particularly strong, as many weak interactions can have a large effect.[11] There are various ways in which molecules can interact with each other, but as our work centres on purely organic molecules, containing only carbon, hydrogen, oxygen, and nitrogen atoms, we will focus on hydrogen bonding, charge-assisted hydrogen bonding, and π-π interactions.

Hydrogen bonds are relatively strong and long-range, so they can direct the structure of materials as they form, but are not so rigid that the components of the crystal cannot be slightly altered without the entire structure changing.[10] Hydrogen bonds also have the added benefit of directionality (i.e. they tend to be linear),[12] which makes them easier to predict and potentially control and use in a design strategy.[11]

In 2011 the IUPAC recommended a definition for the term hydrogen bonding, together with a list of criteria and characteristics: "*The hydrogen bond is an attractive interaction between a hydrogen atom from a molecule or a molecular fragment X–H in which X is more electronegative than H, and an atom or a group of atoms in the same or a different molecule, in which there is evidence of bond formation*".[13] A hydrogen bond therefore consists of a hydrogen bond donor (X−H), and acceptor atom (A) and is most often described by the distance between H and A (*d*) and the angle XĤA (θ) (Figure 1.2).[14]

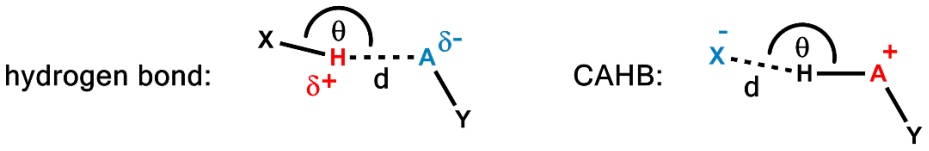

Figure 1.2 Basic components of a hydrogen bond and a charge-assisted hydrogen bond (CAHB).

Hydrogen bonds are mainly electrostatic in nature as the hydrogen atom is partially positive and the acceptor partially negative (Figure 1.2). This interaction can be strong, e.g. X and A can be N, O, F, Cl, Br, I[15] or weak, like C−H···O or O−H···π interactions (or even C−H···π)[14] (Table 1.1). The most important determining factor is perhaps the dipole moment in the X-H fragment – the stronger the dipole, the more positively charged the proton, and the stronger the interaction.[10]

Table 1.1 Additional information regarding the nature of the types of hydrogen bonds. Data in this table has been adapted from references 11 and 14.

	Very strong	**Strong**	**Weak**
Examples	$[F{-}H{-}F]^-$	O−H···O−H	C−H···O
	$[N{-}H{-}N]^+$	O−H···N−H	O−H···π
		N−H···O=C	
		N−H···O−H	
		N−H···N−H	
H···A (*d*, Å)	1.2 − 1.5	1.5 − 2.5	2.0 − 3.0
X−H···A (θ, °)	175 − 180	130 − 180	90 − 180
Bond energy (kcal mol^{-1})	15 − 40	4 − 15	<4

The extreme of this (see the electrostatic limit in Figure 1.3) is when there is a proton shift to the acceptor atom, forming a salt, and resulting in a charge-assisted hydrogen bond (CAHB).[16] CAHBs are hydrogen bonds, but instead of only partial charges (H is δ+ and the acceptor atom is δ-), the donor and acceptor atoms are now charged positive and negative (Figure 1.2), reinforcing the electrostatic nature of the bond.[10,14] This further polarises and therefore strengthens the interaction to produce a more robust network.[10]

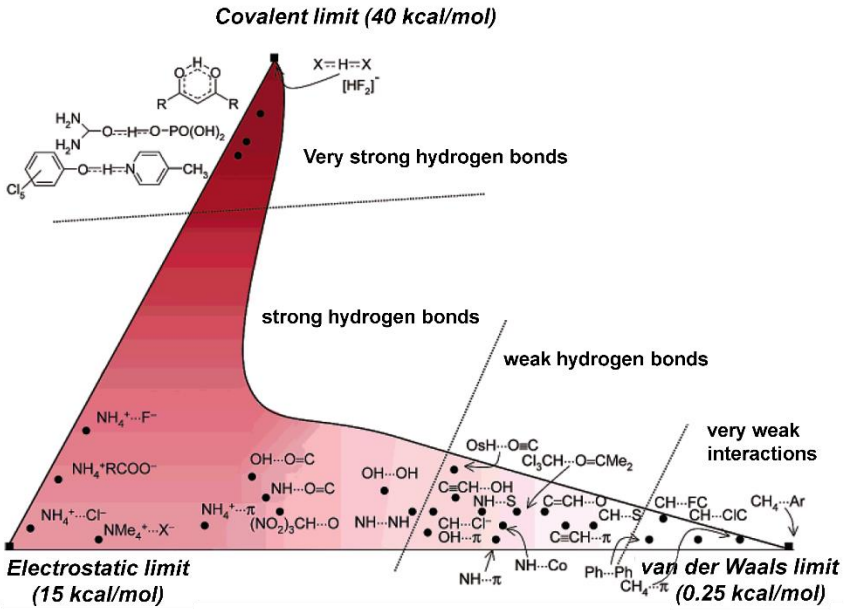

Figure 1.3 Graphical representation of the relative strengths of the different types of hydrogen bonds. The darker red colouring represents stronger interactions, the strongest of which are covalent in nature. At the electrostatic limit there are CAHBs, with the normal, weaker hydrogen bonds being less electrostatic, and tending more towards van der Waals interactions. Figure reproduced from reference 17.

Another type of interaction that plays an important role in the packing of organic molecules, is the π-π interactions that can occur between cyclised aromatic hydrocarbons. These interactions are not as strong or directional as hydrogen bonds, but are still very common, and will affect molecular packing in the absence of conflicting stronger interactions.[2] The formation of π-π interactions stems from the polarizability of the delocalised π electrons – these can form relatively strong dispersion interactions between aromatic rings.[18] Furthermore, π-π interactions are somewhat directional due to the C-H bonds being polarised to a small extent. This produces an area of slightly negative charge in the centre of the aromatic ring, while the rim, or σ-framework, is slightly positive.[18] Based on the likelihood of positive and negative areas attracting each other, we observe two main types of π-π interactions, namely offset face-to-face, and edge-to-face (Figure 1.4).[18] It is possible for the aromatic rings to stack in an eclipsed manner directly on top of each other, but this arrangement is unfavourable and uncommon (Figure 1.4).[18] The face-to-face interactions often propagate throughout the structure, and so this type of interaction is sometimes also called π-π stacking. Due to the geometric predictability of these types of interactions, they are often considered when designing new materials.

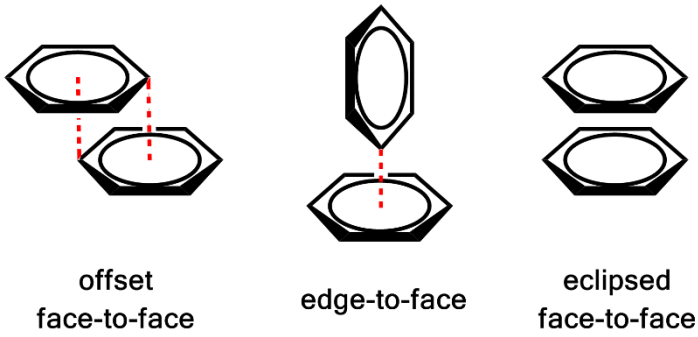

Figure 1.4 The different types of π-π interactions, namely offset face-to-face, edge-to-face, and eclipsed face-to-face (unfavourable), depicted with benzene molecules.

1.4 Close packing

Of course, it is not only chemical interactions that govern crystal packing, but simple geometry as well. Most notably, the affinity of molecules to close pack. In 1955 Kitaigorodskii postulated the close-packing principle: organic molecules will arrange in such a way as to fill the space available as efficiently as possible.[19]

1.5 Polymorphism

"*...every compound has different polymorphic forms and that, in general, the number of forms known for a given compound is proportional to the time and energy spent in research on that compound.*" [20]

W. McCrone (1965)

Often a molecule, or a combination of molecules in the case of multi-component crystals,[21] can arrange itself in more than one way in the solid state.[22] Such molecules are polymorphic, and the different arrangements are called polymorphs.[23,24] As with most concepts in this broad field of research, there has been a lot of debate about this definition. A simple and straightforward definition was proposed by Haleblian and McCrone, one which we shall also use: polymorphs have different solid-state crystal structures, while being identical in solution and in the vapour state.[25] When determining which polymorph is present, it is important to use more than one method of analysis, as polymorphs are often indistinguishable when using certain instrumentation.[22] For example, two polymorphs may have very similar powder X-ray diffraction patterns if the molecules pack in a very similar manner, while their unit cell parameters or space group differ. In addition, crystals of

polymorphs often grow concomitantly, that is, they grow at the same time, under the same conditions.[26] Polymorphs can also differ significantly with regards to their chemical and physical properties, such as crystal colour and shape, density, melting point, solubility, stability, reactivity, hardness, etc.[27] The relationship between polymorphism and isomerism, tautomerism, conformers, and other common confusions will be discussed below.

1.5.1 Types of polymorphism

Tautomeric polymorphism occurs when the difference between the two forms of a compound is simply the shift of a hydrogen atom.[28] This is surprisingly rare compared to the abundance of tautomers in solution. The structures of 2-amino-3-hydroxy-6-phenylazopyridine are a common example demonstrating such an intramolecular hydrogen shift.[29] Similarly, a shift in protonation can also form zwitterions which could in essence be polymorphic to the packing of the neutral species.[30] A hydrogen shift between the donor- and acceptor atoms of a hydrogen bond would change the charge of the molecules, but again, this charged species might pack very similarly to the neutral form.[22]

Conformational polymorphism occurs when two conformers of the same molecule pack in a different way.[31] In general, packing even slightly differently will undoubtedly affect the conformation of the molecules, but in practice, only molecules with vastly different conformations are usually called conformational polymorphs.[31] All the intramolecular bond lengths and angles will almost never be exactly the same for two polymorphs,[22] but they are usually very similar, as considerable energy is needed to change them.[32] Even rigid aromatic systems rotate and bend slightly due to steric hindrance occurring when the packing changes.[33] On the other hand, changing torsion angles uses much less energy and so conformational polymorphism is possible.[32]

In pharmaceutical research, solvates (when a solvent is included in a structure) are sometimes called pseudopolymorphs or pseudopolymorphic solvates.[22] This means that the same crystals containing solvent, and those without any solvent, are pseudopolymorphic. However, in our opinion this does not fall under polymorphism, as the addition of an extra solvent molecule will undoubtedly change the packing, not to mention that they are not the same in solution or in the vapour state, which was included in our definition of polymorphism. Other types of polymorphism include liquid crystal polymorphism,[34] protein

polymorphism,[35] inorganic polymorphism as well as polymorphism in polymers (synthetic and biological) and thin films.[36]

1.5.2 Polymorph stability

It is often of interest to know how polymorphs relate to one another, how they are different, and how they can interconvert. While most polymorphs have similar lattice energies (they differ by less than 4 kJ mol^{-1}),[23] there is usually one that is more stable under a certain set of conditions. In monotropic polymorphism one form is more stable than the others at all temperatures, meaning the less stable (metastable) form will always tend to convert to this form.[22] Polymorphs could also have an enantiotropic relationship, which means that each polymorph is stable over a specific temperature range. Depending on the temperature, either polymorph could then convert to the other.[22] This is explained in more detail in Chapter 3.

1.5.3 Isolation of different polymorphs

Many techniques can be used to control which polymorph forms during crystallisation. Seeding is an old and well-known technique that is often used to control which polymorph crystallises from solution. A seed is a crystal of the desired form that can be added to a supersaturated solution to promote formation of that particular polymorph – even if it is the metastable form.[37] Seeding can also be used to promote the growth of a single enantiomer from a racemic mixture.[38] However, seeding is not always straightforward. This problem was first described in 1995 in the seminal paper by Dunitz and Bernstein, entitled "Disappearing Polymorphs", and revisited 20 years later in a review by Bučar *et al*. In these papers,[39,40] they show (with a multitude of examples) that researchers sometimes lose the ability to make a certain once-abundant polymorph. The leading theory is that this is caused by the air being seeded with one polymorph, which then inhibits or impedes the formation of the other. This frustration is just one more reminder that there is more going on than meets the eye.

Another way to direct the growth of polymorphs is by adding soluble additives to the solution. An additive is a molecule that can promote or inhibit/significantly slow down the growth or nucleation of a particular polymorph without being included into the crystals that form.[37] For rationalisation, and subsequent design modification, it is important to understand how the additive interacts with the polymorph(s). Molecular modelling can be

used to design new additives to ensure that (at least) the fastest growing face of one polymorph is inhibited without hindering fast growth of the other.[41] Sometimes the addition of additives is unintentional - in the form of impurities. However, this can still be very useful if the results are favourable and the impurities can be identified.[42,43] Although the use of additives is usually restricted to solution crystallisation, Kamali *et al.* reported the use of such additives to control polymorphism in the gas phase, i.e. during sublimation.[44]

Another extreme version of additive control is of course when the solvent itself determines which polymorph forms due to interactions it has with one or more of the polymorphs.[45] Even more similar to the use of additives is the use of liquid-assisted grinding to produce different polymorphs. A few drops of solvent is added to the mechanochemical synthesis to speed up the transformation and can also determine the polymorph that forms.[46] In addition, the concentration of solute in the crystallisation solvent can also have an effect on which polymorph forms.[47]

Templating is another way of controlling polymorphism and is based on the fact that heterogeneous crystal nucleation starts on a surface and so can possibly be controlled by altering this surface (homogeneous nucleation does not occur at a surface, but is less common). It works on the same principle as seeding, except that now it is a different molecule that is used to promote formation of the particular polymorph.[37] Other materials such as polymers,[48] Langmuir-Blodgett (LB) films[49] and self-assembled monolayers (SAM templating)[50] can also be used to stimulate formation of a specific form.

Other less common techniques used to control which polymorph forms include controlling the level of supersaturation by using microporous membranes[51] and potentiometric cycling (based on pH control).[52] Confinement techniques are also sometimes used – this includes crystallising metastable forms in a capillary[53] or in nanoscopic confinement to separate polymorphs by nucleus size,[54] or performing a contact line crystallisation.[55,56] External effects are also utilised in the form of sonocrystallisation[57] and non-photochemical laser induced nucleation (NPLIN).[58]

1.5.4 Polymorph prediction

It would undoubtedly be very useful if it were possible to predict which molecules can form polymorphs, and what those forms were. A lot of research is being carried out with this goal in mind, but unfortunately, the problem has not quite been solved. It is possible to predict (using the appropriate software) what the lowest energy forms of a molecule might be, and what the structures could look like, but these are numerous, and where experimental work has also been carried out, more forms are often predicted than are observed experimentally.[59,60] It is often assumed that the lowest energy forms are the ones that are observed, but this is not always the case.[61]

Various reasons for this lack of success have been postulated, including the fact that a number of approximations need to be made during calculation. Crystal growth and the effect of the solvent thereon[62] is also quite complex. During nucleation and crystal growth, molecules reorder – it is a process not just a result. Final crystal structures are also not as rigid and perfect as a calculation would suggest; there are flaws, faults, and disorder, and products are not necessarily crystalline. The observation of metastable polymorphs also proves that it is not always the most stable forms that crystallise. In fact, our experimental data is undoubtedly not complete, as not all possible experiments have been performed, not to mention experiments that cannot be performed due to technical limitations.[59]

1.5.5 Polymorphism in the pharmaceutical industry

Polymorphs are of special interest when doing research in the pharmaceutical industry, as drug molecules are often polymorphic. This is important because different arrangements of atoms in the solid state lead to different lattice energies. In turn, this leads to polymorphs having different physicochemical properties such as solubility[63] and to a lesser extent also stability, dissolution rate, and bioavailability.[22] It is therefore very important that the desired polymorph can be made reproducibly (without converting to the other over time) so that the correct drug can be put on the market.[22] One well-known example of the effect of polymorphism on drug "effectiveness" is that of Chloramphenicol palmitate, where only one of the three known polymorphs is metastable with suitable bioavailability, resulting from its solubility.[64] Some physical properties of other products are also polymorph-dependant, such as explosives,[65] dyes,[66] fats/wax products,[67] soaps,[68] petroleum products,[69] and many types of food, including chocolate.[70]

1.6 Multi-component crystals

The term 'multi-component crystal' is a broad term, representing any crystal containing more than one type of chemical entity, and includes co-crystals, salts, and solvates. These usually consist of a molecule of specific interest, and one or more co-formers (other molecules). The formation of multi-component crystals can be beneficial, as it is possible to alter the properties and structure of a material without altering its chemical properties (much like polymorphism). An example of where this is often used is in the pharmaceutical industry. Important pharmaceutical compounds can be combined with other harmless molecules (co-formers) to alter their physical properties. This includes their solubility,[71] stability,[72] dissolution rate,[73] bioavailability,[74] melting point,[75] and compressibility.[76] These co-formers are chosen from lists of compounds that are safe for human consumption, e.g. GRAS (generally recognised as safe)[77] or EAFUS (Everything Added to Food in the United States)[78] lists. Drug-drug salts and co-crystals can also be formed when the co-former is another drug molecule.[79] Apart from this, multi-component crystals also have application possibilities in the fields of optoelectronics[80] and can be used in an attempt to form porous framework-type materials.[16] These framework-type materials can be used for gas or other small molecule- separation and storage, as well as catalysis. Such frameworks have been reported to capture gases like carbon dioxide,[81] selectively separate gases like ethane/ethene,[82] and selectively absorb solvents like hexane.[83]

1.6.1 Co-crystals

"Two crystals living together – I'd call this a co-crystal for sure." [84]

G. Desiraju (2003)

There is disagreement as to what exactly comprises a co-crystal[84–87] (often also called a molecular complex or molecular adduct), and whether salts and solvates are considered co-crystals – or whether this term is needed at all. The consensus of the majority seems to be along these lines: a co-crystal is formed when two or more neutral molecules are combined in a definite stoichiometric relationship to form a structurally homogenous material, where at least two of the molecules did not play the role of the crystallisation solvent.[88]

Co-crystals are held together by noncovalent intermolecular interactions. Most often, these are hydrogen bonds as they tend to be stronger than other interactions between purely

organic molecules.[89] Molecules with many hydrogen bonding donor and acceptor atoms will therefore make good co-crystallisation agents.[90] Other intermolecular interactions, such as π-π interactions, can also be present, but are weaker and so will have less of an effect.[91] For co-crystals to form successfully, these heterogeneous intermolecular interactions between different molecules need to be stronger than those between the molecules themselves.[92] This will promote the formation of a heteromeric co-crystal instead of merely separate molecular solids (i.e. simple recrystallisation taking place). Studying the possible hydrogen bonds or synthons that can form between molecules,[93] as well as their relative strengths (whether by calculation[94] or experimental studies[95]), is thus important when you want to predict the outcome of multi-component crystallisations.[96] For example, the amide···carboxylic acid interaction is more favourable than the amide···amide hydrogen-bonding interaction.[97] This is similar to determining the order of reactivity in organic synthesis, but it is not nearly as well studied or understood. So much so that most researchers still prefer performing extensive screening tests, above trying to predict which molecules will co-crystallise. In fact, much more intensive and time-consuming first-principle calculations would need to be performed to be anywhere near predicting co-crystal formation.[98]

As a side note, co-crystals can also be hydrated or solvated, possibly forming hydrogen-bonded organic frameworks (HOFs),[99] or supramolecular organic frameworks (SOFs).[100]

1.6.2 Salts

When the components of a co-crystal are acids and bases there is often proton transfer that occurs so that the product is in fact a salt.[101] The acid and base components are then connected by stronger charge-assisted hydrogen bonds, instead of by hydrogen bonds. The possibility of this proton transfer occurring is thus dependent on the strength of the acid and base. The potential for salt formation can be determined by using the quantified pKa rule.[102] This rule states that when the difference in pKa between the acid and base (ΔpKa) is more than 4, proton transfer usually occurs to form a salt. Conversely, if the pKa(protonated base) – pKa(acid) is less than –1, co-crystal formation is more likely. In the intermediary region of ΔpKa between –1 and 4, it is not as clear cut. Previously it was assumed that no prediction can be made for these systems,[103] but Cruz-Cabeza has derived a linear relationship between the probability of salt formation and ΔpKa values within this range.[102] This rule has certain

limitations,[104] such as not always being satisfied when there is not a 1:1 ratio of acid:base,[105] but serves as a sufficient guideline for predicting ionisation.

Other than this difference in charge, all that was said about co-crystals also applies here. As with co-crystals, to form a salt, the priority of intermolecular interactions need to be taken into account so that the heteromeric salt is formed instead of recrystallisation occurring. Salt formation is very common, and about half of all pharmaceuticals are sold in the form of salts.[103] Salts can also be hydrated or solvated to possibly form ionic organic frameworks.[16]

1.7 A series of organic zwitterions

In recent years, our group has investigated a series of organic zwitterions formed from the addition of a variety of pyridine derivatives to acetylenedicarboxylic acid. Investigations carried out on some of these zwitterions have revealed some interesting and potentially useful properties. Our aim in this work was thus to expand this study and investigate the remaining zwitterions in the series, as well as two further zwitterions.

The first paper on these zwitterions was published in July of 2014 by Loots *et al.*[106] (Figure 1.4). Here the formation of seven novel pyridinium zwitterionic compounds was described – although many more syntheses were attempted. The crystals of some of these were shown to contain solvent/water molecules, and two salts were also obtained where the covalent bond between the acid and base is not formed.

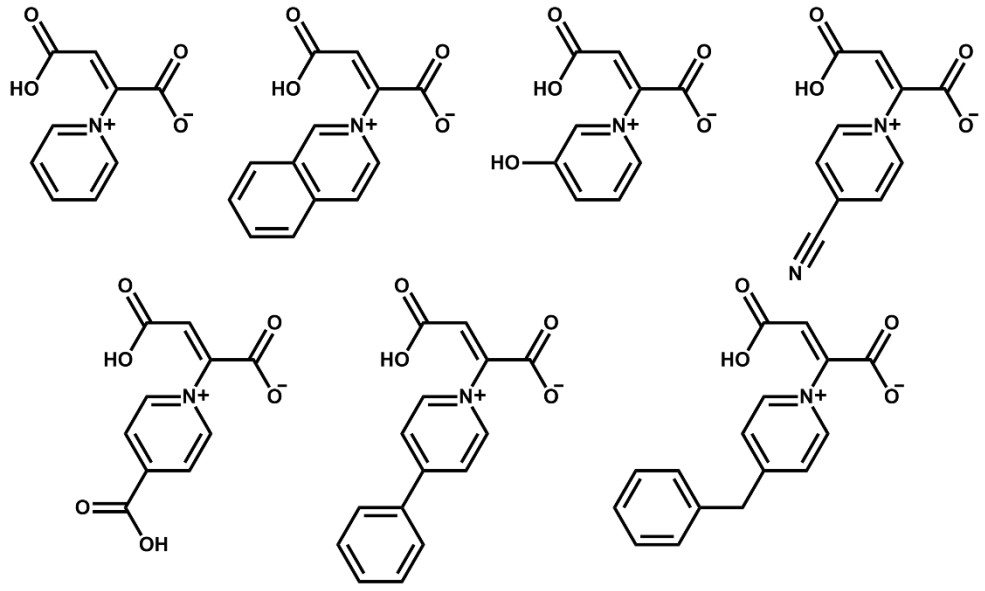

Figure 1.4 The first series of zwitterions that was reported by Loots *et al.*[106]

Two subsequent studies were carried out to further investigate two of the reported zwitterions. The first was published in 2015 and reports on the benzylpyridine-functionalised zwitterion.[107] This more in-depth study proved very interesting, as the zwitterion was discovered to be polymorphic, as well as porous. Four polymorphs and three solvates were obtained, and their solvent-mediated interconversions were demonstrated. One of the polymorphs was also shown to be porous to 1,4-dioxane. The second study has not been published yet, but reports on the 4-phenylpyridine zwitterion.[108] This zwitterion exists as two polymorphic apohosts, and three solvated forms. Interconversions between all forms were studied. In both these studies a salt of the starting materials was also obtained and determined to be the kinetic product of the reaction, with the zwitterion being the thermodynamic product.

1.8 Aims and objectives

The aim of this project was to investigate the various solid-state forms that can be adopted by a series of organic zwitterionic molecules. By doing a thorough and systematic study we hoped to be able to better gauge the usefulness of these molecules as supramolecular building blocks. The solid-state structures of all new materials obtained were investigated by both single-crystal- and powder X-ray diffraction, so that we could understand how these molecules interact and pack together in the solid state. Their properties were also studied in detail using a variety of other analytical techniques.

Previous work has shown that the unusual shape and hydrogen-bonding capability of such zwitterions can be the origin of interesting phenomena such as polymorphism and porosity. A series of these zwitterions has been discovered, but only two have been studied in great depth. Therefore, our first objective was to determine exactly how the others in the series can be formed, and whether they can also exist as different polymorphs or solvates. We then continued to study the relationships between all forms obtained and investigated the possibility of interconversion, porosity, and selectivity (where applicable).

The second part of this study was based on two new zwitterions that had recently been discovered in the group. These zwitterions are derived from nicotinamide and isonicotinamide. Once again, our aim was to determine exactly how they can be formed, and whether they can also exist as different polymorphs or solvates. They differ from all of the previously reported zwitterions as they have an additional amide functionality on the

pyridyl moiety. Our aim was to use this functionality to inhibit close packing in the zwitterions and so increase the possibility of the structures being porous (Figure 1.6).

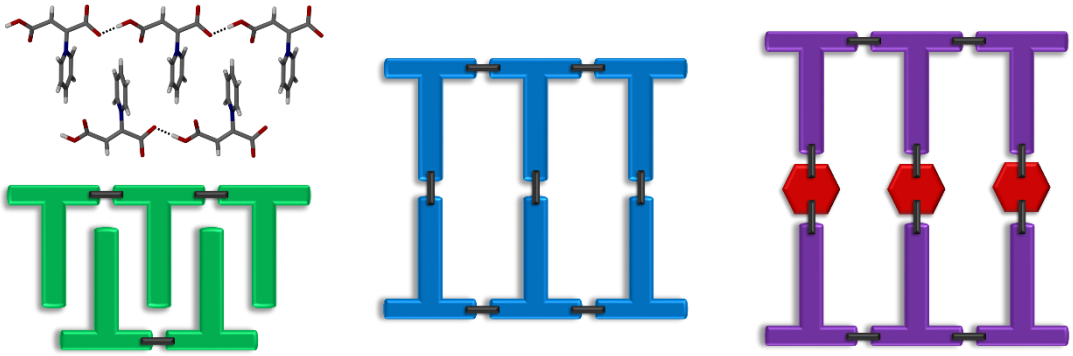

Figure 1.6 (a) General packing motif for the original series of zwitterions.[106] Chains of zwitterions interdigitate to form a close-packed structure. (b) We postulated that zwitterions containing an extra hydrogen bonding group would form a more open structure. (c) The addition of co-formers could possibly increase the pore size.

Additionally, we intended to combine these zwitterions with other small organic co-formers, with complementary functional groups, to crystallise multi-component or framework materials. The latter two zwitterions could be well-suited for this due to the extra hydrogen-bonding groups that could interact with the co-former (Figure 1.6). Because the zwitterions are already charged, our aim was to form not only hydrogen bonds, but also CAHBs, as these are stronger and could aid in forming open, porous frameworks. Such frameworks could demonstrate useful properties such as selectivity and porosity, while co-crystal- and salt formation is useful for altering the physicochemical properties of molecules.

Throughout this whole project, our objective was to use only organic molecules to form our materials, and to use mechanochemistry as much as possible. Using organic components to create frameworks and multi-component crystals has a number of advantages: there is a wide variety of molecules available, different functional groups can easily be incorporated by co-crystallisation of molecules and simple synthesis methods can generally be used. In addition these compounds form by self-assembly and can easily be re-dissolved and re-formed. To further optimise the process, we aimed to utilise mechanochemistry.[109] Mechanochemistry is a rapid technique that uses very small amounts of solvent (if any). It is still not very widely used and our aim was to demonstrate its usefulness in synthesis and co-crystal/salt screening tests.

The completion of this project would mean a better understanding of the forces holding zwitterions together, how they like to pack in 3D space, and whether they prefer to crystallise on their own, or with other co-formers or solvent molecules. Once we are able to understand why they behave the way they do, we may be able to use this knowledge to design and obtain further useful materials.

1.9 Thesis outline

Chapter 2 contains brief descriptions of the techniques and instrumentation used in this study. Chapter 3 describes the polymorphic behaviour of two zwitterions, while Chapter 4 describes the new nicotinamide and isonicotinamide zwitterions and their ability to form salts. Chapter 5 is an additional research chapter (not pertaining to zwitterions) containing solvent-competition experiments that were carried out with another organic system. Chapter 6 is a summary of the important results, conclusions made, as well as possible future work. As a supplementary, Appendix A contains details of this work that has not been included in the previous chapters, including the formation of another zwitterion. The attached CD contains information on the crystal structures presented in this work (i.e. CIF files) as well as NMR plots for the selectivity study in Chapter 5.

1.10 References

1 J.-M. Lehn, *Angew. Chem. Int. Ed. Eng.*, 1988, **27**, 89–112.

2 J. W. Steed, D. R. Turner and K. Wallace, *Core Concepts in Supramolecular Chemistry and Nanochemistry*, John Wiley & Sons, Ltd, Chichester, 2007.

3 R. J. D. Tilley, *Understanding solids: the science of materials*, John Wiley & Sons, Ltd, Chichester, 2013.

4 J. D. Dunitz, *Pure Appl. Chem.*, 1991, **63**, 177–185.

5 S. L. Price, *Chem. Soc. Rev.*, 2014, **43**, 2098–2111.

6 G. R. Desiraju, *Angew. Chemie Int. Ed.*, 1995, **34**, 2311–2327.

7 A. Burrows, in *Encyclopedia of Supramolecular Chemistry*, eds. J. L. Atwood and J. W. Steed, Marcel Dekker, Inc., New York, 2004, pp. 319–321.

8 T. S. Thakur and G. R. Desiraju, *Cryst. Growth Des.*, 2008, **8**, 4031–4044.

9 A. Mukherjee, *Cryst. Growth Des.*, 2015, **15**, 3076–3085.

10 M. D. Ward, in *Molecular networks*, ed. M. W. Hosseini, Springer, Berlin, 2009, pp. 1–23.

11 G. R. Desiraju, J. J. Vittal and A. Ramanan, *Crystal Engineering A Textbook*, World Scientific Publishing Co. Pte. Ltd., Singapore, 2011.

12 Z. P. Shields, J. S. Murray and P. Politzer, *Int. J. Quantum Chem.*, 2010, **110**, 2823–2832.

13 E. Arunan, G. R. Desiraju, R. A. Klein, J. Sadlej, S. Scheiner, I. Alkorta, D. C. Clary, R. H. Crabtree, J. J. Dannenberg, P. Hobza, H. G. Kjaergaard, A. C. Legon, B. Mennucci and D. J. Nesbitt, *Pure Appl. Chem.*, 2011, **83**, 1–5.

14 G. R. Desiraju, in *Encyclopedia of Supramolecular Chemistry*, eds. J. L. Atwood and J. W. Steed, Marcel Dekker, Inc., New York, 2004, pp. 658–665.

15 G. R. Desiraju and T. Steiner, *The Weak Hydrogen Bond*, Oxford University Press, Oxford, 1999.

16 H. Wahl, D. A. Haynes and T. le Roex, *Chem. Commun.*, 2012, **48**, 1775–1777.

17 G. R. Desiraju, *Acc. Chem. Res.*, 2002, **35**, 565–573.

18 I. Dance, in *Encyclopedia of Supramolecular Chemistry*, eds. J. Atwood and J. Steed, Marcel Dekker, Inc., New York, 2004, pp. 1076–1080.

19 A. Kitaigorodskii, *Molecular crystals and molecules*, Academic Press, Inc., New York, 1973.

20 W. C. McCrone, in *Physics and chemistry of the organic solid state*, eds. D. Fox, M. M. Labes and A. Weissberger, Wiley Interscience, New York, USA, 1965, pp. 725–767.

21 S. Aitipamula, P. S. Chow and R. B. H. Tan, *CrystEngComm*, 2014, **16**, 3451–3465.

22 T. L. Threlfall, *Analyst*, 1995, **120**, 2435–2460.

23 A. J. Cruz-Cabeza, S. M. Reutzel-Edens and J. Bernstein, *Chem. Soc. Rev.*, 2015, **44**, 8619–8635.

24 J. Bernstein, Ed., *Polymorphism in molecular crystals*, Oxford: Clarendon Press, New York, 2002.

25 J. Haleblian and W. McCrone, *J. Pharm. Sci.*, 1969, **58**, 911–912.

26 J. Bernstein, R. J. Davey and J.-O. Henck, *Angew. Chem. Int. Ed.*, 1999, **38**, 3440–3461.

27 D. Braga, F. Grepioni, L. Maini and M. Polito, in *Molecular networks*, ed. M. W. Hosseini, Springer, Berlin, 2009, pp. 25–50.

28 J. Elguero, *Cryst. Growth Des.*, 2011, **11**, 4731–4738.

29 G. R. Desiraju, *J. Chem. Soc. Perkin Trans. 2*, 1983, 1025–1030.

30 F. Lai, J. J. Du, P. A. Williams, L. Váradi, D. Baker, P. W. Groundwater, J. Overgaard, J. A. Platts and D. E. Hibbs, *Phys. Chem. Chem. Phys.*, 2016, **18**, 28802–28818.

31 A. J. Cruz-Cabeza and J. Bernstein, *Chem. Rev.*, 2014, **114**, 2170–2191.

32 J. Bernstein and A. T. Hagler, *J. Am. Chem. Soc.*, 1978, **100**, 673–681.

33 K. M. Barkigia, M. W. Renner, L. R. Furenlid, C. J. Medforth, K. M. Smith and J. Fajer, *J. Am. Chem. Soc.*, 1993, **115**, 3627–3635.

34 O. A. Turanova, G. G. Garifzyanova and A. N. Turanov, *Russ. J. Gen. Chem.*, 2010, **80**, 2317–2322.

35 I. A. Ketto, T. M. Knutsen, J. Øyaas, B. Heringstad, T. Ådnøy, T. G. Devold and S. B. Skeie, *Int. Dairy J.*, 2016, 1–10.

36 S. Rastogi and L. Kurelec, *J. Mater. Sci.*, 2000, **35**, 5121–5138.

37 A. Llinàs and J. M. Goodman, *Drug Discov. Today*, 2008, **13**, 198–210.

38 R. Tamura, M. Mizuta, S. Yabunaka, D. Fujimoto, T. Ariga, S. Okuhara, N. Ikuma, H. Takahashi and H. Tsue, *Chem. Eur. J.*, 2006, **12**, 3515–3527.

39 J. D. Dunitz and J. Bernstein, *Acc. Chem. Res.*, 1995, **28**, 193–200.

40 D. K. Bučar, R. W. Lancaster and J. Bernstein, *Angew. Chem. Int. Ed.*, 2015, **54**, 6972–6993.

41 R. J. Davey, N. Blagden, G. D. Potts and R. Docherty, *J. Am. Chem. Soc.*, 1997, **119**, 1767–1772.

42 S. K. Poornachary, P. S. Chow and R. B. H. Tan, *Cryst. Growth Des.*, 2008, **8**, 179–185.

43 N. Blagden, R. J. Davey, R. Rowe and R. Roberts, *Int. J. Pharm.*, 1998, **172**, 169–177.

44 N. Kamali, A. Erxleben and P. McArdle, *Cryst. Growth Des.*, 2016, **16**, 2492–2495.

45 N. Blagden and R. J. Davey, *Cryst. Growth Des.*, 2003, **3**, 873–885.

46 M. Rafilovich and J. Bernstein, *J. Am. Chem. Soc.*, 2006, **128**, 12185–12191.

47 J. I. E. Lu, X. Wang, X. I. A. Yang and C. Ching, *J. Pharm. Sci.*, 2007, **96**, 2457–2468.

48 M. Lang, A. L. Grzesiak and A. J. Matzger, *J. Am. Chem. Soc.*, 2002, **124**, 14834–14835.

49 F. Lu, G. Zhou, H.-J. Zhai, Y.-B. Wang and H.-S. Wang, *Cryst. Growth Des.*, 2007, **7**, 2654–2657.

50 X. Yang, B. Sarma and A. S. Myerson, *Cryst. Growth Des.*, 2012, **12**, 5521–5528.

51 G. Di Profio, S. Tucci, E. Curcio and E. Drioli, *Cryst. Growth Des.*, 2007, **7**, 526–530.

52 A. Llinàs, J. C. Burley, T. J. Prior, R. C. Glen and J. M. Goodman, *Cryst. Growth Des.*, 2008, **8**, 114–118.

53 L. J. Chyall, J. M. Tower, D. A. Coates, T. L. Houston and S. L. Childs, *Cryst. Growth Des.*, 2002, **2**, 505–510.

54 B. D. Hamilton, J.-M. Ha, M. A. Hillmyer and M. D. Ward, *Acc. Chem. Res.*, 2012, **45**, 414–423.

55 J. S. Capes and R. E. Cameron, *Cryst. Growth Des.*, 2007, **7**, 108–112.

56 S. K. P. Poornachary, J. V. Parambil, P. S. Chow, R. B. H. Tan and J. Y. Y. Heng, *Cryst. Growth Des.*, 2013, **13**, 1180–1186.

57 H. Hatakka, H. Alatalo, M. Louhi-Kultanen, I. Lassila and E. Hæggström, *Chem. Eng. Technol.*, 2010, **33**, 751–756.

58 W. Li, A. Ikni, P. Scouflaire, X. Shi, N. El Hassan, P. Gémeiner, J. M. Gillet and A. Spasojević-De Biré, *Cryst. Growth Des.*, 2016, **16**, 2514–2526.

59 S. L. Price, *Acta Crystallogr. Sect. B Struct. Sci. Cryst. Eng. Mater.*, 2013, **69**, 313–328.

60 A. M. Reilly, R. I. Cooper, C. S. Adjiman, S. Bhattacharya, A. D. Boese, J. G. Brandenburg, P. J. Bygrave, R. Bylsma, J. E. Campbell, R. Car, D. H. Case, R. Chadha, J. C. Cole, K. Cosburn, H. M. Cuppen, F. Curtis, G. M. Day, R. A. DiStasio Jr, A. Dzyabchenko, B. P. van Eijck, D. M. Elking, J. A. van den Ende, J. C. Facelli, M. B. Ferraro, L. Fusti-Molnar, C.-A. Gatsiou, T. S. Gee, R. de Gelder, L. M. Ghiringhelli, H. Goto, S. Grimme, R. Guo, D. W. M. Hofmann, J. Hoja, R. K. Hylton, L. Iuzzolino, W. Jankiewicz, D. T. de Jong, J. Kendrick, N. J. J. de Klerk, H.-Y. Ko, L. N. Kuleshova, X. Li, S. Lohani, F. J. J. Leusen, A. M. Lund, J. Lv, Y. Ma, N. Marom, A. E. Masunov, P. McCabe, D. P. McMahon, H. Meekes, M. P. Metz, A. J. Misquitta, S. Mohamed, B. Monserrat, R. J. Needs, M. A. Neumann, J. Nyman, S. Obata, H. Oberhofer, A. R. Oganov, A. M. Orendt, G. I. Pagola, C. C. Pantelides, C. J. Pickard, R. Podeszwa, L. S. Price, S. L. Price, A. Pulido, M. G. Read, K. Reuter, E. Schneider, C. Schober, G. P. Shields, P. Singh, I. J. Sugden, K. Szalewicz, C. R. Taylor, A. Tkatchenko, M. E. Tuckerman, F. Vacarro, M. Vasileiadis, A. Vazquez-Mayagoitia, L. Vogt, Y. Wang, R. E. Watson, G. A. de Wijs, J. Yang, Q. Zhu and C. R. Groom, *Acta Crystallogr. Sect. B Struct. Sci. Cryst. Eng. Mater.*, 2016, **72**, 439–459.

61 S. L. Price, *Acc. Chem. Res.*, 2009, **42**, 117–126.

62 M. Lahav and L. Leiserowitz, *Chem. Eng. Sci.*, 2001, **56**, 2245–2253.

63 M. Pudipeddi and A. T. M. Serajuddin, *J. Pharm. Sci.*, 2005, **94**, 929–939.

64 A. J. Aguiar, J. Krc, A. W. Kinkel and J. C. Samyn, *J. Pharm. Sci.*, 1967, **56**, 847–853.

65 A. Saracibar, A. Van der Ven and M. E. Arroyo-de Dompablo, *Chem. Mater.*, 2012, **24**, 495–503.

66 N. C. Debnath and S. A. Vaidya, *Prog. Org. Coatings*, 2006, **56**, 159–168.

67 M. Abes and S. S. Narine, *Chem. Phys. Lipids*, 2007, **149**, 14–27.

68 J. S. Raut, V. M. Naik, S. Singhal and V. A. Juvekar, *Ind. Eng. Chem. Res.*, 2008, **47**, 6347–6353.

69 S. P. Srivastava, J. Handoo, K. M. Agrawal and G. C. Joshi, *J. Phys. Chem. Solids*, 1993, **54**, 639–670.

70 K. W. Smith, I. Zand and G. Talbot, *J. Agric. Food Chem.*, 2008, **56**, 1602–1605.

71 E. Skořepová, D. Bím, M. Hušák, J. Klimeš, A. Chatziadi, L. Ridvan, T. Boleslavská, J. Beránek, P. Šebek and L. Rulíšek, *Cryst. Growth Des.*, 2017, **17**, 5283–5294.

72 M. Mukaida, K. Sugano and K. Terada, *Chem. Pharm. Bull.*, 2015, **63**, 18–24.

73 M. F. Arafa, S. A. El-Gizawy, M. A. Osman and G. M. El Maghraby, *J. Drug Deliv. Sci. Technol.*, 2017, **38**, 9–17.

74 S. Jasud, S. Warad, S. Rahul, G. Jagdale and S. Zinjad, *World J. Pharm. Pharm. Sci.*, 2013, **2**, 4682–4697.

75 J. B. Nanubolu and K. Ravikumar, *CrystEngComm*, 2016, **18**, 1024–1038.

76 Z. Rahman, R. Samy, V. A. Sayeed and M. A. Khan, *Pharm. Dev. Technol.*, 2012, **17**, 457–465.

77 *GRAS: Generally Recognized as Safe (GRAS)*, U.S. FDA: College Park, MD, 2011. http://www.fda.gov/Food/IngredientsPackagingLabeling/GRAS/default.htm (accessed July 30, 2017).

78 *EAFUS: Everything Added to Food in the United States (EAFUS)*, U.S. FDA, 2011. http://www.fda.gov/food/ingredientspackaginglabeling/ foodadditivesingredients/ucm115326.htm (accessed July 30, 2017).

79 B. Sekhon, *DARU J. Pharm. Sci.*, 2012, **20**, 45–47.

80 G. Fan, X. Yang, R. Liang, J. Zhao, S. Li and D. Yan, *CrystEngComm*, 2016, **18**, 240–249.

81 S. Nandi, D. Chakraborty and R. Vaidhyanathan, *Chem. Commun.*, 2016, **52**, 7249–

7252.

82 P. Li, Y. He, H. D. Arman, R. Krishna, H. Wang, L. Weng and B. Chen, *Chem. Commun.*, 2014, **50**, 13081–13084.

83 X. Z. Luo, X. J. Jia, J. H. Deng, J. L. Zhong, H. J. Liu, K. J. Wang and D. C. Zhong, *J. Am. Chem. Soc.*, 2013, **135**, 11684–11687.

84 G. R. Desiraju, *CrystEngComm*, 2003, **5**, 466–467.

85 J. D. Dunitz, *CrystEngComm*, 2003, **5**, 506–506.

86 A. D. Bond, *CrystEngComm*, 2007, **9**, 833–834.

87 E. Grothe, H. Meekes, E. Vlieg, J. H. ter Horst and R. de Gelder, *Cryst. Growth Des.*, 2016, **16**, 3237–3243.

88 P. A. Wood, N. Feeder, M. Furlow, P. T. A. Galek, C. R. Groom and E. Pidcock, *CrystEngComm*, 2014, **16**, 5839–5848.

89 M. C. Etter and G. M. Frankenbach, *Chem. Mater.*, 1989, **1**, 10–12.

90 M. Gryl, T. Seidler, K. Stadnicka, I. Matulková, I. Němec, N. Tesařová and P. Němec, *CrystEngComm*, 2014, **16**, 5765–5768.

91 J. Lin, Y. Chen, D. Zhao, X. Lu and Y. Lin, *J. Mol. Struct.*, 2017, **1149**, 452–456.

92 C. B. Aakeröy and D. J. Salmon, *CrystEngComm*, 2005, **72**, 439–448.

93 M. C. Etter, *Acc. Chem. Res.*, 1990, **23**, 120–126.

94 K. E. Riley, M. Pitoňák, J. Černý and P. Hobza, *J. Chem. Theory Comput.*, 2010, **6**, 66–80.

95 C. B. Aakeröy, A. M. Beatty and B. A. Helfrich, *J. Am. Chem. Soc.*, 2002, **124**, 14425–14432.

96 A. Delori, P. T. A. Galek, E. Pidcock, M. Patni and W. Jones, *CrystEngComm*, 2013, **15**, 2916–2928.

97 L. Leiserowitz and F. Nader, *Acta Crystallogr. Sect. B Struct. Crystallogr. Cryst. Chem.*, 1977, **B33**, 2719–2733.

98 M. K. Corpinot, S. A. Stratford, M. Arhangelskis, J. Anka-Lufford, I. Halasz, N. Judaš, W. Jones and D.-K. Bučar, *CrystEngComm*, 2016, **18**, 5434–5439.

99 Y.-F. Han, Y.-X. Yuan and H.-B. Wang, *Molecules*, 2017, **22**, 266–275.

100 J. Tian, L. Chen, D.-W. Zhang, Y. Liu and Z.-T. Li, *Chem. Commun.*, 2016, **52**, 6351–6362.

101 D. A. Haynes, Z. F. Weng, W. Jones and W. D. S. Motherwell, *CrystEngComm*, 2009, **11**, 254–260.

102 A. J. Cruz-Cabeza, *CrystEngComm*, 2012, **14**, 6362–6365.

103 P. H. Stahl and G. Wermuth, *Handbook of Pharmaceutical Salts: Properties, Selection, and Use*, Wiley-VCH, Weinheim, 2002.

104 S. L. Childs, G. P. Stahly and A. Park, *Mol. Pharm.*, 2007, **4**, 323–328.

105 S. M. Pratik and A. Datta, *J. Phys. Chem. B*, 2016, **120**, 7606–7613.

106 L. Loots, D. A. Haynes and T. le Roex, *New J. Chem.*, 2014, **38**, 2778–2786.

107 L. Loots, J. P. O'Connor, T. le Roex and D. A. Haynes, *Cryst. Growth Des.*, 2015, **15**, 5849–5857.

108 J. Lombard, L. Loots, D. A. Haynes and T. le Roex, *Manuscript in preparation*, 2017.

109 T. Friščić, *Chem. Soc. Rev.*, 2012, **41**, 3493–3510.

CHAPTER 2

EXPERIMENTAL AND ANALYTICAL TECHNIQUES

2.1 Methodology for zwitterion formation

The reaction to synthesise the zwitterions described in this thesis (Figure 2.1) is a simple Michael addition-type reaction between acetylenedicarboxylic acid (ADC) and various pyridine derivatives. The two components were simply combined with the solvent/solvent mixture in a small vial and stirred for 5-10 minutes at various temperatures. All chemicals and solvents were obtained from Sigma Aldrich South Africa and used without further purification.

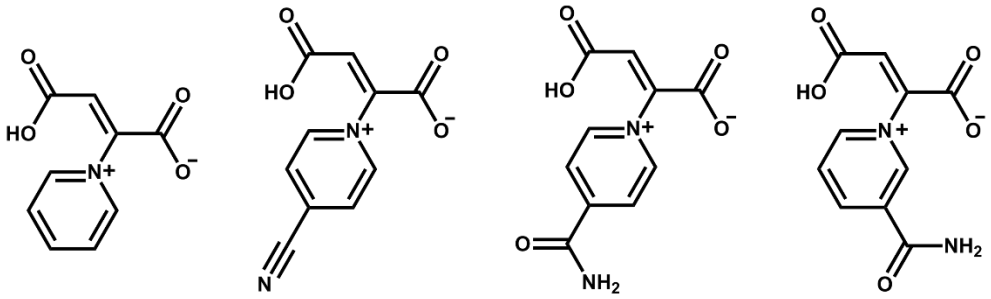

Figure 2.1 The zwitterions that will be discussed in this thesis.

Due to the simplicity of this synthesis, our key variable was the choice of solvent. For all zwitterions we first attempted the reaction in 16 common laboratory solvents (namely: water, methanol, ethanol, dimethylformamide, dimethyl sulfoxide, acetone, acetonitrile, chloroform, dichloromethane, diethyl ether, 1,4-dioxane, tetrahydrofuran, toluene, cyclohexane, ethyl acetate, and benzene). However, not all of the solvents could dissolve the starting materials – in fact very few did. DMSO, DMF, and water were always successful, while methanol and ethanol were successful for two of the zwitterions. We will refer to the different solvents as soluble or insoluble solvents for each set of starting materials. The next step was to use two-component solvent systems to perform the synthesis. All possible solvent combinations between soluble solvents were attempted, followed by all soluble-insoluble combinations. This amounted to about 60 solvents/combinations per

zwitterion (depending on whether methanol and ethanol were classified as soluble- or insoluble solvents for that particular set of starting materials).

Other than the solvent used, we also investigated the effect of temperature and reagent ratios on the product obtained. To test the effect of temperature, we repeated some of the syntheses at temperatures ranging from room temperature to 100 °C. To determine whether the solvent ratio could change the product that is obtained, we again repeated a few experiments, but added an excess of each of the reagents alternately.

Four analogous zwitterions will be discussed in this thesis, namely those that are obtained when ADC is combined with pyridine, 4-cyanopyridine, nicotinamide, and isonicotinamide. The synthesis of two of these zwitterions is accompanied by the formation of a salt by-product. From previous work[1,2] this salt seems to be the kinetic product of the reaction that forms from a simple acid-base proton transfer. It forms faster and at lower temperatures than the zwitterion, and so it is easy to remove by filtration before the solution is left to crystallise once more to form the more thermodynamically stable zwitterion.

2.2 Crystal growth

Solid-state supramolecular chemistry relies heavily on crystal structures and the accurate information it provides. Thus, we always endeavour to grow crystals of all products. The technique of 'slow evaporation' was the main technique used during this project: material was simply dissolved in the solvent(s) and then left to crystallise slowly as the solvent evaporated and the solution became saturated. Slow crystal growth is important to obtain larger crystals suitable for single-crystal X-ray diffraction. Practically, the speed of crystallisation was controlled by either covering vials with non-sealing lids, perforated parafilm, or by not covering them at all. The choice of solvent was also very important to ensure optimal crystal growth, and often a multi-component solvent was needed. It is important that the solvent can be supersaturated with the material, i.e. one in which the material is not too insoluble, but also not too soluble – practically this is often achieved by combining a solvent in which the material is soluble with one in which the material is insoluble. Varying the ratios of solvents in such a solvent mixture can also aid in slowing down crystallisation. Of course, the difference in solvent volatility need also be taken into account.

As an addendum we experimented with the effect of temperature on crystal growth. Vials of solutions were left to crystallise in the refrigerator, or on a warm surface. Vials were also suspended in an oil bath, where the temperature could be controlled to cool down very slowly over a period of time.

2.3 Methodology for multi-component crystal formation

We attempted to form multi-component crystals by combining each zwitterion with other organic molecules. To obtain a clear picture of the ability of these zwitterions to form multi-component crystals, co-formers of varying sizes and containing various functional groups were used. The specific co-formers used includes: urea, isonicotinamide, nicotinamide, uracil, terephthalic acid, melamine, 1,4-Diazabicyclo[2.2.2]octane, 2-amino-pyrimidine, 2-aminopyridine, 2,6-diaminopyridine, thymine, pyrogallol, 2,2'-biphenol, isoquinoline, pyridine, 4-methylphenol, 2,3-dihydroxynapthalene, napthalene, phloro-glucinol dihydrate, N-phenyl-2-napthylamine, pamoic acid, hydroquinone, piperazine, pyrazinecarboxylic acid, 4-phenylpyridine, 4-hydroxybenzaldehyde, α,α'-dibromo-o-xylene and 2-amino-benzonitrile. We also attempted to co-crystallise the zwitterions with each other as they are similar in size and contain complementary functional groups.

We attempted to form multi-component crystals *via* solution methods by simply stirring the components together in a solvent, with mild heating to aid dissolution. Due to the insoluble nature of these zwitterions, we could only achieve dissolution in water, and even then it almost always resulted in recrystallisation of the zwitterion, or the coformer, on its own. The crystallisations were repeated with the addition of a few drops of pyridine, as this appeared to aid dissolution. The idea was that recrystallisation might not occur if the two components did not have such vastly differing solubilities, however this too was unsuccessful.

As mechanochemistry is less affected by this difference in solubility, it proved to be a useful tool for quick co-former screening, and so lead to the discovery of the salts discussed in Chapter 4.

2.4 Mechanochemistry

Mechanochemistry is a solid-state synthesis and crystallisation technique where reagents are ground together in a mortar and pestle. Neat grinding, liquid-assisted grinding (LAG)[3] and polymer-assisted grinding (POLAG)[4] are all useful, but differ slightly in reaction rate and efficiency, as well as solvent inclusion ability. Using mechanochemical methods is very effective and quick, and therefore very useful for co-crystal/salt-formation screening purposes. It is also environmentally friendly with respect to solvent use, and is less likely to yield a mixture of products.[5] With respect to forming multicomponent materials, mechanochemical methods are often more successful than conventional methods as they are not as dependant on the solubility of the components.[5] However, the solubility difference between molecules should not be too great – both components should be saturated in the solvent drop(s) when LAG is used.[6] Neat grinding does not work for all cases,[6] but LAG has a high success rate, with the rate of conversion increasing with the amount of solvent used and being dependent on the choice of solvent.[6]

In this work mechanochemistry (manual grinding with mortar and pestle at room temperature) was not successful in synthesising the zwitterions as heat is needed to form this thermodynamic product (although the kinetic salt product can be formed by grinding). On the other hand, this technique was very useful for making the multi-component materials. The components (e.g. the zwitterion and melamine) were manually ground together for 10 minutes with a few drops of either water, methanol, ethanol, or THF, to afford a powder of the salt that could be recrystallised from water to obtain single crystals. Other methods that can be used to obtain crystals, after a salt or co-crystal has been identified *via* mechanochemistry, include recrystallisation with seeding, recrystallisation from the melt, sublimation, etc.

2.5 Instrumentation

2.5.1 Thermogravimetric Analysis (TGA)

TGA is a form of thermal analysis where a sample is heated while the change in its mass is measured. Information regarding the loss of solvent and degradation can be obtained. Analysis was performed on a TA Q500 instrument. Each sample, ranging from 3-15 mg, was loaded into an open aluminium pan and suspended in the furnace of the instrument. The

sample was then heated at 10 °C min^{-1} from room temperature (20-30 °C) to 500 °C while under a constant flow of nitrogen (50 ml min^{-1}). Data were exported using Universal Analysis 2000 v 4.5A (TA Instruments) and analysed using Microsoft Excel 2013.

2.5.2 Differential Scanning Calorimetry (DSC) analysis

DSC is another useful thermal analysis technique where the change in heat flow (in W/g) is measured as the sample is heated up and cooled down. Peaks and troughs (exo- and endotherms) in the trace indicate physical or chemical changes in the sample. Analysis was performed on a TA Q20 instrument. Each sample, ranging from 3-10 mg, was loaded into an aluminium pan and closed with a perforated lid. A reference pan was made in the same way. The sample and reference pan were placed on thermocouples inside the instrument and subjected to two heating-cooling cycles while under a flow of nitrogen (50 ml min^{-1}). For the first cycle the temperature was increased at 10 °C min^{-1} from 25 °C to just before decomposition. This was followed by cooling at 5 °C min^{-1} to -20 °C. For the second cycle the sample was heated once again, and subsequently cooled to room temperature at the same speed used previously.

2.5.3 Nuclear magnetic resonance (NMR) spectroscopy

NMR was used to identify products when single crystals were not available. Samples were prepared by dissolving 15-20 mg of a powdered sample in an appropriate deuterated solvent, such as D_2O or DMSO-d_6, and pipetting the solution into a Wilmad® NMR tube. Analysis was performed using an Agilent spectrometer at 300 MHz. MestReNova Version 7.1.2 (Mnova)[7] was used to analyse the data and generate spectra.

2.5.4 Single-crystal X-ray diffraction (SCD)

SCD is a powerful technique that can be used to obtain the relative coordinates of all the atoms/molecules in a crystalline material (3D crystal structure) based on electron density. Single crystals are needed to obtain accurate data and these are usually cooled to 100 K to minimise atomic movement.

For our analysis, crystals were placed in paratone oil so that a suitable crystal could be chosen. The crystal was then picked up using a MiTeGen mount which was then attached to a goniometer head in the instrument cabinet.

SCD for all compounds, except **3-Melamine**, was carried out using a Bruker SMART Apex II diffractometer. The diffractometer makes use of MoKα radiation of wavelength 0.71073 Å produced using a microfocus sealed tube and a 0.5 mm MonoCap collimator. Frames were detected by a Bruker APEX SMART CCD area-detector. An Oxford Cryosystems cryostat (Cryostream Plus 700 Controller) was used to keep the single crystals at 100 K throughout all data collections.

Single-crystal X-ray Diffraction (SCD) of **3-Melamine** was carried out using a Bruker Apex II DUO Quasar CCD area-detector diffractometer. This dual source diffractometer was operated using MoKα radiation of wavelength 0.71073 Å produced by an Incoatec $I_{\mu S}$ microsource coupled with a multilayer mirror optics monochromator. An Oxford Cryosystems cryostat (Cryostream Plus 700 Controller) was used to keep the single crystal at 100 K throughout the data collection.

Data were collected, and reduced using the Bruker software package SAINT[8] in the ApexIII software. SADABS[9,10] was used for the absorption correction and correcting for other systematic errors. Finally, the structures were solved (SHELXS-13)[11] using direct methods and refined (SHELXL-16)[12] through the graphical user interface XSeed.[13,14] Hydrogen atoms on sp^2-hybridised carbon atoms were placed in calculated positions using riding models, while O–H and N–H hydrogen atoms were placed on maxima in the electron density difference maps. All images were created using POV-Ray.[15]

2.5.5 Powder X-ray diffraction (PXRD)

PXRD is a useful technique for analysing bulk powdered, but crystalline, samples. A fingerprint plot is obtained that can easily be compared to known patterns for positive identification. Samples were prepared by lightly grinding the material in a mortar and pestle and placing it in a zero-background holder inside the instrument. PXRD patterns were collected on a Bruker D2 Phaser powder X-ray diffractometer with 1.54183 Å CuKα radiation; operated at 30 kV and 10 mA. Data were collected from $2\theta = 4$ to 40° at a scan speed of 0.5 seconds per step (step size of 0.0161). Data analysis was performed with the

program X'Pert HighScore Plus (version 2.2e) and images generated with Microsoft Excel 2013.

2.5.6 Fourier transform infrared spectroscopy

FTIR was carried out using a Bruker Alpha spectrometer with Platinum ATR attachment, using the OPUS Version 7.5 software.[16] A background scan was acquired before each sample scan. This technique was very useful for determining whether our multi-component materials were co-crystals or salts. By looking at the C=O stretching frequency one can determine whether there is a carboxylate (1550 – 1635 cm^{-1}) or carboxylic acid group (ca. 1720 cm^{-1}) present, i.e. whether it is a salt or a co-crystal.

2.6 Computer software

2.6.1 Mercury CSD 3.9

Mercury is a useful tool developed by the Cambridge Crystallographic Data Centre (CCDC) to visualise crystal structures and intermolecular interactions, and to statistically analyse data from the CSD (the Cambridge Structural Database).[17–20] We specifically made use of its functionality to calculate UNI intermolecular potentials using the 'UNI' force field.[21,22]

2.6.2 ConQuest 1.18

ConQuest[20] is developed by the CCDC in order to easily search for crystal structures on the CSD (a database containing all published crystal structures). This software has a variety of useful functionalities; for our purposes, we made use of its ability to search for specific interactions within crystal structures in order to determine the propensity of these interactions to form.

2.6.3 CrystalExplorer 17.5

CrystalExplorer[23] can be used to investigate crystal packing and intermolecular interactions, and to generate surfaces within a crystal structure that correspond to specific properties such as electron density and electrostatic potential. We made use of CrystalExplorer's ability to calculate intermolecular interaction energies from model energies consisting of electrostatic, polarisation, dispersion, and exchange-repulsion components. For our

purposes, the Tonto computational chemistry package was used for wavefunction calculations,[24] carried out at the B3LYP/6-31G(d,p) level of theory.

2.7 References

1 L. Loots, J. P. O'Connor, T. le Roex and D. A. Haynes, *Cryst. Growth Des.*, 2015, **15**, 5849–5857.

2 J. Lombard, L. Loots, D. A. Haynes and T. le Roex, *Manuscript in preparation*, 2017.

3 D. Braga, L. Maini and F. Grepioni, *Chem. Soc. Rev.*, 2013, **42**, 7638–7648.

4 D. Hasa, G. Schneider Rauber, D. Voinovich and W. Jones, *Angew. Chem. Int. Ed.*, 2015, **54**, 7371–7375.

5 N. Shan, F. Toda and W. Jones, *Chem. Commun.*, 2002, 2372–2373.

6 T. Friščić, S. L. Childs, S. A. A. Rizvi and W. Jones, *CrystEngComm*, 2009, **11**, 418–426.

7 *MestReNova, version 7.1.2-100008*, Mestrelab Research S. L., 2012.

8 *SAINT Data Collection Software, version V7.99A*, Bruker AXS Inc., 2012, Madison, WI.

9 *SADABS, version 2012/1*, Bruker AXS Inc., 2012, Madison, WI.

10 R. H. Blessing, *Acta Crystallogr. Sect. A Found. Crystallogr.*, 1995, **51**, 33.

11 G. M. Sheldrick, *Acta Crystallogr. Sect. A Found. Crystallogr.*, 2008, **64**, 112.

12 G. M. Sheldrick, *Acta Crystallogr. Sect. C*, 2015, **71**, 3–8.

13 L. J. Barbour, *J. Supramol. Chem*, 2001, **1**, 189–191.

14 J. L. Atwood and L. J. Barbour, *Cryst. Growth Des.*, 2003, **3**, 3–8.

15 *POV-RayTM for Windows, version 3.6*, Persistence of Vision Raytracer Pty. Ltd., 2004, Williamstown, Australia.

16 *OPUS 7.5, build: 7, 5, 18 (20140810)*, Bruker Optik GmbH, 2014.

17 C. F. Macrae, P. R. Edgington, P. McCabe, E. Pidcock, G. P. Shields, R. Taylor, M.

Towler and J. van de Streek, *J. Appl. Crystallogr.*, 2006, **39**, 453–457.

18 C. F. Macrae, I. J. Bruno, J. A. Chisholm, P. R. Edgington, P. McCabe, E. Pidcock, L. Rodriguez-Monge, R. Taylor, J. van de Streek and P. A. Wood, *J. Appl. Crystallogr.*, 2008, **41**, 466–470.

19 R. Taylor and C. F. Macrae, *Acta Crystallogr. Sect. B Struct. Sci.*, 2001, **B57**, 815–827.

20 I. J. Bruno, J. C. Cole, P. R. Edgington, M. Kessler, C. F. Macrae, P. McCabe, J. Pearson and R. Taylor, *Acta Crystallogr. Sect. B Struct. Sci.*, 2002, **B58**, 389–397.

21 A. Gavezzotti, *Acc. Chem. Res*, 1994, **27**, 309–314.

22 A. Gavezzotti and G. Filippini, *J. Phys. Chem.*, 1994, **98**, 4831–4837.

23 M. J. Turner, S. K. McKinnon, D. J. Wolff, P. R. Grimwood, D. Spackman, D. Jayatilaka and M. A. Spackman, *CrystalExplorer17 (2017)*, University of Western Australia. http://hirshfeldsurface.net.

24 Tonto, A Fortran Based Object-Oriented System for Quantum Chemistry and Crystallography, D. Jayatilaka and D. J. Grimwood, *Computational Science - ICCS* 2003, **4**, 142-151.

CHAPTER 3

POLYMORPHIC BEHAVIOUR OF TWO ORGANIC ZWITTERIONS: A RARE CASE OF NO OBSERVABLE CONVERSION BETWEEN POLYMORPHS

This chapter is presented as a draft of a paper that has been published in Crystal Growth and Design (DOI 10.1021/acs.cgd.7b01271). The version that was submitted is included as Appendix C. All the experimental work in this chapter was carried out by myself, except for the following: the conformational scan was carried out by Bernard Dippenaar, and the CASTEP calculations were carried out by Thalia Carstens. The draft included here was written by me.

3.1 Abstract

The solid-state behaviour of two organic zwitterions, (Z)-3-carboxy-2-(4-cyanopyridin-1-ium-1-yl)-acrylate (**1**) and (Z)-1-(3-carboxy-1,1-dihydroxyprop-2-en-1-ide-2-yl)-pyridin-1-ium (**2**), has been extensively investigated. Variation of crystallisation conditions resulted in the identification of two conformational polymorphs of **1**, a kinetic and thermodynamic form. Three polymorphs of **2**, where the formation of a particular polymorph depends entirely on solvent of crystallisation, were also identified. The relationship between the polymorphs of both **1** and **2** has been extensively studied, and attempts were made to interconvert between forms to determine their relative stability. No interconversion between polymorphs is observed in either **1** or **2**. In the case of **1**, this is likely due to restrictions on rotation of the carboxylic group in the solid state, which is required for conversion between polymorphs.

3.2 Introduction

In the rapidly developing field of crystal engineering, significant effort is still devoted to understanding in more detail why molecules pack in certain ways in the solid state. One useful way to gain more insight into this question is the detailed study of polymorphism. As with most scientific concepts, the definition of polymorphism and the depth to which it has

been studied has varied throughout its development. Despite its first recognition in 1822 by Mitscherlich,[1] the first widely accepted definition, given by McCrone, only appeared in 1965.[2] Since then there has been much debate regarding the significance of isomerism,[3,4] tautomerism,[5] and large conformational changes[6] to this definition, and whether allotropism,[7] amorphous materials,[8] and pseudopolymorphism should be included in the definition of polymorphs.[9] Nevertheless, the most common and innocuous definition remains that polymorphism[10–12] is when a molecule (or a combination of molecules in the case of multi-component frameworks[13]) can arrange in more than one way in the solid state.[14] Simply put, polymorphs have different solid-state crystal structures, but are identical in solution and in the vapour state.[15]

In order to control which polymorph is isolated it is often of interest to know how polymorphs relate to one another, how they are different, and how they can interconvert. Many polymorphs can be interconverted by changing the temperature, changing the pressure,[16] dissolution of the crystals in different solvents,[17,18] grinding (neat or liquid-assisted),[19] the presence of moisture in the air,[20] the addition of acids or bases[21] or by melting.[22] Monotropic polymorphism is when one polymorph is more stable than another at all temperatures and is therefore more likely to be formed. The less stable form is often called the metastable polymorph.[14] For monotropic polymorphs, changing the temperature would only result in conversion from the metastable to the stable form. Enantiotropic polymorphism occurs when each polymorph is stable over a certain temperature range, such that there is a low-temperature form and a high-temperature form. At the juncture temperature both are equally stable and so either one could be converted to the other. At temperatures above this point the low-temperature polymorph will convert to the high-temperature form, and *vice versa.*[14] Very rarely, there are reports of polymorphs that do not interconvert at all.[23]

Recently, we reported the synthesis and solid-state behaviour of a series of organic zwitterions.[24–26] These molecules have extensive hydrogen bonding capability as well as an interesting T-shape, which lead us to study their interactions in the solid state. The zwitterions are synthesized directly from reaction of acetylenedicarboxylic acid (ADC) with various pyridine derivatives (Scheme 3.1) and previous studies showed that several of these zwitterions display interesting inclusion behaviour and polymorphism. The focus of this

study was thus to carry out an extensive investigation of two of these zwitterions, which are formed by reaction of ADC with 4-cyanopyridine (**1**) or with pyridine (**2**).

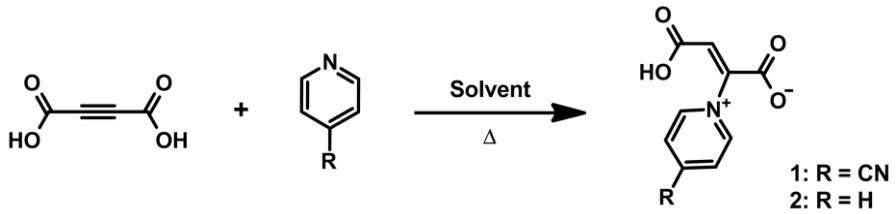

Scheme 3.1 General reaction scheme for the formation of zwitterions **1** and **2**.

3.3 Results and discussion

3.3.1 Synthesis and crystallisation

Zwitterions **1α** and **2α** (CSD refcodes: BIXMIG & BIXLUR[24]) have previously been described by our group. Systematic variation of the crystallisation solvent yielded three new polymorphs (**1β**, **2β**, and **2γ**). Crystals of all five polymorphs formed directly from the reaction mixture by slow evaporation, between 24 hours and one week after the reaction, and were of suitable size for single-crystal X-ray diffraction, needing no further purification.

Zwitterion **1α** crystallised from solvent mixtures of either methanol or ethanol with a series of common solvents, whilst **1β** was synthesized and crystallised from a range of solvent mixtures containing water (see supplementary information for details). Using lower reaction temperatures (room temperature instead of 60 °C) or shorter stirring times produced a mixture of both **1α** and **1β**. When crystals of **1α** were filtered and the filtrate left to allow further crystallisation, a mixture of polymorphs was isolated.

Zwitterion **2α** crystallised from methanol, as well as from several other solvent mixtures, often containing methanol. Zwitterion **2β** crystallised from a mixture of methanol and DMF, as well as other solvent mixtures containing DMF (see supplementary information for all solvents/solvent mixtures used). Zwitterion **2γ** only crystallises from a mixture of water and THF and is often accompanied by the simultaneous formation of **2α**. The temperature of reaction and crystallisation had no noticeable effect on the product in the case of zwitterion **2**.

Attempts were made to use liquid-assisted grinding (LAG) to synthesize crystalline **1** and **2**. The combination of ADC and pyridine resulted in the formation of an unknown product (**3**) when LAG was used, while the mechanochemical combination of ADC and 4-cyanopyridine left the starting materials unchanged. Single crystal data of **3** have not been obtained, but it is strongly suspected to be a salt formed *via* proton transfer, based on ^{1}H and ^{13}C NMR and PXRD (See supplementary information). From previous work[24–26] it seems that the salt is most likely the kinetic product of the reaction between ADC and the pyridine derivative that forms without sufficient heating.

3.3.2 Crystal structures

Zwitterions **1** and **2** both contain a pyridinium moiety and a backbone consisting of the four-carbon chain and the carboxylic acid/carboxylate groups – these terms will be used in the following descriptions. The structures of **1α** and **2α** have been reported previously,[24] however they are described again here for comparative purposes. Crystallographic data are summarized in Table 3.1 and hydrogen-bond distances and angles in Table 3.2.

Table 3.1 Crystallographic data for the polymorph structures.

Structure	**1α***	**1β**	**2α***	**2β**	**2γ**
Chemical formula	$C_{10}H_6N_2O_4$	$C_{10}H_6NO_4$	$C_9H_7NO_4$	$C_9H_7NO_4$	$C_9H_7NO_4$
Formula weight /g mol^{-1}	218.17	218.17	193.16	193.16	193.16
Crystal system	Monoclinic	Monoclinic	Orthorhombic	Triclinic	Monoclinic
Space group	$P2_1/c$	$P2_1/c$	$P2_12_12_1$	$P\bar{1}$	$P2_1/n$
a /Å	7.1931(1)	8.0518(8)	7.9762(3)	7.332(2)	10.2397(7)
b /Å	20.060(3)	11.8523(1)	8.3938(3)	8.0634(2)	7.9983(5)
c /Å	7.4716(1)	20.020(2)	12.6089(5)	9.107(3)	10.6591(7)
α /°	90.00	90.00	90.00	65.923(3)	90
β /°	112.495(2)	94.3020(1)	90.00	75.200(4)	107.223(2)
γ /°	90.00	90.00	90.00	64.146(3)	90
Calculated density /g cm^{-3}	1.455	1.521	1.520	1.457	1.539
Volume /Å^3	996.1(3)	1905.2(3)	844.17(6)	440.4(2)	833.84(1)
Z	4	8	4	2	4
Temperature /K	100(2)	100(2)	100(2)	100(2)	100(2)
μ /mm^{-1}	0.12	0.12	0.12	0.12	0.12
Independent reflections	2208	4359	2254	2336	2084
R_{int}	0.0256	0.0178	0.0371	0.0595	0.0330
R_1 [I > 2σ(I)]	0.0419	0.0450	0.0398	0.0454	0.0352

*Although reported previously, these structures have been redetermined from new data and the CIF files included.

Table 3.2 Summary of the hydrogen-bond geometries of the polymorphs.

Structure	D–H···A	D—H /Å	H···A /Å	D···A /Å	D—H···A /°	Symmetry codes
1α	O1–H1···O7	0.99(3)	1.52(3)	2.5045(2)	178(2)	*x, y, z+1*
1β	O2A–H2A···O8A	0.99(3)	1.56(3)	2.5512(2)	177(3)	*x+1, y, z*
	O2B–H2B···O8B	0.87(3)	1.65(3)	2.5246(2)	175(3)	*x-1, y, z*
2α	O2–H2···O8	1.00(4)	1.49(4)	2.475(2)	170(4)	*x+1, y, z*
2β	O2–H2···O8	0.99(3)	1.50(3)	2.4934(2)	178(3)	*x, y-1, z*
2γ	O2–H2···O8	1.05(3)	1.42(3)	2.49698(1)	174(2)	*x, y+1, z*

*3.3.2.1 Crystal structures of **1α** and **1β***

Zwitterion **1α** (BIXMIG[24]) crystallises in the monoclinic space group $P2_1/c$ and has one zwitterion per asymmetric unit (ASU). The angle between the planes formed by the backbone and the pyridinium moiety is 97.47(5)°. These planes were fitted to all non-hydrogen atoms – the first to those of the backbone, and the second to those of the ring. The angle was chosen in such a way as to allow for comparison between the different forms. One-dimensional chains of zwitterions are formed via O–H···O hydrogen bonding between the backbones; these run along the *c*-axis (Figure 3.1 a). Each chain then forms a pair with another so that they form a herringbone pattern as the pyridinium moieties interdigitate (Figure 3.1 b & c). These pairs then pack together to form sheets of zwitterion chains with cyano groups all pointing in the same direction. Sheets then pack together in an ABAB fashion with cyano groups pointing in the opposite direction on each adjacent sheet (Figure 3.1 d).

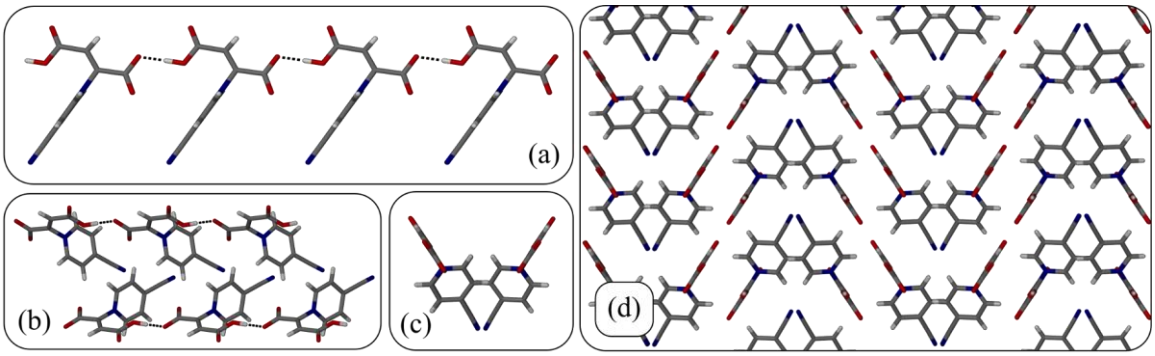

Figure 3.1 (a) Chain of zwitterion **1α** showing the hydrogen bonding between neighbouring zwitterions. (b) Pairs of zwitterion chains of **1α** viewed down the *a*-axis - showing the herringbone pattern - and (c) down the *c*-axis. (d) Packing diagram of **1α** viewed down the *c*-axis.

Polymorph **1β** is similar to **1α**. Like **1α** it also crystallises in $P2_1/c$, but with two zwitterions in the ASU. The angles between the planes formed by the backbone and pyridinium moiety in the two zwitterions are 96.43(4)° and 77.53(4)°. One-dimensional chains of zwitterions are formed via O–H···O hydrogen bonding between the carboxylate backbones; these run along the *a*-axis. Each chain then forms a pair with another to give a two-dimensional ladder-like structure as the pyridinium moieties interdigitate (Figure 3.2 a & b). These ladders then pack in alternating directions along the *a*-axis, leaving no open spaces in the structure (Figure 3.2 c).

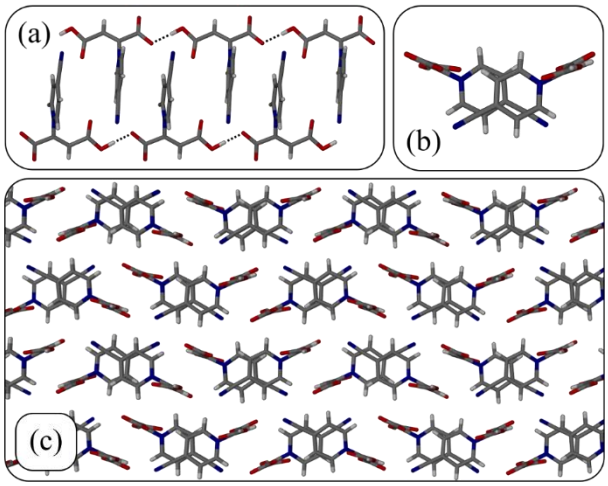

Figure 3.2 (a) Pair of zwitterion chains, or ladder, of **1β** viewed down the *b*-axis, and (b) down the *a*-axis. (c) Packing diagram of **1β** viewed down the *a*-axis.

*3.3.2.2 Comparison of **1α** and **1β***

The polymorphs of zwitterion **1** are similar – both consist of pairs of chains of zwitterions close-packed together – but there are slight differences leading to the herringbone pattern of **1α** and the ladder structure of **1β**. The most notable difference is the position of protonation (Figure 3.3). In polymorph **1β** (as well as in all three polymorphs of zwitterion **2**) the oxygen atom *trans* to the pyridinium ring is protonated, while in **1α** the *cis* oxygen atom of that carboxylic acid group is protonated. This leads to a different chain geometry in **1α**, i.e. the zwitterion backbones do not pack end-on in a collinear fashion to form a straight line but are rather tilted with respect to each other (Figure 3.3). The more perpendicular arrangement of **1β** allows the pyridinium moieties to interdigitate (Figure 3.4) so that the cyanopyridinium rings now fit in between the backbones. As a result the backbones are slightly farther apart to accommodate these rings (Figure 3.4).

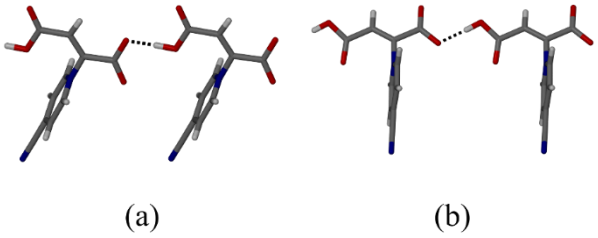

Figure 3.3 Hydrogen bonding between the zwitterions in (a) **1α** and (b) **1β**.

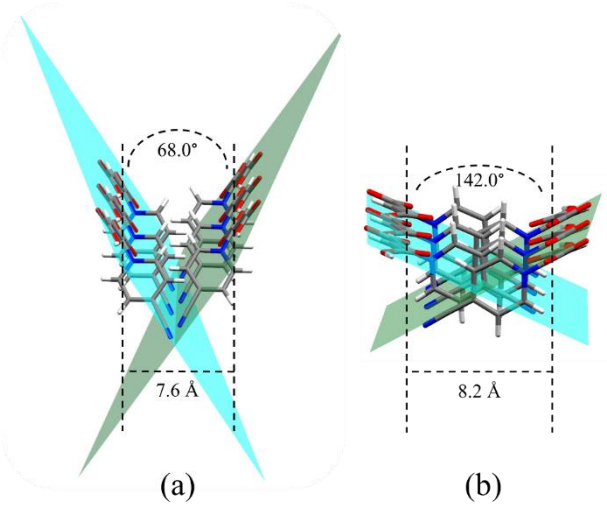

Figure 3.4 Comparison of the pairs of chains in **1α** and **1β**. Planes are constructed to show the angle of the zwitterion chains relative to each other. Distances between the zwitterion chains were measured from the sp^2 carbon in the backbones. (a) In **1α** the two nearest zwitterion chains are separated by an angle of 68.00(4)° and a distance of 7.621(4) Å. (b) In **1β** the two nearest chains are 142.00(5)° and 8.216(3) Å from each other leaving more space in between the backbones for the pyridinium moieties.

It should also be noted that **1β** has two molecules in the ASU while **1α** has only one. The angle between the planes made by the pyridinium moiety and backbone of **1α** is 97.47(5)°. While half of the molecules in **1β** have a very similar conformation (96.43(4)°), every second zwitterion is slightly twisted to make this angle 77.53(4)°. It could be that this smaller twist in **1β** allows the zwitterions to pack together more closely. In fact, from the crystallographic data, **1β** is more dense than **1α** (1.521 *vs* 1.455 g cm^{-3}). According to the density rule[27] based on the close packing principle of Kitaigorodskii,[28] crystal structures that are more dense, are more stable.

*3.3.2.3 Crystal structures of **2α**, **2β** and **2γ***

Zwitterion **2α** crystallises in the chiral, orthorhombic space group $P2_12_12_1$ and has one zwitterion per ASU. The angle between the planes formed by the backbone and pyridinium ring is 78.35(5)°. Once again, one-dimensional chains of zwitterions are formed via O–H···O hydrogen bonding between the backbones; these run along the *a*-axis (Figure 3.5 a). Each chain then forms a pair with another as the pyridinium moieties interdigitate and partially overlap to give a similar ladder-like structure to that formed in **1β** (Figure 3.5 b & c), except that the pyridinium rings of the two chains in the ladder are not quite parallel to one another. These pairs of chains pack together in 3-dimensions to form the structure (Figure 3.5 d).

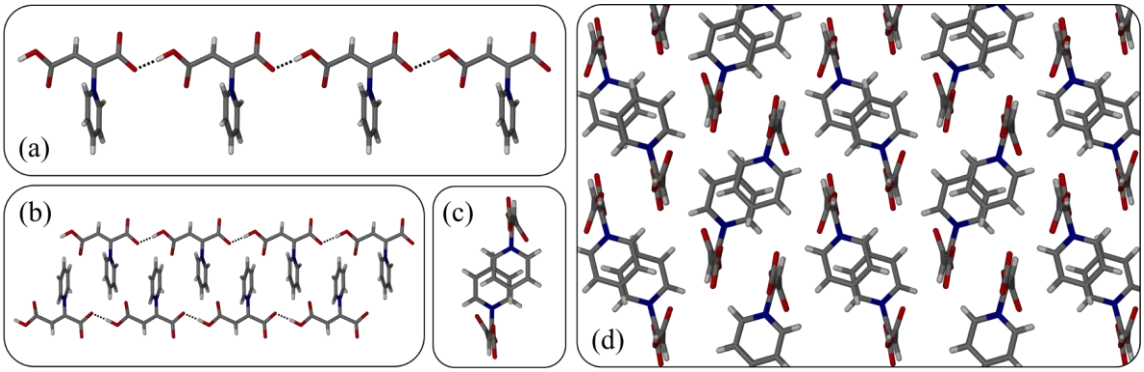

Figure 3.5 (a) Chain of zwitterion **2α** showing the hydrogen bonding between neighbouring zwitterions. (b) Pair of zwitterion chains, or ladder, of **2α** viewed down the *c*-axis and (c) down the *a*-axis. (d) Packing diagram of **2α** viewed down the *a*-axis.

Zwitterion **2β** crystallises in the triclinic space group $P\bar{1}$, and has one zwitterion per ASU. The angle between the planes formed by the backbone and pyridinium moiety is 69.11(4)°. One-dimensional chains of zwitterions are formed via O–H···O hydrogen bonding between the backbones; these run along the *b*-axis (Figure 3.6 a). Each one-dimensional chain then forms a pair with another resulting in a two-dimensional ladder-like structure as the pyridine moieties interdigitate (Figure 3.6 b). When two neighbouring ladders are examined (Figure 3.6 c) it is clear that all the pyridinium rings are parallel to each other. These ladders then pack into sheets that form a layered structure. When viewed down the *b*-axis the backbones of neighbouring ladders line up along the *a*-axis resulting in hydrophilic and hydrophobic layers (Figure 3.6 d).

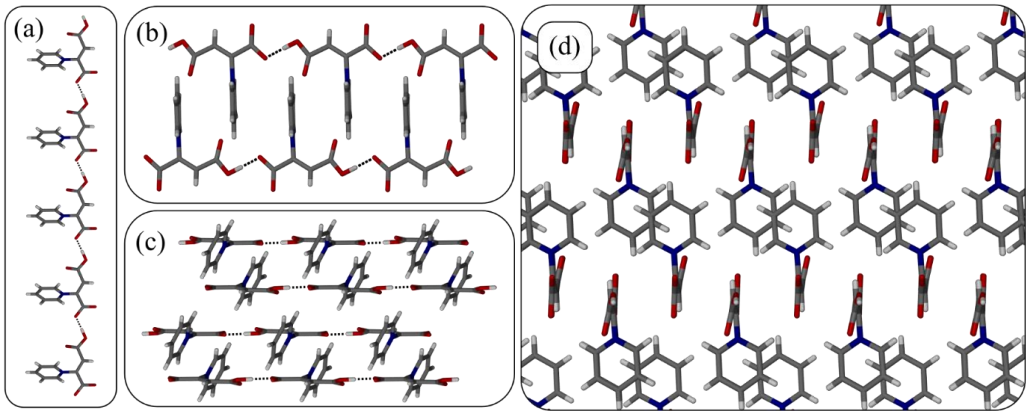

Figure 3.6 (a) Chain of zwitterion **2β** showing the hydrogen bonding between neighbouring zwitterions. (b) Pair of zwitterion chains, or ladder, of **2β** viewed down the *a*-axis, and (c) down the *c*-axis. Here two ladders are shown to demonstrate that all pyridine moieties are parallel (d) Packing diagram of **2β** viewed down the *b*-axis.

Zwitterion **2γ** crystallises in the monoclinic space group $P2_1/n$ and has one zwitterion per ASU. The angle between the planes formed by the backbone and pyridinium moiety is 114.7(4)°. One-dimensional chains of zwitterions are formed via O–H···O hydrogen bonding between the backbones; these run along the *b*-axis (Figure 3.7 a). Each one-dimensional chain then forms a pair with another to form a two-dimensional ladder-like structure as the pyridinium moieties interdigitate and are parallel to each other (Figure 3.7 b). When two neighbouring ladders are viewed it is clear that the pyridinium rings are parallel to those in the same ladder, but not to those in adjacent ladders (Figure 3.7 c). These ladders pack into sheets that form a layered structure. When viewed down the *b*-axis the backbones of neighbouring ladders line up, resulting in hydrophilic and hydrophobic layers (Figure 3.7 d) very similar to those seen in **2β**.

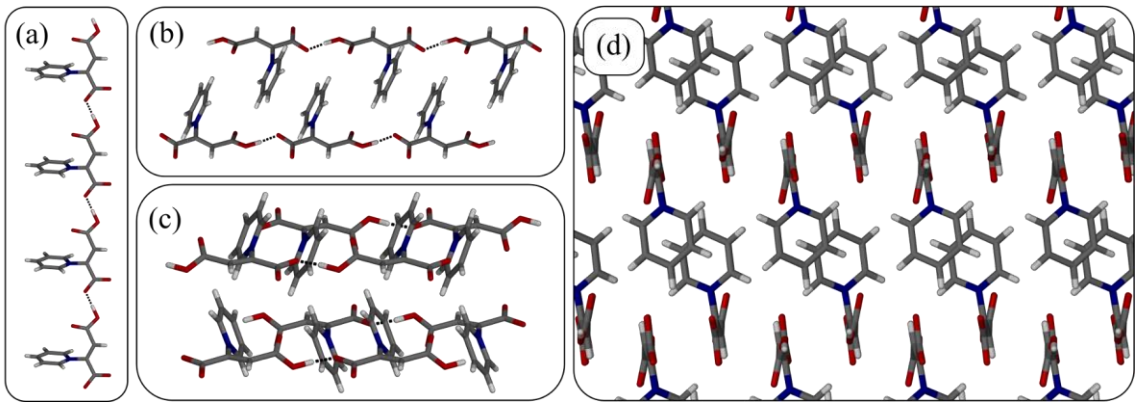

Figure 3.7 (a) Chain of zwitterion **2γ** showing the hydrogen bonding between neighbouring zwitterions. (b) Pair of zwitterion chains, or ladders, of **2γ** viewed down the *c*-axis, and (c) down the *a*-axis. Here two ladders are shown, making it clear that all rings are not parallel (d) Packing diagram of **2γ** viewed down the *b*-axis showing how similar it is to **2β**.

*3.3.2.4 Comparison of **2α**, **2β** and **2γ***

For zwitterion **2** the main difference between the polymorphs is not in the hydrogen bonding, but the conformation of the zwitterion itself. For **1α** and **1β**, the angle between the plane formed by the backbone and by the ring is roughly the same for both polymorphs (97.47(5)° and 96.43(4)°/77.53(4)°). However, this angle differs considerably for the polymorphs of zwitterion **2**. For **2α** this angle is 78.35(5)°, for **2β** the angle is 69.11(4)°, and in **2γ** the planes are separated by 114.7(4)° (Figure 3.8). Furthermore, there is a C–C bond rotation causing a change in the orientation of the carboxylic acid group relative to the backbone (Figure 3.8). This is to ensure that the hydrogen atom is in the correct position to form a hydrogen bond with the carboxylate group of the next zwitterion in the chain.

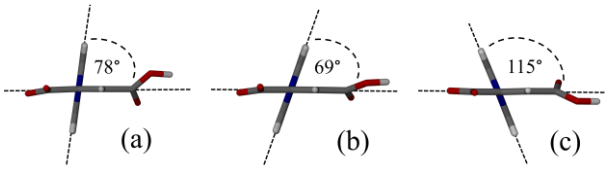

Figure 3.8 The conformational change in the polymorphs of zwitterion **2** can clearly be seen when viewed down the plane of the pyridinium ring. (a) In **2α** the angle between the ring and backbone is 78.35(5)°. (b) In **2β** the angle between the ring and backbone is 69.11(4)°. (c) In **2γ** the angle between the ring and backbone is 114.7(4)°.

For each polymorph there is also a difference in the angle of the pyridinium rings with respect to those of the surrounding zwitterions. In **2α** the pyridinium rings in one zwitterion chain are all parallel to each other, but not parallel to those of the other chain in the same

ladder. In **2β** the pyridinium rings in both chains of the ladder are parallel, in fact, they are parallel through the whole structure. In **2γ** we have an intermediate arrangement where the rings in both chains of the ladder are parallel to each other, but neighbouring ladders are not parallel to one another (Figure 3.9).

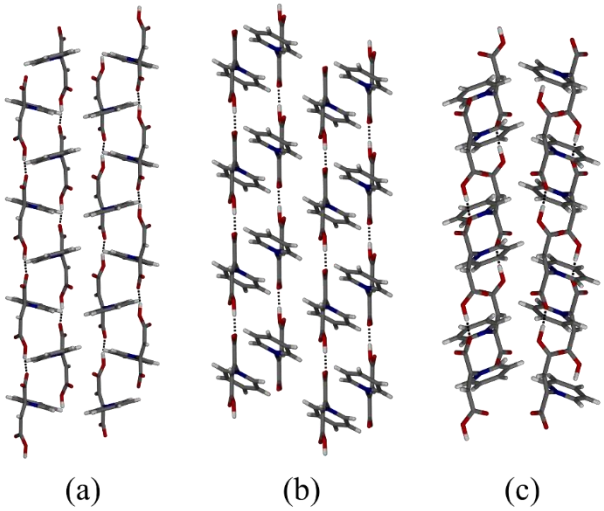

Figure 3.9 Pairs of ladders of (a) **2α** viewed down the *b*-axis, (b) **2β** viewed down the *c*-axis, and (c) **2γ** viewed down the *a*-axis. The difference in the angles of the pyridinium rings with respect to each other can clearly be seen.

3.3.3 Conformational polymorphism

As we know, polymorphism occurs when a compound can arrange itself in more than one way in the solid state. When these solid-state forms have vastly different conformations, they are specifically called conformational polymorphs. In other words, when the torsion angles in a molecule rotate rapidly in solution, conformational polymorphs can be formed if the torsion angle gets 'stuck' in different rotational energy minima in the solid state. On the other hand, if the torsion angles within a molecule do not rotate rapidly in solution, it is possible to simply have different conformational isomers. When these crystallise, they will undoubtedly have different crystal structures, just like different molecules would, and so are not called polymorphs, just different isomers.[6]

In the case of zwitterion **1**, the crystal structures of **1α** and **1β** show different conformations, with the carboxylic acid hydrogen atom either *cis* or *trans* to the pyridyl moiety (Figure 3.3). Therefore, to prove that these are in fact polymorphs (conformational polymorphs) we need to demonstrate free rotation in solution.

To measure the rotational barriers of zwitterion **1** in solution, we investigated the energy of **1** as the carboxylic acid group is rotated about the C–C bond (Figure 3.10).* Two minima are observed that correspond to the crystal structures of the two polymorphs - **1β** being approximately 3 kJ mol^{-1} lower in energy than **1α**.

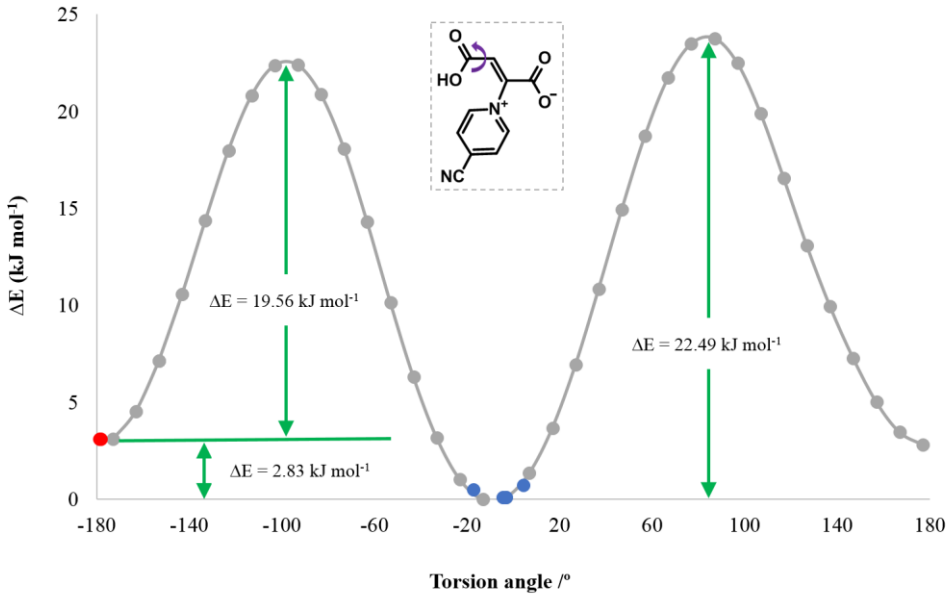

Figure 3.10 Conformational energy diagram indicating how the energy of **1** changes as the carboxylate group is rotated around the O=C−C=C torsion angle (indicated in the inset). The energy of the crystal structures and calculated gas-phase minima of **1α** and **1β** are indicated as red and blue dots respectively.

The rotational barriers between the two minima are calculated as 19.56 and 22.49 kJ mol^{-1} (Figure 3.10). The Eyring equation can be used to calculate the rate constant (k), and therefore the rate of conversion between the minima:

$$k = \frac{k_b T}{h} e^{-\Delta G/RT} \qquad (3.1)$$

Where k_b is the Boltzmann constant, T is the temperature, and h is Planck's constant. The value of k, that is, the rate of conversion between the minima at 25 °C, was found to be of the order of 10^9-10^{10} s^{-1}. This confirms that there is rapid conversion between the conformers in solution, indicating that **1α** and **1β** are in fact conformational polymorphs.

* The conformational scan (excluding data analysis) was carried out by another student, Bernard Dippenaar.

3.3.4 Polymorph stability and interconversion

Several attempts were made to interconvert between the polymorphs of both **1** and **2**. All polymorphic forms were ground (neat and liquid-assisted), allowed to stand in different solvents and out in air, slurried in a variety of solvents, and analysed as the temperature was changed from -20 °C to just before decomposition (and back again). There was no evidence for conversion between forms for either **1** or **2**. The polymorphs do not melt, but merely decompose at high temperatures (between 170 and 200 °C). Visually all five polymorphs seem to dissolve at about the same rate in water, and not at all in other common solvents. TGA shows no mass loss for any of the polymorphs of **1** or **2** and DSC shows no endo- or exotherms. Unlike most polymorphs, it appears that the polymorphs of **1** and **2** do not have a monotropic or enantiotropic relationship, as all seem to be equally stable once formed.

Even though these polymorphs seem equally stable once formed, in the case of zwitterion **1** stability still appears to play a role in determining which polymorph forms. It seems that although the polymorphs can grow under the same conditions, **1β** forms much more slowly – **1α** forms in 1 day, but **1β** needs at least 3 days to crystallise. When a solvent mixture containing water (lower vapour pressure) is used, it evaporates more slowly and **1β** has time to form. This in confirmed by the fact that when crystals of **1α** are removed by filtration, and the filtrate left to continue to crystallise, it yields a mixture of products as **1β** has now had enough time to form. **1α** is thus likely to be the kinetic product and **1β** the thermodynamic product. This corresponds to the energy values obtained from conformational analysis – **1β** is lower in energy than **1α**, and therefore more energetically favourable (Figure 3.10). This also correlates to the densities of the two forms, as mentioned previously, **1β** is more dense than **1α**, a further indication that **1β** is more stable.

No such relationship is observed for the polymorphs of zwitterion **2** and all three forms appear to be equally stable and similar in energy. Each form can be obtained at both high and low temperatures, and the outcome of an experiment only depends on the solvent used for synthesis and crystallisation.

3.3.5 Calculations

The total packing energy of each polymorph (with hydrogen normalization), as well as various intermolecular potentials, was calculated using the UNI intermolecular force field[29,30] in Mercury.[31–34] This force field is only a rough approximation, but can give a good indication of the relative energies, especially when similar molecules are compared.[35] The total packing energy of **1α** and **1β** is -102.7 kJ mol^{-1} and -123.6 kJ mol^{-1} respectively. This corresponds to all previous observations indicating that **1β** is more stable than **1α**.

The centroid-to-centroid distance between neighbouring aromatic rings in **1α** is 5.386(1) Å with the shortest C-C contact being 3.639(3) Å, while in **1β** the centroid-to-centroid distances are 3.943(1) Å and 4.547(2) Å alternating down the ladder, with many shorter C-C interactions than in **1α** (e.g. 3.437(2), 3.465(2), 3.527(2), and 3.553(2) Å). The higher stability of **1β** is therefore possibly as a result of weak offset π-π interactions that are present due to the better alignment of the aromatic rings compared to **1α** (Figure 3.11). **1α** has no π-π interactions as the rings are too far away from each other. Loots *et al.* showed how such π-π stacking has an effect on the packing of similar zwitterions.[24]

The total packing energies for the polymorphs of zwitterion **2** were calculated to be -106.2, -93.7, and -93.5 kJ mol^{-1} for **2α**, **2β**, and **2γ**, respectively.

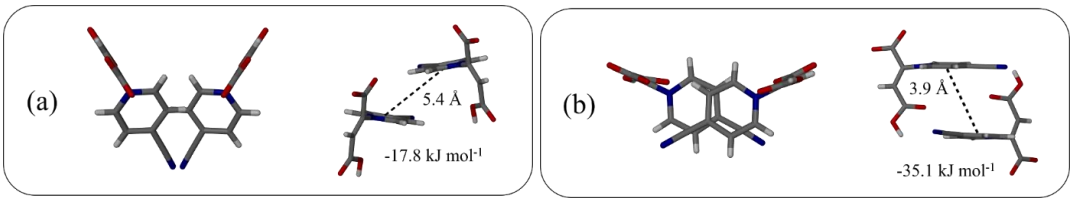

Figure 3.11 The interactions between the aromatic rings in the crystal structures are indicated (as calculated with the UNI force field) as well as the centroid-to-centroid distances. (a) The rings in **1α** hardly overlap, are not parallel to each other, and are too far away for π-π interactions to form. The interaction between these two molecules has a potential energy of -17.8 kJ mol^{-1}. (b) The aromatic rings in **1β** overlap better, are closer together, and are also parallel. The interaction between the two nearest molecules in the ladder has a potential energy of -35.1 kJ mol^{-1}.

Packing energy calculations were followed up by more rigorous lattice energy calculations† using the module CASTEP in Materials Studio.[36] The following formula was used to calculate the lattice energy:

$$E_{latt} = \frac{E_{cryst}}{Z} - \sum_{i}^{n} E_{mol_n} \qquad (3.2)$$

E_{mol} is the single point energy for a single molecule (performed for the *n* crystallographically unique molecules in the asymmetric unit). Z is the number of formula units per unit cell and E_{cryst} is the single point energy calculated for the whole unit cell. The value obtained in this way for **1β** was divided by 2 in order to account for *Z*' = 2. These calculations were carried out in order to determine whether there could be a thermodynamic driving force behind the formation of the polymorphs.

The lattice energy of **1α** is calculated as -281.0 kJ mol^{-1}, while that of **1β** is calculated as -262.83 kJ mol^{-1}. These values differ from all our previous results and indicate that **1α** may be more stable than **1β**. Environmental factors, such as the solvent used, were not taken into account when these calculations were performed, and could lead to the variations in the results.

Lattice energies calculated for **2α**, **2β**, and **2γ** are -273.40 kJ mol^{-1}, -260.49 kJ mol^{-1}, and -286.50 kJ mol^{-1} when CASTEP is used. These values do not vary as much between the different forms, indicating that there is no significant difference between the stabilities of these polymorphs.

3.4 Conclusion

Two groups of polymorphs have been described – their formation seems to be governed by different factors. The polymorphs of **1** seem to exist as a kinetic and thermodynamic pair. **1α** crystallises quickly, but is the less stable conformer with no π-π interactions forming due to inefficient overlap of the aromatic rings. **1β** crystallises more slowly and is the more stable conformer due to better overlap of the aromatic rings and thus additional weak π-π

† Lattice energy calculations were carried out by another student, Thalia Carstens.

interactions. On the other hand, the formation of the three polymorphs of **2** appear to be driven purely by solvent choice, which affects the conformation of the zwitterion.

In the case of zwitterion **1**, the balance of evidence indicates that **1β** is more stable, yet **1α** cannot convert to this more stable form. In the case of zwitterion **2**, the three polymorphs are similar in energy, and so we would also expect interconversion between different forms, however this is not the case. The inability of these polymorphs to interconvert is unusual, but indicates some energetic hurdle that cannot be crossed. In all crystal structures the ladders of zwitterion are very closely interlocked and major shifts in the crystal structure and hydrogen bonding would need to occur if one form were to change to another.

Determining how to control which polymorphic form of a particular molecule is obtained is essential, and this has been successfully achieved for both zwitterions in this study. Likewise, it is important to know how the polymorphs relate to one another and how they can interconvert. Two rare examples of polymorphs that do not interconvert have been presented. This is a potentially useful property for molecules to have – polymorphs can have very different physical and chemical properties and a system in which it is known with certainty that no interconversion will occur could be advantageous.

3.5 Experimental

Further details of the crystallisation conditions, as well as all PXRD, TGA, DSC, and NMR data are available in the Supporting Information.

3.5.1 Synthesis and crystallisation

All chemicals and solvents were obtained from Sigma Aldrich South Africa and used without further purification.

1α [(Z)-3-carboxy-2-(4-cyanopyridin-1-ium-1-yl)-acrylate] was synthesized by stirring acetylenedicarboxylic acid (ADC, 0.020 g, 0.175 mmol) and 4-pyridinecarbonitrile (0.018 g, 0.173 mmol) in a solvent mixture containing methanol (1 ml) and 1,4-dioxane (1 ml) for 10 minutes at 60 °C. Crystallisation *via* slow evaporation at room temperature produced large, colourless crystals after 24 hours.

1β [(Z)-3-carboxy-2-(4-cyanopyridin-1-ium-1-yl)-acrylate] was made by stirring acetylenedicarboxylic acid (ADC, 0.020 g, 0.175 mmol) and 4-pyridinecarbonitrile

(0.018 g, 0.173 mmol) in a solvent mixture containing dimethylformamide (1 ml) and water (1 ml) for 10 minutes at 60 °C. Crystallisation *via* slow evaporation at room temperature produced large, colourless crystals after about 3 days.

2α [(Z)-1-(3-carboxy-1,1-dihydroxyprop-2-en-1-ide-2-yl)-pyridin-1-ium] was made by stirring acetylenedicarboxylic acid (ADC, 0.020 g, 0.175 mmol) and pyridine (0.014 g, 0.172 mmol) in 2 ml methanol for 5 minutes at 60 °C (the addition of 2 ml ethanol or water can used to speed up product formation). Crystallisation *via* slow evaporation at room temperature produced colourless, block-like crystals after 24 hours.

2β [(Z)-1-(3-carboxy-1,1-dihydroxyprop-2-en-1-ide-2-yl)-pyridin-1-ium] was made by stirring acetylenedicarboxylic acid (ADC, 0.020 g, 0.175 mmol) and pyridine (0.014 g, 0.172 mmol) in a solvent mixture containing methanol (2 ml) and dimethyl formamide (2 ml) for 5 minutes at 60 °C. Crystallisation *via* slow evaporation at room temperature produced colourless, block-like crystals after 24 hours.

2γ [(Z)-1-(3-carboxy-1,1-dihydroxyprop-2-en-1-ide-2-yl)-pyridin-1-ium] was made by stirring acetylenedicarboxylic acid (ADC, 0.020 g, 0.175 mmol) and pyridine (0.014 g, 0.172 mmol) in a solvent mixture containing THF (2 ml) and water (1 ml) for 10 minutes at 60 °C. Crystallisation *via* slow evaporation at room temperature produced colourless, plate-like crystals after 3 days.

The salt, **3**, was made by combining acetylenedicarboxylic acid (ADC, 0.020 g, 0.175 mmol) with pyridine (0.014 g, 0.172) and grinding them together in a mortar and pestle for 10 minutes. **2α** was also obtained when the salt **3** was dissolved in methanol. δ_H (300 MHz, D_2O) 8.07 (2H, J = 7.0 Hz, t), 8.62 (1H, J = 7.9 Hz, 1.4 Hz, tt), 8.78 (2H, m). δ_C (300 MHz, D_2O) 73.44, 125.18, 138.80, 144.96, 155.17.

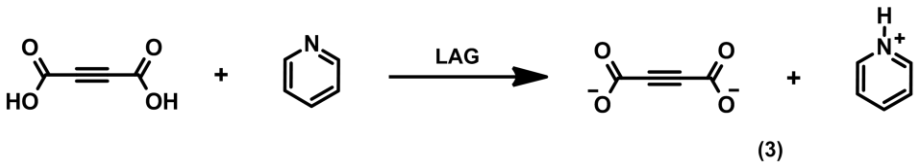

(3)

Scheme 3.2 General reaction scheme for the preparation of salt **3** from acetylenedicarboxylic acid and pyridine.

3.5.2 Calculations

Structures were optimized starting from the crystal structure geometries using B3LYP/6-311++G(d,p) in Gaussian 09 Rev E01.[37] Further frequency calculations confirmed that a minimum energy conformation was obtained. The potential energy scan was performed by the addition of two dummy atoms in order to rotate the relevant torsion angle in increments of 10°. Single-point energies were calculated at each increment at the B3LYP/6-311++G(d,p) level of theory.

Lattice energy calculations were carried out using the module CASTEP in Materials Studio using GGA-PBE with GD2 dispersion correction.[36]

3.6 Acknowledgements

We would like to thank the Wilhelm Frank Scholarship Fund, the National Research Foundation of South Africa and Stellenbosch University for funding. The use of NMR instruments managed by the Central Analytical Facility at the University of Stellenbosch is also acknowledged. We thank Thalia Carstens and A. Bernard Dippenaar for assistance with calculations, and Catharine Esterhuysen for helpful discussions.

3.7 Associated content

Details on synthetic procedures, all solvents/solvent combinations used, and instrumental characterization and analysis for all compounds (PXRD, TGA, DSC, NMR), as well as X-ray crystallographic files in CIF format are available. This material is available free of charge *via* the Internet at http://pubs.acs.org. CCDC 1572494-1572498 contain the supplementary crystallographic data for this paper. These data can be obtained free of charge from The Cambridge Crystallographic Data Centre *via* www.ccdc.cam.ac.uk/data_request/cif.

3.8 References

1 E. Mitscherlich, *Ann. Chim. Phys.*, 1822, **19**, 350–419.

2 W. C. McCrone, in *Physics and chemistry of the organic solid state*, eds. D. Fox, M. M. Labes and A. Weissberger, Wiley Interscience, New York, USA, 1965, pp. 725–767.

3 S. A. Bourne, *Supramolecular Isomerism*, John Wiley & Sons, Ltd, Chichester, UK, 2012.

4 B. Moulton and M. J. Zaworotko, *Chem. Rev.*, 2001, **101**, 1629–1658.

5 J. Elguero, *Cryst. Growth Des.*, 2011, **11**, 4731–4738.

6 A. J. Cruz-Cabeza and J. Bernstein, *Chem. Rev.*, 2014, **114**, 2170–2191.

7 H. Reinke, H. Dehne and M. Hans, *J. Chem. Educ.*, 1993, **70**, 101–103.

8 M. J. Buerger, *Trans. Am. Crystallogr. Assoc.*, 1971, **7**, 1–23.

9 A. Nangia and G. R. Desiraju, *Chem. Commun.*, 1999, **7**, 605–606.

10 J. Bernstein, Ed., *Polymorphism in molecular crystals*, Oxford: Clarendon Press, New York, 2002.

11 S. Aitipamula and A. Nangia, in *Supramolecular Chemistry: From Molecules to Nanomaterials, Volume 6*, John Wiley & Sons, Ltd, Chichester, UK, 2012, pp. 2957–2974.

12 A. J. Cruz-Cabeza, S. M. Reutzel-Edens and J. Bernstein, *Chem. Soc. Rev.*, 2015, **44**, 8619–8635.

13 S. Aitipamula, P. S. Chow and R. B. H. Tan, *CrystEngComm*, 2014, **16**, 3451–3465.

14 T. L. Threlfall, *Analyst*, 1995, **120**, 2435–2460.

15 J. Haleblian and W. McCrone, *J. Pharm. Sci.*, 1969, **58**, 911–912.

16 R. H. Barbour, A. A. Freer and D. D. MacNicol, *J. Chem. Soc. Chem. Commun.*, 1983, 362–363.

17 T. Nakashima, R. Fujii and T. Kawai, *Chem. - A Eur. J.*, 2011, **17**, 10951–10957.

18 J. Boeckmann, N. Evers and C. Näther, *CrystEngComm*, 2012, **14**, 1094–1104.

19 A. V Trask, N. Shan, W. D. S. Motherwell, W. Jones, S. Feng, R. B. H. Tan and K. J. Carpenter, *Chem. Commun.*, 2005, **7**, 880–2.

20 M. Mathlouthi, G. Benmessaoud and B. Rogé, *Food Chem.*, 2012, **132**, 1630–1637.

21 Y. Noishiki, H. Takami, Y. Nishiyama, M. Wada, S. Okada and S. Kuga,

Biomacromolecules, 2003, **4**, 896–899.

22 Y. Abe, S. Karasawa and N. Koga, *Chem. - A Eur. J.*, 2012, **18**, 15038–15048.

23 L. A. Stevens, K. P. Goetz, A. Fonari, Y. Shu, R. M. Williamson, J.-L. Brédas, V. Coropceanu, O. D. Jurchescu and G. E. Collis, *Chem. Mater.*, 2015, **27**, 112–118.

24 L. Loots, D. A. Haynes and T. le Roex, *New J. Chem.*, 2014, **38**, 2778–2786.

25 L. Loots, J. P. O'Connor, T. le Roex and D. A. Haynes, *Cryst. Growth Des.*, 2015, **15**, 5849–5857.

26 J. Lombard, L. Loots, D. A. Haynes and T. le Roex, *Manuscript in preparation*, 2017.

27 S. Lohani and J. D. W. Grant, in *Polymorphism in the pharmaceutical industry*, ed. R. Hilfiker, Wiley-VCH Verlag GmbH & Co., Weinheim, Germany, 2006, pp. 21–42.

28 A. Kitaigorodskii, *Molecular crystals and molecules*, Academic Press, Inc., New York, 1973.

29 A. Gavezzotti and G. Filippini, *J. Phys. Chem.*, 1994, **98**, 4831–4837.

30 A. Gavezzotti, *Acc. Chem. Res*, 1994, **27**, 309–314.

31 C. F. Macrae, I. J. Bruno, J. A. Chisholm, P. R. Edgington, P. McCabe, E. Pidcock, L. Rodriguez-Monge, R. Taylor, J. van de Streek and P. A. Wood, *J. Appl. Crystallogr.*, 2008, **41**, 466–470.

32 C. F. Macrae, P. R. Edgington, P. McCabe, E. Pidcock, G. P. Shields, R. Taylor, M. Towler and J. van de Streek, *J. Appl. Crystallogr.*, 2006, **39**, 453–457.

33 I. J. Bruno, J. C. Cole, P. R. Edgington, M. Kessler, C. F. Macrae, P. McCabe, J. Pearson and R. Taylor, *Acta Crystallogr. Sect. B Struct. Sci.*, 2002, **B58**, 389–397.

34 R. Taylor and C. F. Macrae, *Acta Crystallogr. Sect. B Struct. Sci.*, 2001, **B57**, 815–827.

35 A. Gavezzotti, *Zeitschrift für Krist.*, 2005, **220**, 499–510.

36 *Dassault Systèmes BIOVIA*, BIOVIA Materials Studio, Release 2017, San Diego: Dassault Systèmes, 2017.

37 Gaussian 09, Revision E.01, Frisch, M. J.; Trucks, G. W.; Schlegel, H. B.; Scuseria, G. E.; Robb, M. A.; Cheeseman, J. R.; Scalmani, G.; Barone, V.; Mennucci, B.; Petersson, G. A.; Nakatsuji, H.; Caricato, M.; Li, X.; Hratchian, H. P.; Izmaylov, A. F.; Bloino, J.; Zheng, G.; Sonnenberg, J. L.; Hada, M.; Ehara, M.; Toyota, K.; Fukuda, R.; Hasegawa, J.; Ishida, M.; Nakajima, T.; Honda, Y.; Kitao, O.; Nakai, H.; Vreven, T.; Montgomery, J. A., Jr.; Peralta, J. E.; Ogliaro, F.; Bearpark, M.; Heyd, J. J.; Brothers, E.; Kudin, K. N.; Staroverov, V. N.; Kobayashi, R.; Normand, J.; Raghavachari, K.; Rendell, A.; Burant, J. C.; Iyengar, S. S.; Tomasi, J.; Cossi, M.; Rega, N.; Millam, J. M.; Klene, M.; Knox, J. E.; Cross, J. B.; Bakken, V.; Adamo, C.; Jaramillo, J.; Gomperts, R.; Stratmann, R. E.; Yazyev, O.; Austin, A. J.; Cammi, R.; Pomelli, C.; Ochterski, J. W.; Martin, R. L.; Morokuma, K.; Zakrzewski, V. G.; Voth, G. A.; Salvador, P.; Dannenberg, J. J.; Dapprich, S.; Daniels, A. D.; Farkas, Ö.; Foresman, J. B.; Ortiz, J. V.; Cioslowski, J.; Fox, D. J. Gaussian, Inc., Wallingford CT, 2009.

3.9 Supplementary information

Synthesis and crystallisation

All chemicals and solvents were obtained from Sigma Aldrich South Africa and used without further purification.

1α [(Z)-3-carboxy-2-(4-cyanopyridin-1-ium-1-yl)-acrylate] was synthesized by stirring acetylenedicarboxylic acid (ADC, 0.020 g, 0.175 mmol) and 4-pyridinecarbonitrile (0.018 g, 0.173 mmol) in a solvent mixture containing methanol (1 ml) and 1,4-dioxane (1 ml) for 10 minutes at 60 °C. Crystallisation *via* slow evaporation at room temperature produced large, colourless crystals after 24 hours. Other solvent(s) used are summarised in Table S1.

1β [(Z)-3-carboxy-2-(4-cyanopyridin-1-ium-1-yl)-acrylate] was made by stirring acetylenedicarboxylic acid (ADC, 0.020 g, 0.175 mmol) and 4-pyridinecarbonitrile (0.018 g, 0.173 mmol) in a solvent mixture containing dimethylformamide (1 ml) and water (1 ml) for 10 minutes at 60 °C. Crystallisation *via* slow evaporation at room temperature produced large, colourless crystals after about 3 days. Other solvent(s) used are summarised in Table S1.

Using lower reaction temperatures (room temperature instead of 60 °C) or shorter stirring times produced a mixture of polymorphs. When crystals of **1α** were filtered and the filtrate left to allow further crystallisation, a mixture of polymorphs was isolated.

Table S1 Summary of solvents and solvent mixtures used in the crystallisation of **1**, grouped according to the product. Reported ratios are volume ratios.

1α	**1α**	**1β**
MeOH	EtOH	H_2O
MeOH/MeCN (1:1)	EtOH/DMF (1:1)	H_2O/MeOH (1:1)
MeOH/THF (1:1)	EtOH/MeCN (1:1)	H_2O/Cyclohexane (1:1)
MeOH/DMF (1:1)	EtOH/THF (1:1)	H_2O/EtOH (1:1)
MeOH/DMSO (1:1)	EtOH/DMSO (1:1)	H_2O/THF (1:1)
MeOH/Acetone (1:1)	EtOH/Acetone (1 :1)	H_2O/DMF (1:1)
MeOH/DCM (1:1)	EtOH/DCM (1:1)	H_2O/Toluene (1:1)
MeOH/$CHCl_3$ (1:1)	EtOH/$CHCl_3$ (1:1)	H_2O/EtherH_2O (1:1)
MeOH/EtOAc (1:1)	EtOH/EtOAc (1:1)	H_2O/Benzene (1:1)
MeOH/Et_2O (1:1)	EtOH/Et_2O (1:1)	H_2O/Acetone (5:1)
MeOH/Benzene (1:1)	EtOH/Benzene (1:1)	H_2O/DMSO (2:1)
MeOH/Cyclohexane (1:1)	EtOH/Cyclohexane (1:1)	H_2O/$CHCl_3$ (5:1)
MeOH/Toluene (1:1)	EtOH/Toluene (1:1)	H_2O/DCM (5:1)
MeOH/EtOH (1:1)		H_2O/Dioxane (5:1)
MeOH/Dioxane (1:1)		

2α [(Z)-1-(3-carboxy-1,1-dihydroxyprop-2-en-1-ide-2-yl)-pyridin-1-ium] was made by stirring acetylenedicarboxylic acid (ADC, 0.020 g, 0.175 mmol) and pyridine (0.014 g, 0.172 mmol) in 2 ml methanol for 5 minutes at 60 °C (the addition of 2 ml ethanol or water could be used to speed up product formation). Crystallisation *via* slow evaporation at room temperature produced colourless crystal blocks after 24 hours. Other solvent(s) used are summarised in Table S2.

2β [(Z)-1-(3-carboxy-1,1-dihydroxyprop-2-en-1-ide-2-yl)-pyridin-1-ium] was made by stirring acetylenedicarboxylic acid (ADC, 0.020 g, 0.175 mmol) and pyridine (0.014 g, 0.172 mmol) in a solvent mixture containing methanol (2 ml) and dimethyl formamide (2 ml) for 5 minutes at 60 °C. Crystallisation *via* slow evaporation at room temperature

produced colourless crystal blocks after 24 hours. Other solvent(s) used are summarised in Table S2.

2γ [(Z)-1-(3-carboxy-1,1-dihydroxyprop-2-en-1-ide-2-yl)-pyridin-1-ium] was made by stirring acetylenedicarboxylic acid (ADC, 0.020 g, 0.175 mmol) and pyridine (0.014 g, 0.172 mmol) in a solvent mixture containing THF (2 ml) and water (1 ml) for 10 minutes at 60 °C. Crystallisation *via* slow evaporation at room temperature produced colourless crystal plates after 3 days. Other solvent(s) used are summarised in Table S2.

The salt, **3**, was made by combining acetylenedicarboxylic acid (ADC, 0.020 g, 0.175 mmol) with pyridine (0.014 g, 0.172) and grinding them together in a mortar and pestle for 10 minutes. **2α** was also obtained when the salt **3** was dissolved in methanol. δ_H (300 MHz, D_2O) 8.07 (2H, J = 7.0 Hz, t), 8.62 (1H, J = 7.9 Hz, 1.4 Hz, tt), 8.78 (2H, m). δ_C (300 MHz, D_2O) 73.44, 125.18, 138.80, 144.96, 155.17.

Table S2 Summary of solvents and solvent mixtures used in the crystallisation of **2**, grouped according to the product formed. Reported ratios are volume ratios.

2α		**2β**	
MeOH	MeOH & Acetone (2:1)	DMF	DMF & DCM (2:3)
MeOH & H_2O (2:1)	MeOH & Dioxane (2:1)	DMF & EtOAc (2:1)	DMF & EtOH (1:2)
MeOH & EtOH (1:1)	MeOH & Cyclohex. (3:1)	DMF & MeOH (1:1)	
MeOH & Benzene (1:1)	MeOH & EtOAc (1:1)		
MeOH & THF (2:1)	H_2O & Acetone (1:4)	**2γ**	
MeOH & Toluene (2:1)	H_2O & Dioxane (1:4)	H_2O & THF (1:2)	
MeOH & DCM (2:1)			
Mixture of 2β and 2γ		**Mixture of 2α and 2β**	
H_2O & EtOH		DMF & Acetone (1:2)	MeOH & MeCN (1:1)
		DMF & Dioxane (1:1)	EtOH & H_2O (2:1)

Powder X-Ray diffraction patterns

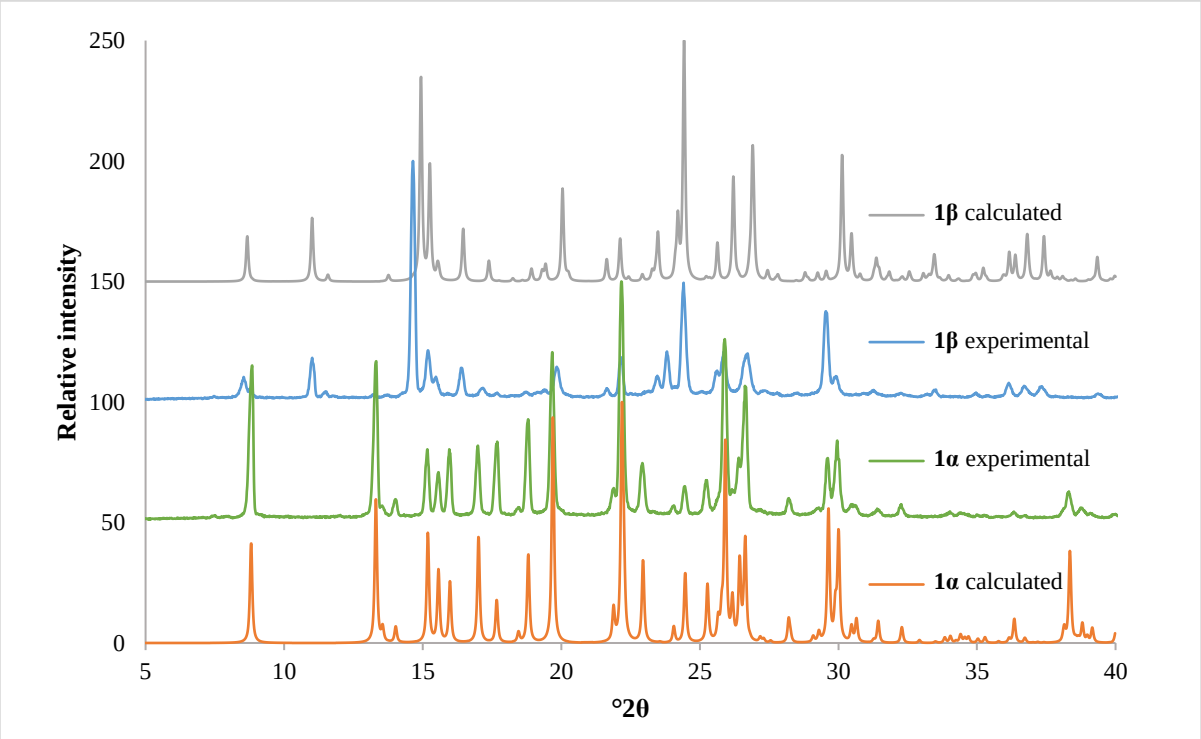

Figure S1 Comparison of the experimental and calculated powder patterns of the two polymorphs of **1**. The slight shift in angle between the calculated and experimental patterns is due to the difference in temperature (powder pattern at room temperature; crystal structure at 100 K).

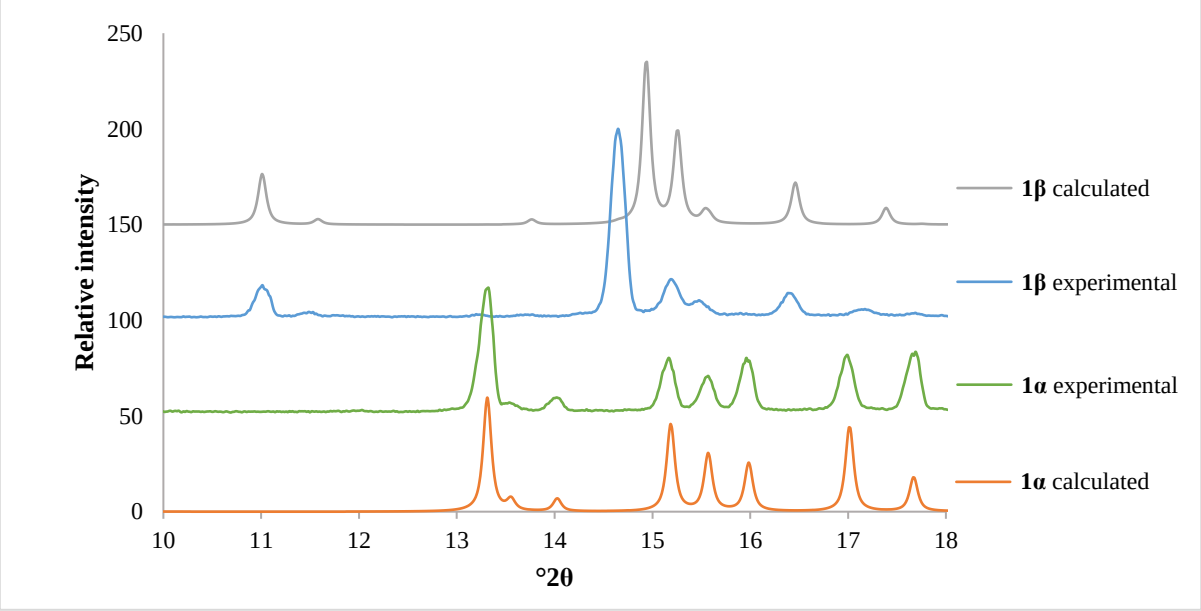

Figure S2 Comparison of the truncated experimental and calculated powder patterns of the two polymorphs of **1**, zoomed in to clearly show the region where they differ most notably.

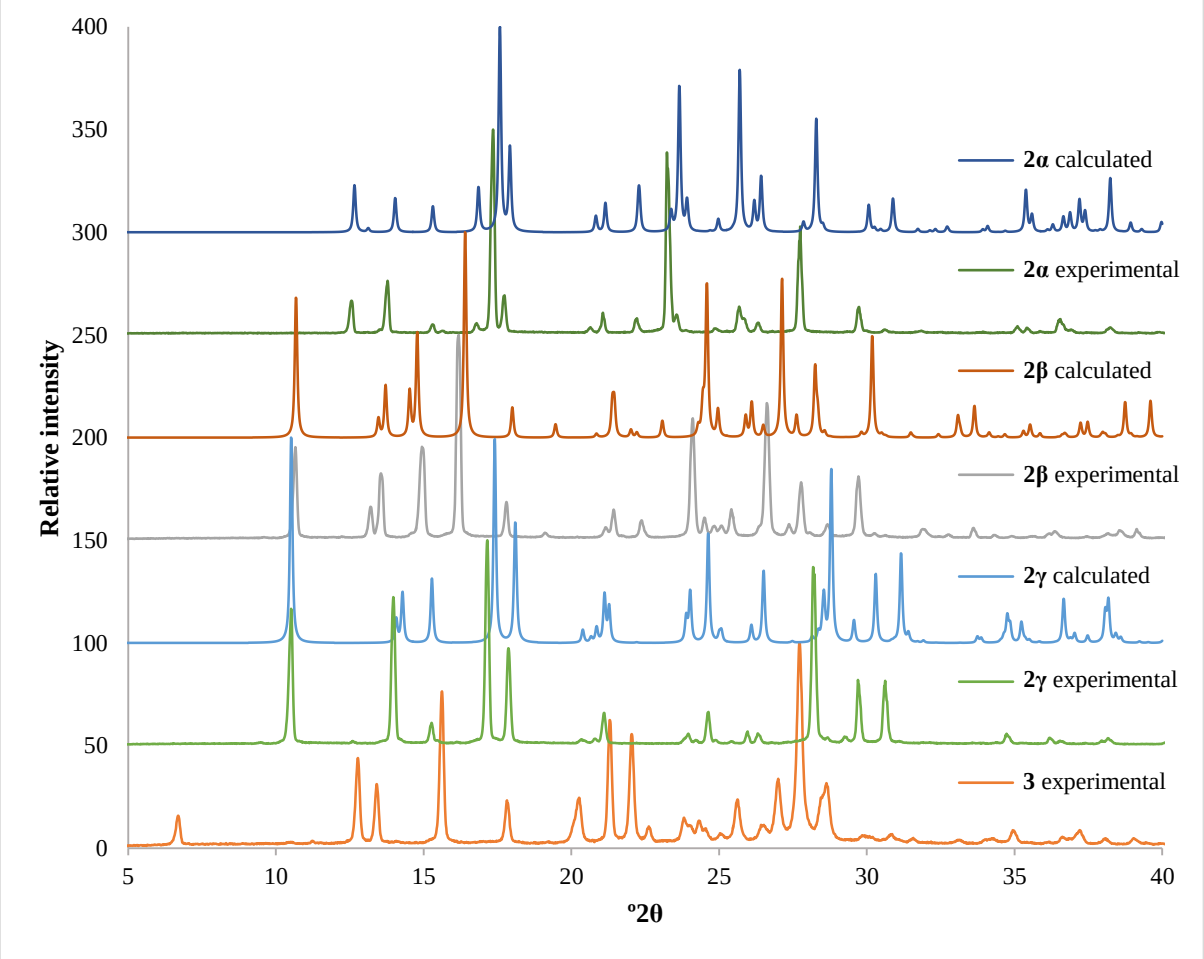

Figure S3 Comparison of the experimental and calculated powder patterns of the three polymorphs of **2**. The slight shift in angle between the calculated and experimental patterns is due to the difference in temperature (powder pattern at room temperature; crystal structure at 100 K). The experimental powder pattern of what is thought to be the salt **3** is also shown.

Thermal analysis (TGA and DSC)

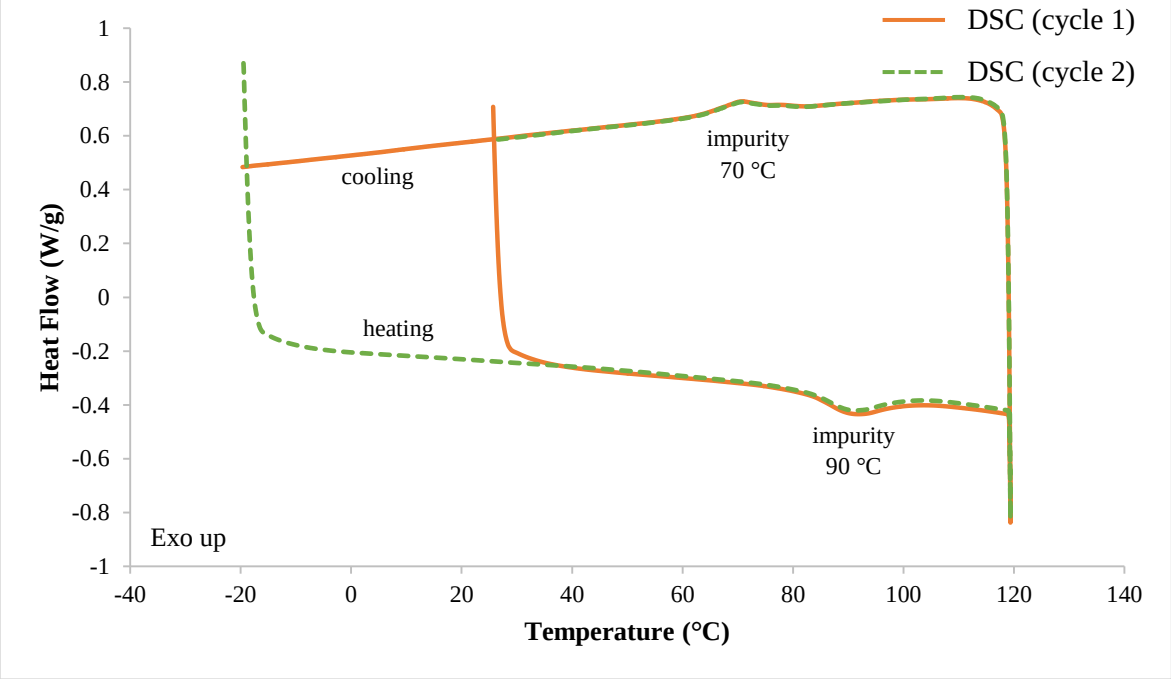

Figure S4 DSC trace for the starting material ADC used as an example. An impurity in the instrument resulted in a small endotherm during heating (90 °C) and a small exotherm on cooling (70 °C). This impurity can be seen in some of the following DSC curves and can be ignored (the higher the mass of the sample tested, the smaller the impurity peaks).

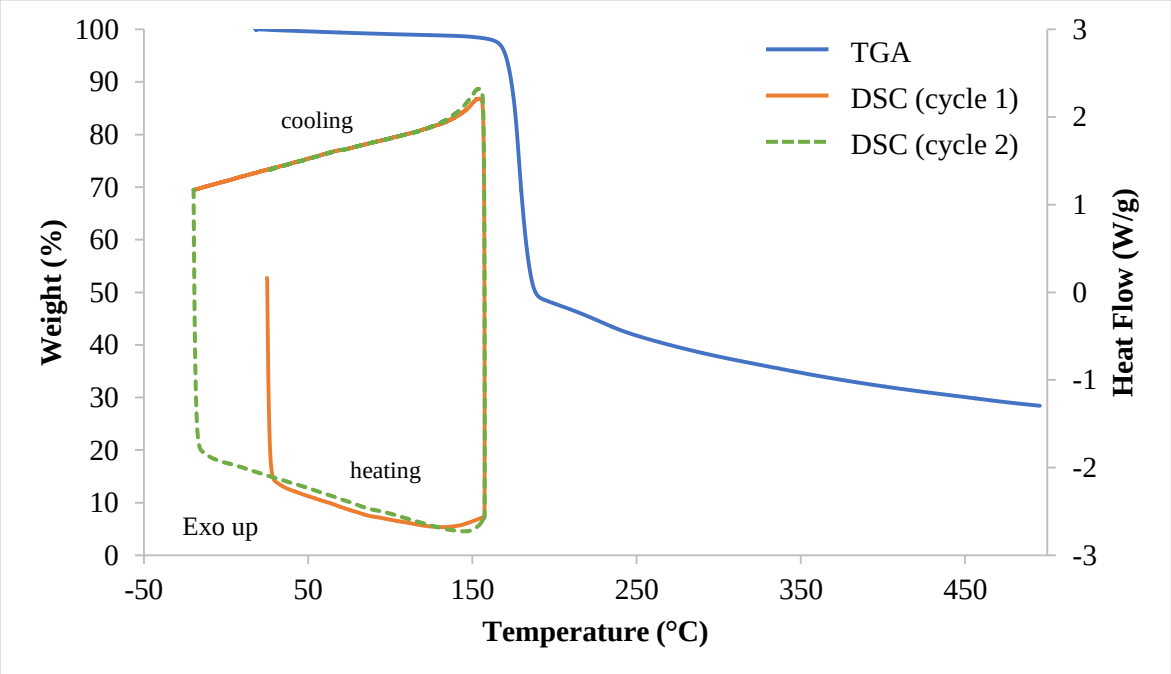

Figure S5 Thermal analysis results for **1α**. TGA trace shown in blue and DSC trace in orange (cycle 1) and green dashes (cycle 2).

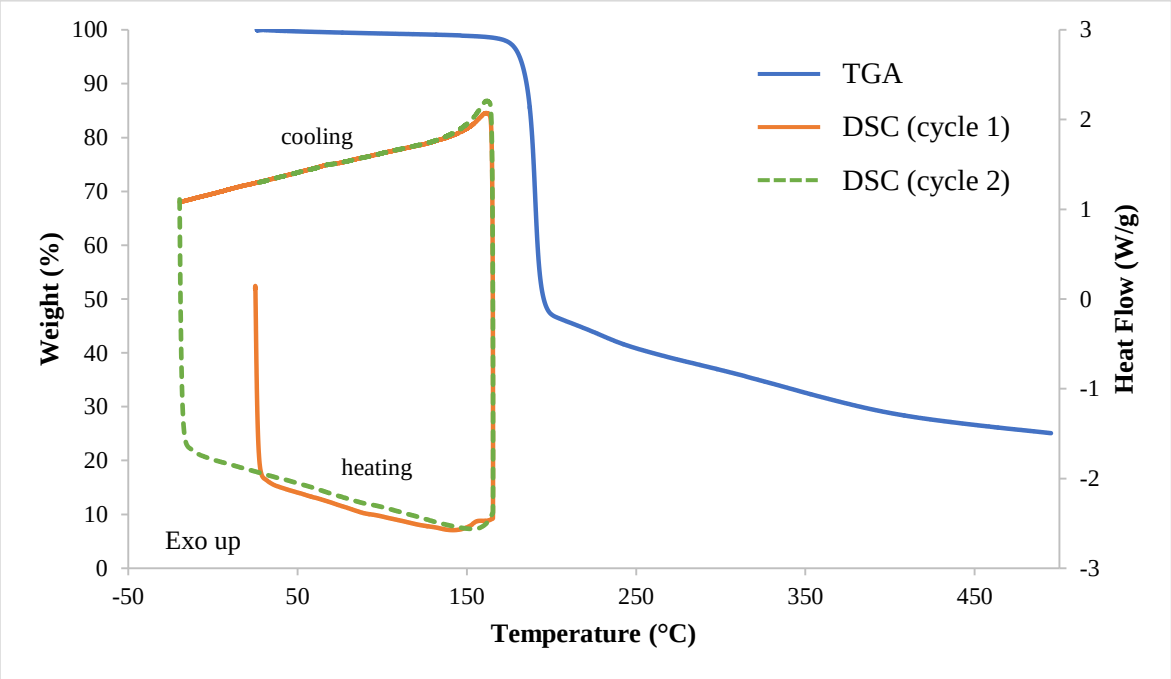

Figure S6 Thermal analysis results for **1β**. TGA trace shown in blue and DSC trace in orange (cycle 1) and green dashes (cycle 2).

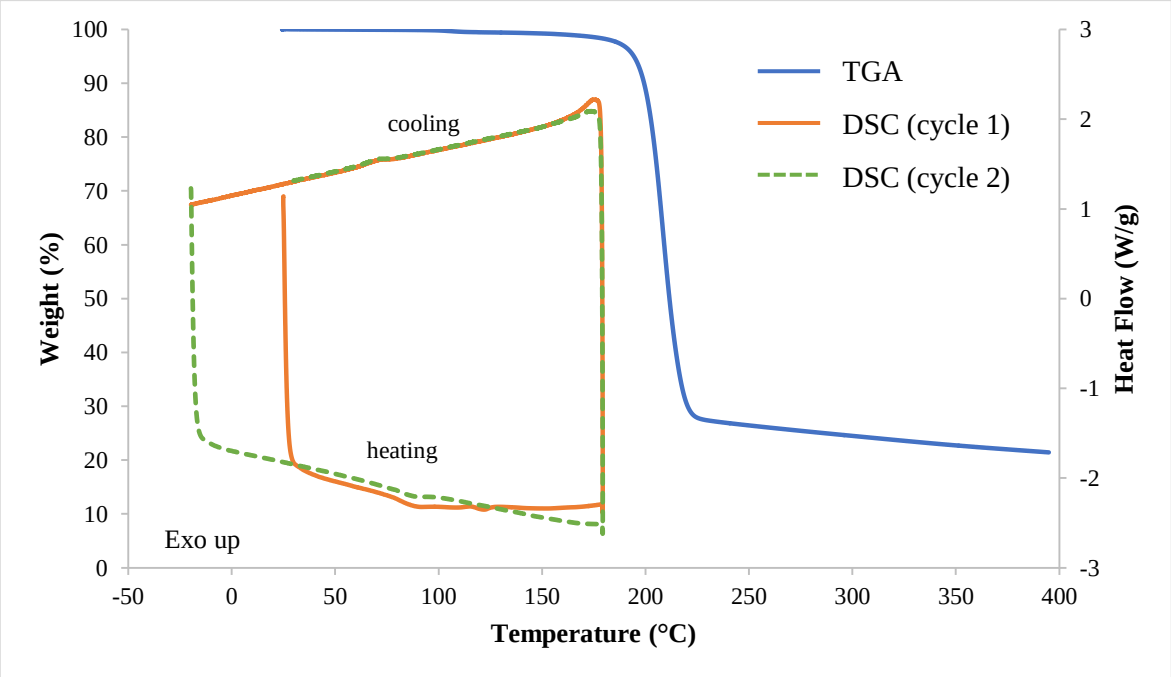

Figure S7 Thermal analysis results for **2α**. TGA trace shown in blue and DSC trace in orange (cycle 1) and green dashes (cycle 2). The small exo- and endotherms in the DSC are due to an impurity present in the instrument.

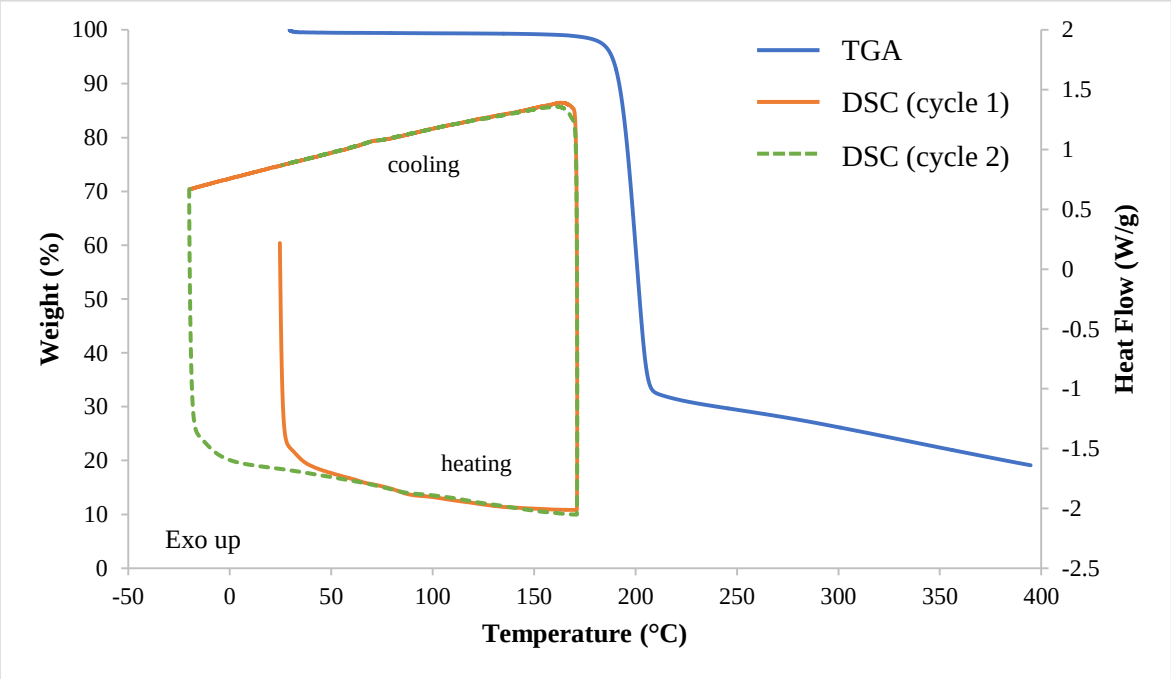

Figure S8 Thermal analysis results for **2β**. TGA trace shown in blue and DSC trace in orange (cycle 1) and green dashes (cycle 2).

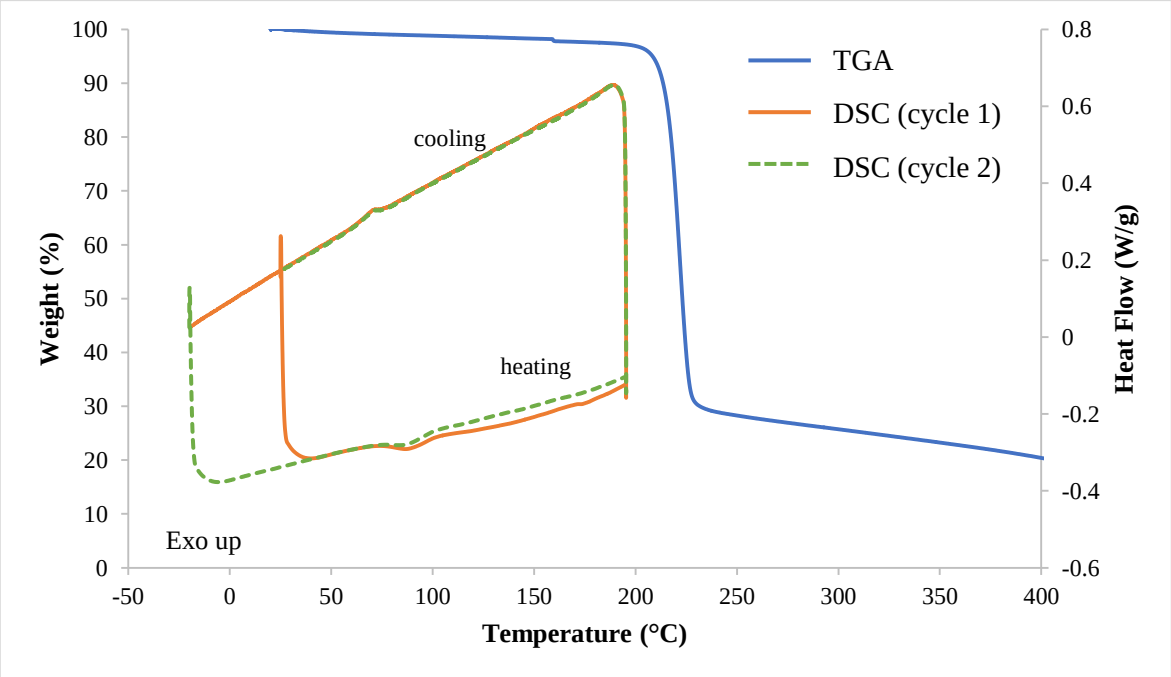

Figure S9 Thermal analysis results for **2γ**. TGA trace shown in blue and DSC trace in orange (cycle 1) and green dashes (cycle 2). The small exo- and endotherms in the DSC are due to an impurity present in the instrument.

NMR

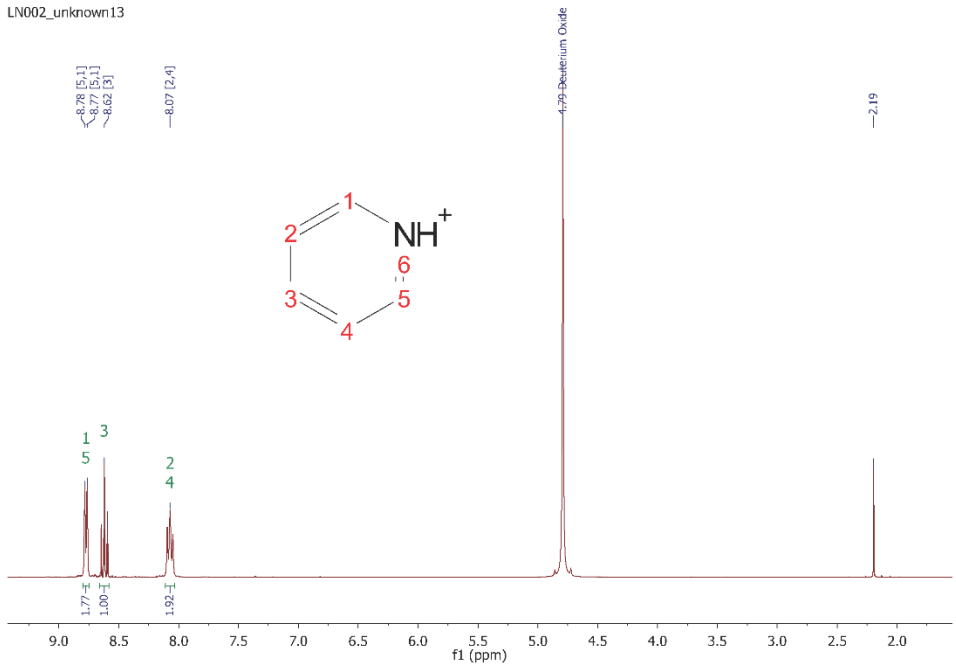

Figure S10 ^{1}H NMR (300MHz) of **3** showing the proton signals for pyridinium (The ADC dianion does not contain any protons).

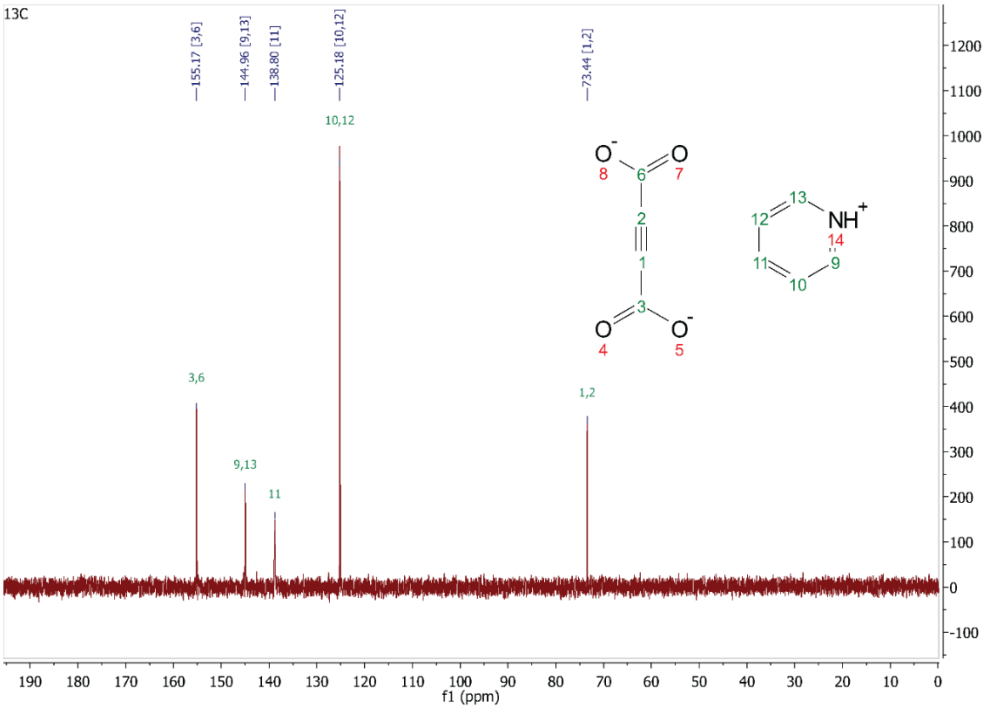

Figure S11 ^{13}C NMR (300MHz) showing the peaks corresponding to the carbon atoms in ADC and pyridinium.

CHAPTER 4

NICOTINAMIDE- AND ISONICOTINAMIDE-DERIVED ZWITTERIONS AND THEIR SALTS

This chapter is presented as a draft of a paper that is about to be submitted to CrystEngComm. All the experimental work in this chapter was carried out by myself. The draft included here was written by me.

4.1 Abstract

The reaction between acetylenedicarboxylic acid and nicotinamide or isonicotinamide produces two new zwitterionic molecules, namely (Z)-2-(3-carbamoylpyridin-1-ium-1-yl)-3-carboxyacrylate (**1**) and (Z)-3-carboxy-2-(4-carboxypyridin-1-ium-1-yl)acrylate (**2**), as well as a salt by-product, **2a**. The solid-state behaviour of the zwitterions has been investigated by altering variables such as the solvent(s) used, and the temperature at which synthesis and crystallisation occurs. These zwitterions, as well as a previously reported zwitterion, (Z)-3-carboxy-2-(4-cyanopyridin-1-ium-1-yl)-acrylate (**3**), were subsequently combined with various small organic co-formers in an attempt to form multi-component crystals *via* mechanochemical or solution methods. Three new hydrated salts were formed with melamine (**1-Melamine**, **2-Melamine**, and **3-Melamine**), all of which display charge-assisted hydrogen bonding (CAHB). Zwitterions **1** and **2** also form characteristic $R_2^2(8)$ hydrogen-bonded units between the amide group and melamine. Based on these observed trends in hydrogen bonding, further crystallisation experiments were attempted with molecules similar to melamine. Although single crystals were not obtained, six potential salts have been identified based on NMR and IR data. Compared to the number of co-formers used, the discovery of only three salts per zwitterion is unusual – a search of the Cambridge Structural Database (CSD) indicates that this may be due to the high propensity of the CAHBs between the zwitterions in the solid state.

4.2 Introduction

Multi-component crystals, in which two or more different molecules are included in one crystalline material,[1] are increasingly being studied by solid-state chemists as they are of interest in many areas, including the development of new materials and the pharmaceutical industry. Their formation is often linked to a change in physicochemical properties,[2] such as solubility,[3,4] stability,[5] tabletability,[6] and many others linked to the practical application of solids. Multi-component crystals include co-crystals, salts, and solvates, but many other intermediary categories have also been suggested, such as salt solvates, co-crystal salts, co-crystal solvates, and co-crystal salt solvates.[7] These terms are still under dispute, especially the term co-crystal – with respect to its necessity, specificity, elegance, and even spelling.[7–9] While confusion can be avoided by simply calling them multi-component systems, more specific terms do aid in accurately describing a material. For this reason, we will continue with the following simple, but important, definitions: co-crystals form when two or more neutral molecules are combined into one crystalline material. When there is a proton transfer between these components, they are called salts. In addition, when one of the components played the role of the solvent in the reaction, the product is called a solvate.

Multi-component crystals are usually formed after some thought is put into the possible intermolecular interactions that molecules could have with each other,[10] be it hydrogen bonds, π-π stacking, halogen bonds, van der Waals interactions, etc. Therefore, it is imperative to understand trends in intermolecular interactions if we want to be able to design useful salts, co-crystals and solvates.

The synthesis and structures of a series of pyridyl-derived zwitterions were recently reported by our group,[11] and some of these zwitterions have been found to show interesting inclusion abilities,[12] conversions[13] and polymorphic behaviour.[13] Based on this, two new zwitterions (with the potential to form multi-component crystals) have been synthesised in the same way. Zwitterions are neutral molecules that contain positive and negative charges – giving them the added benefit of not only hydrogen bonding, but also a higher probability of forming even stronger charge-assisted hydrogen bonds (CAHBs).[14] The zwitterions used in this study consist of a dicarboxylic acid backbone with pyridinium or a pyridinium derivative branching out to give them their characteristic T-shape. This characteristic molecular shape, together with their hydrogen-bonding capability, makes them potentially useful supramolecular building blocks.

In this study we have investigated two new zwitterions (Scheme 4.1), namely (Z)-2-(3-carbamoylpyridin-1-ium-1-yl)-3-carboxyacrylate (**1**) and (Z)-3-carboxy-2-(4-carboxy-pyridin-1-ium-1-yl)-acrylate (**2**). These zwitterions were specifically chosen as they have an extra hydrogen bond donor/acceptor group attached to the pyridinium ring in the form of an amide functional group. As the amide-amide interaction is a known synthon,[15] the idea was that this extra "sticky end" perpendicular to the carboxylic acid groups would allow the supramolecular structure to propagate in more dimensions, through additional intermolecular interactions, stabilising the structure and potentially resulting in interesting properties.

Here we describe the solid-state structures of these two zwitterions on their own, as well as structures obtained when the zwitterions were combined with other small organic molecules (Scheme 4.1). A zwitterion that was reported previously by our group[13] shows similar behaviour when combined with these co-formers – although the zwitterion will not be discussed here, its ability to form salts will. The structures are compared to gain insight into the trends in hydrogen bonding and to establish the potential use of these zwitterions in forming further solid-state supramolecular structures.

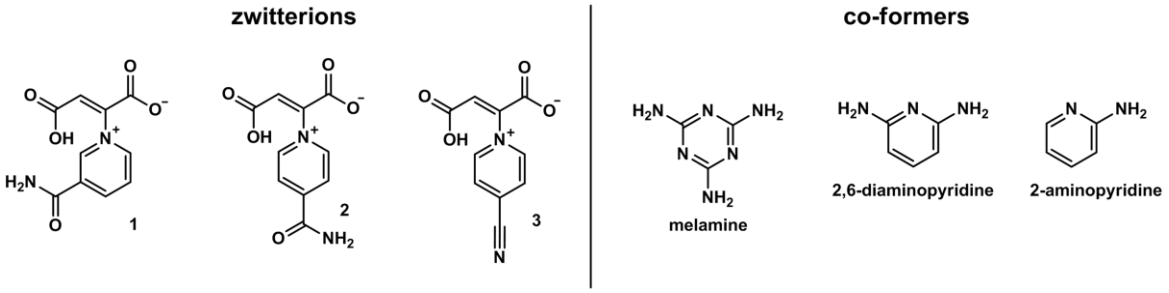

Scheme 4.1 Structures of the three zwitterions discussed in this paper, as well as the three co-formers that were successfully combined with each zwitterion.

4.3 Results and discussion

4.3.1 Synthesis and crystallisation

The zwitterions were synthesised in a straightforward manner: the combination of acetylenedicarboxylic acid (ADC) and the pyridine derivative (nicotinamide/ isonicotinamide) in a particular solvent or solvent system, with mild heating and stirring for a few minutes, yields reasonably sized, colourless crystals after 24 hours (Scheme 4.2). In

the case of the isonicotinamide zwitterion, a salt of the same starting materials can be formed using the same method, but a different solvent combination. Unlike the zwitterions, this salt, **2a**, can also be formed mechanochemically with the addition of a few drops of tetrahydrofuran. To investigate the formation of polymorphs or solvates, various solvent mixtures were used during synthesis of the zwitterions, and crystallisation temperature and reagent ratios were also varied. Combinations of methanol, ethanol, water, dimethylformamide and dimethyl sulfoxide with each other, as well as with 11 other common laboratory solvents, were utilised.

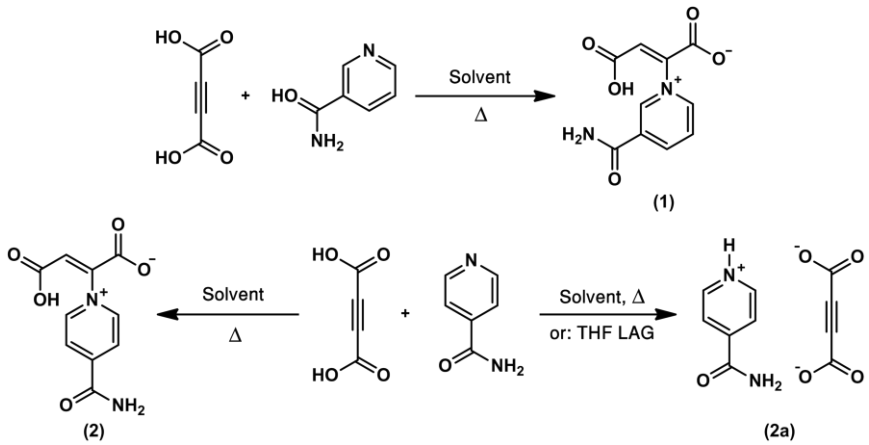

Scheme 4.2 Synthesis of zwitterions **1** and **2** as well as the salt **2a**. In each case the reagents (acetylenedicarboxylic acid and nicotinamide/isonicotinamide) are added to a particular solvent, or solvent mixture, and stirred for a few minutes with mild heating. The salt, **2a**, can also be made *via* liquid-assisted grinding with a few drops of tetrahydrofuran.

Synthesis of zwitterion **1** always gave the same product, with no observed polymorphs or solvates, despite the fact that approximately 60 solvent combinations were used, and crystallisation at both room temperature and in the refrigerator was attempted. The combination of ADC and isonicotinamide, on the other hand, can result in the formation of zwitterion **2**, which crystallises as a hydrate, or in the formation of a salt of the two components, **2a**, *via* simple charge transfer. In our previous work[12] it was observed that when such a salt is formed, it is the kinetic product of the reaction, which forms more quickly and at lower temperatures than the zwitterion itself. It is therefore simple to dispose of the unwanted salt by-product by removing crystals that form too quickly (i.e. after 24 hours) before the filtrate is left to crystallise once more. No other polymorphs or solvates of zwitterion **2** were observed. The synthesis of zwitterion **3** is similar to that of zwitterion **1** and **2** and is reported in a previous publication.[11]

The salts, **1-Melamine**, **2-Melamine**, and **3-Melamine** can easily be formed by grinding a 1:1 molar ratio of the zwitterion and melamine together with a few drops of solvent. Depending on the specific salt, crystals could then be obtained by recrystallisation of this powder, or by dissolution of a 1:1 molar ratio of the starting materials in water.

Many co-crystallisations were attempted with zwitterions **1**, **2** and **3**. The co-formers were chosen based on known interactions that they could have with amide- and carboxylic acid groups, such as the zwitterions have – the idea was to form co-crystals. Unfortunately, the insoluble nature of the zwitterions (to our knowledge they only dissolve in water at 100 °C) made these crystallisations extremely difficult practically, especially since most organic co-formers are very soluble. This discord is also one of the reasons why most of our attempts merely resulted in crystallisation of the two molecular components separately. Another reason for this may have to do with the propensity for formation of homomeric zwitterion-zwitterion interactions – this will be discussed later. Nevertheless, using liquid-assisted grinding as a quick screening tool, melamine was identified as a potentially successful co-former. Further crystallisation and recrystallisation experiments lead to the crystal structures of three melamine salts, **1-Melamine**, **2-Melamine** and **3-Melamine**. When these form, a proton transfer occurs from the carboxylic acid group of the zwitterion to one of the nitrogen atoms in the melamine ring. It is important to note that these salts dissolve more easily than the zwitterions on their own.

4.3.2 Crystal structures

Crystallographic data for all structures obtained with zwitterions **1**, **2** and **3** are summarised in Table 4.1. Zwitterion **3** (both of its polymorphs – **3α** and **3β**)[*] has been included for comparative purposes, although it will only be discussed in terms of its salt with melamine.

[*] This zwitterion is described in Chapter 3, where it is called zwitterion **1** (with polymorphs **1α** and **1β**).

Table 4.1 Crystallographic data for the reported zwitterions and salts.

Structure	**1**	**2**	**2a**	**3α***	**3β***	**1-Melamine**	**2-Melamine**	**3-Melamine**
Chemical formula	$C_{10}H_8N_2O_5$	$C_{10}H_{10}N_2O_6$	$C_8H_7N_2O_3$	$C_{10}H_6N_2O_4$	$C_{10}H_6NO_4$	$C_{13}H_{18}N_8O_7$	$C_{13}H_{16}N_8O_6$	$C_{13}H_{14}N_8O_5$
Formula weight /g mol^{-1}	236.18	254.20	179.16	218.17	218.17	398.35	380.34	362.32
Crystal system	Monoclinic	Triclinic	Triclinic	Monoclinic	Monoclinic	Triclinic	Triclinic	Monoclinic
Space group	$P2_1/c$	$P\bar{1}$	$P\bar{1}$	$P2_1/c$	$P2_1/c$	$P\bar{1}$	$P\bar{1}$	$P2_1/c$
a /Å	8.8986(2)	7.2047(1)	3.671(3)	7.1931(1)	8.0518(8)	5.7312(5)	8.6886(3)	17.184(2)
b /Å	7.9933(2)	7.5455(1)	7.594(5)	20.060(3)	11.8523(1)	12.3326(1)	8.9638(3)	7.328(5)
c /Å	14.175(3)	10.8058(2)	13.772(1)	7.4716(1)	20.020(2)	12.8974(1)	11.2137(4)	13.045(9)
α /°	90.00	91.800(2)	95.732(8)	90.00	90.00	71.530(2)	94.473(2)	90.00
β /°	97.628(3)	100.509(2)	93.218(8)	112.495(2)	94.3020(1)	86.574(3)	103.931(2)	111.257(1)
γ /°	90.00	115.757(2)	97.153(8)	90.00	90.00	89.673(3)	106.6570(1)	90.00
Calculated density /g cm^{-3}	1.570	1.636	1.574	1.455	1.521	1.533	1.575	1.572
Volume /Å^3	999.3(3)	516.12(1)	378.1(5)	996.1(3)	1905.2(3)	863.01(1)	801.88(5)	1531(2)
Z	4	2	2	4	8	2	2	4
Temperature /K	100(2)	100(2)	100(2)	100(2)	100(2)	100(2)	100(2)	100(2)
Independent reflections	2350	2301	1758	2208	4359	4460	4114	3395
R_{int}	0.0546	0.0113	0.0518	0.0256	0.0178	0.0383	0.0271	0.0854
R_1 [I > 2σ(I)]	0.0445	0.0317	0.0424	0.0419	0.0450	0.0719	0.0452	0.0560

* This zwitterion is described in Chapter 3, where it is called zwitterion **1** (with polymorphs **1α** and **1β**).

Zwitterion **1** crystallises in the monoclinic space group $P2_1/c$ and has one zwitterion in the asymmetric unit (ASU). The zwitterions form chains by way of O–H···O hydrogen bonds between the carboxylate/carboxylic acid backbones (Figure 4.1 a). Two such chains then interdigitate forming a ladder-like structure as they pair up, *via* hydrogen bonds between an amide hydrogen atom and one of the oxygen atoms of the carboxylic acid moiety in the other chain (Figure 4.1 b & c). When viewed down the *a*-axis the ladders can clearly be seen as they pack next to each other to form a layered structure (Figure 4.1 d).

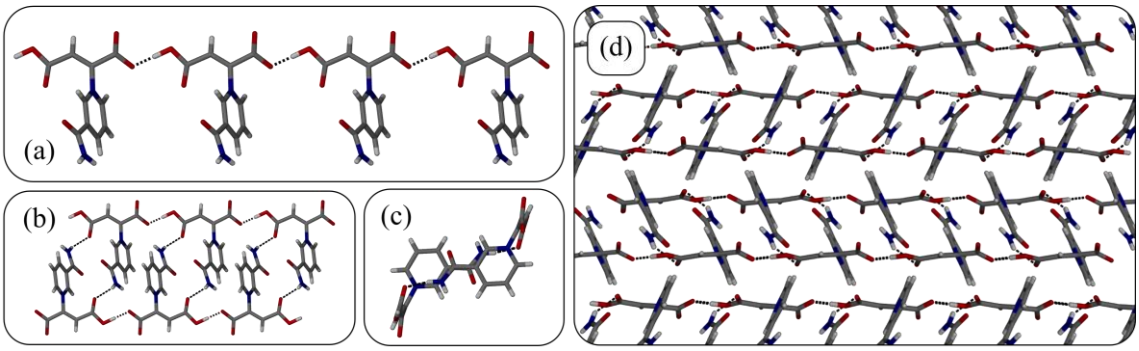

Figure 4.1 (a) Hydrogen-bonded chain of zwitterion **1** viewed down the *c*-axis. (b) Pairs of chains of zwitterion **1** showing the hydrogen bonds holding them together when viewed down the *c*-axis and (c) the *b*-axis. (d) Packing diagram of zwitterion **1** showing the layered structure (viewed down the *a*-axis).

Zwitterion **2** crystallises in the triclinic space group $P\bar{1}$. The ASU of **2** consists of one zwitterion and one molecule of water that is hydrogen bonded through its oxygen atom to the amide functional group of the zwitterion. Once again the zwitterions form chains through hydrogen-bonded carboxylic acid backbones (Figure 4.2 a), and again there is a hydrogen bond between the amide and carbonyl groups of neighbouring chains (Figure 4.2 b). The water molecules only interact with one chain and do not play a role in holding neighbouring chains together. These neighbouring chains do not interdigitate, as with zwitterion **1**, but simply pack next to one another (Figure 4.2 c). The pairs of hydrogen-bonded chains and their layered packing are clearly visible when viewed down the *b*-axis (Figure 4.2 d).

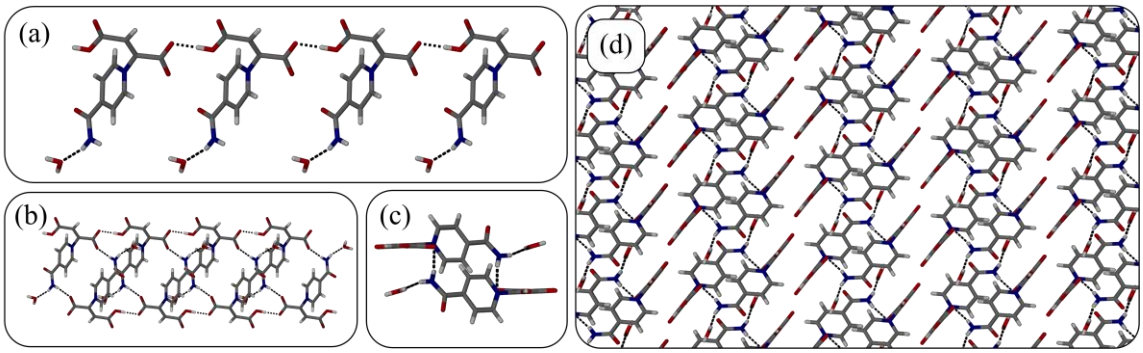

Figure 4.2 (a) Hydrogen-bonded chain of zwitterion **2** viewed perpendicular to the *bc* plane. (b) Pairs of chains of zwitterion **2** showing the hydrogen bonds keeping them together when viewed perpendicular to the *bc* plane and (c) the *b*-axis. (d) Packing diagram of zwitterion **2** showing the layered structure (viewed down the *b*-axis).

The salt **2a** also crystallises in the triclinic space group $P\bar{1}$. There is one isonicotinamide ion and half an ADC ion in the ASU, with a N^{+}–H···$^{-}$O charge assisted hydrogen bond between the positively charged pyridinium nitrogen atom and the negatively charged carboxylate group (Figure 4.3 a). The isonicotinamide ion is also hydrogen bonded to another ADC ion through the amide group. Lastly, two isonicotinamide ions interact by forming the familiar amide-amide 8-atom dimeric unit (Figure 4.3 b).

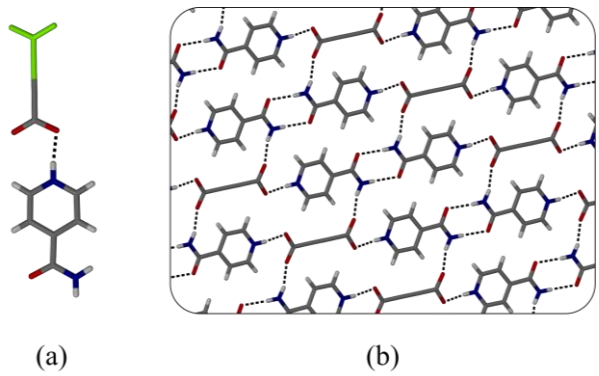

Figure 4.3 (a) The asymmetric unit of the salt **2a** contains one isonicotinamide ion and half an ADC ion. The symmetry-generated half of the ADC ion is shown in green for clarity. (b) Total packing diagram for **2a**, viewed down the *bc* plane, showing the hydrogen bonds that form.

4.3.3 Crystal structures of the melamine salts

The first salt, **1-Melamine**, contains zwitterion **1**, melamine and water in a 1:1:2 mole ratio and crystallises in the triclinic space group $P\bar{1}$. The zwitterion backbone is disordered over two positions in such a manner that the oxygen atoms are on the same positions for both

conformations (i.e. the backbone is flipped by 180°). The structure has a multitude of hydrogen bonds (Figure 4.4 a) due to the many hydrogen-bond donor- and acceptor atoms present in melamine. When viewed down the *a*-axis, these hydrogen bonds can clearly be seen (Figure 4.4 b). Most notable is the hydrogen bond between the amide group of **1**, and melamine – an interaction that seems to play an important role in the formation of these salts (Figure 4.4 a). There is also a CAHB between the zwitterion carboxylate group and the melamine ion (Figure 4.4 a). Water molecules occur in pairs and are located in pockets which line up through the structure. Both water molecules are hydrogen-bonded to the framework. There is no mass loss in the TGA (see supplementary information) that corresponds to the 9.07% water present, indicating that the water molecules are only lost during decomposition.

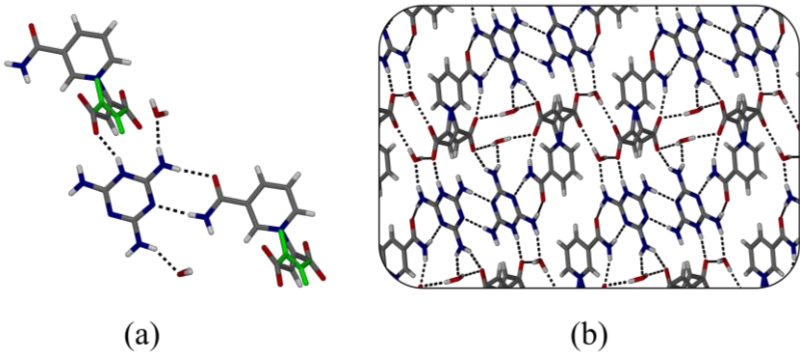

Figure 4.4 (a) Hydrogen bonding in **1-Melamine**. The disorder in the zwitterion backbones is shown in green. (b) Packing diagram of **1-Melamine** viewed down the *a*-axis.

The second salt, **2-Melamine**, contains zwitterion **2**, melamine, and water in a mole ratio of 1:1:1. This salt also crystallises in the triclinic space group, $P\bar{1}$. There are numerous hydrogen bonds present (Figure 4.5 a and b) – note the same $R_2^2(8)$ hydrogen-bonded unit between the amide group and the melamine ion, as well as the charge-assisted hydrogen bond that was also present in **1-Melamine**. The geometry of the latter interaction is however quite different here, as there is an additional hydrogen bond between the neighbouring amine group of melamine and the other oxygen atom of the carboxylate group forming the CAHB (Figure 4.5 a). This hydrogen bond-CAHB double interaction serves to keep melamine and the zwitterion backbone in the same plane. As this propagates through the structure, all of the hydrogen bonds in **2-Melamine** are then in the same plane, so that separate sheets form that are not directly bonded to one another (2D sheets) (Figure 4.5 c). This is in contrast to the hydrogen bonds of **1-Melamine** that extend in three dimensions.

Again, the water molecules are hydrogen bonded to the framework and it does not seem likely that they can be removed without the crystals decomposing. From TGA (see supplementary information) we know that there is a 5.1% mass loss that could be due to water being lost (the mass of one molecule of water is calculated to be 4.8%). This can also be seen from the DSC where there is a broad endotherm that corresponds to this mass loss, however, the mass loss occurs slowly, and is directly followed by decomposition of the crystals, which means that dehydrated crystals cannot be isolated.

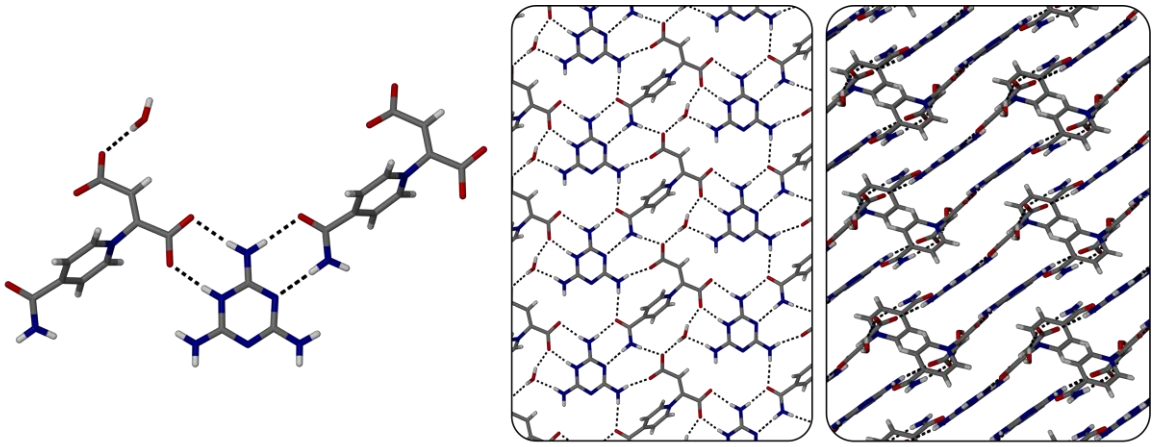

Figure 4.5 (a) Hydrogen bonding in **2-Melamine**. (b) One layer (chosen for clarity) in the packing diagram of **2-Melamine** showing all the hydrogen bonds. (c) Layers in **2-Melamine** pair up (although not held together by hydrogen bonding), but the pairs are then offset to one another in an ABAB manner (viewed down the *a*-axis).

The final salt, **3-Melamine**, contains zwitterion **3**, melamine, and water in a mole ratio of 1:1:1 (Figure 4.6 a). This salt crystallises in the monoclinic space group $P2_1/c$. As with the other two salts, there are numerous hydrogen bonds present, the most notable synthon being that between the carboxylate group of the zwitterion backbone and the melamine ion. As with **2-Melamine**, this interaction consists of a CAHB between an oxygen atom of the carboxylate group and a protonated nitrogen atom in the melamine ring, as well as a hydrogen bond between the neighbouring amine group of melamine and the other oxygen atom of the carboxylate group forming the CAHB (Figure 4.6 a). The packing diagram for this salt (Figure 4.6 b) shows a layered structure: layers of zwitterions separated by sheets of melamine. The pyridinium moieties of the zwitterions are all parallel to each other, and so too are the melamine rings, however the two are at an angle of 105.7(1)° to each other.

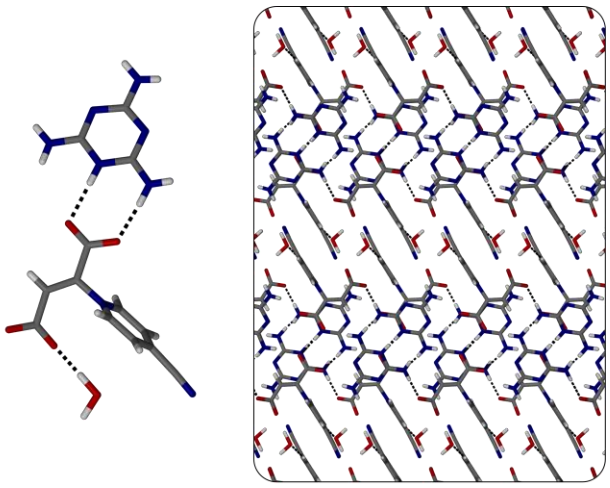

(a) (b)

Figure 4.6 (a) Asymmetric unit of **3-Melamine** showing the hydrogen bonds present. (b) Packing diagram of **3-Melamine** showing the layered structure (viewed down the *b*-axis).

4.3.4 Mechanochemistry

We endeavoured to use mechanochemical methods (specifically grinding in a mortar and pestle) to determine whether bulk material of either the zwitterions or the salts could be produced quickly and easily in this manner. Synthesis of the zwitterions, as well as formation of the salts, were attempted by using neat- and liquid-assisted grinding (for the latter, drops of methanol, ethanol, water and tetrahydrofuran were used). Both of these methods were unsuccessful with regard to zwitterion formation, as it seems more heat is needed to form the covalent bonds, to yield this thermodynamic product. Grinding of the components used to synthesise zwitterion **2** resulted in formation of the kinetic product, **2a**.

Mechanochemical methods were however very successful in forming the zwitterion-melamine salts – both neat and liquid-assisted grinding (using a few drops of methanol or water) were successful, however LAG produced a faster change than neat grinding. Formation of the melamine salts, which have water in the structure, is therefore possible even if water is not deliberately added. Further mechanochemistry experiments, carried out with compounds that are similar to melamine with regard to forming possible intermolecular interactions, were also attempted, namely 2-aminopyridine, 2-aminopyrimidine and 2,6-diaminopyridine. The co-crystallisations of zwitterion **1**, **2**, and **3** with 2-aminopyridine (AP) and 2,6-diaminopyridine (DAP), using LAG with a few drops of methanol, seemed to be successful as powder patterns were obtained that did not match either of the starting

materials, in each case. The combinations of the zwitterions with 2-aminopyrimidine left the starting materials unchanged. It is therefore suspected that salts **1-AP**, **2-AP**, **3-AP**, **1-DAP**, **2-DAP** and **3-DAP** were formed. As of yet, recrystallisation of these six suspected salts has been unsuccessful, as has direct crystallisation from solution. ^{1}H NMR data does however indicate the presence of both starting materials, which supports our hypothesis of salt formation. FTIR indicates that these too are salts, and not co-crystals (the C=O stretching frequency at 1550 – 1635 cm^{-1} indicates the presence of a carboxylate group instead of a carboxylic acid, which would show up around 1720 cm^{-1}).

4.3.5 Hydrogen-bond propensities

For two different types of molecules in solution to recognise each other and form heteromeric molecular solids, the interactions between the different molecules need to be more favourable than interactions between the molecules themselves.[10] Therefore, in order to successfully form multi-component crystals, there needs to be an understanding of the hierarchy of intermolecular interactions. In purely organic molecules, hydrogen bonds are usually the strongest interactions present, and so they are usually all that has to be taken into account.[16] For example, nitrogen-containing heterocycles and carboxylic acids form very strong hydrogen bonds to each other; this interaction is frequently observed in the Cambridge Structural Database (CSD),[10] and can therefore confidently be used in the design of co-crystals. From the CSD it is also clear that the carboxylic acid-amide interaction is more common than the amide-amide and carboxylic acid-carboxylic acid interactions.[17] Combining carboxylic acids and amides is thus also a viable strategy for multi-component crystal formation.

Furthermore, the possibility of proton transfer between molecules also needs to be taken into account. Unexpected proton transfer may result in unexpected intermolecular interactions as CAHBs are likely to form preferentially, as they are stronger than other hydrogen bonds. Here pKa values can be very useful for predicting whether such a proton transfer will occur, i.e. if a salt or co-crystal will form. The pKa rule quantifies this and states that when the difference in pKa between the acid and base (ΔpKa = pKa[protonated base] – pKa[acid]) is more than 4, proton transfer usually occurs to form a salt. Conversely, if ΔpKa < –1, co-crystal formation is more likely. In the intermediary region of ΔpKa between –1 and 4, a linear relationship between the probability of salt formation and ΔpKa

values has been derived.[18] Unfortunately, the pKa values for the zwitterions are not known, and could also not be measured as they are very difficult to dissolve. In the case of the zwitterions, the observed salt formation was unexpected, as the aim was in fact to form co-crystals.

As mentioned previously, one of the factors preventing co-crystal/salt formation, in the case of the zwitterions, is the propensity of the zwitterions to hydrogen bond to each other, instead of interacting with the co-formers. Practically, we can assume that this is happening due to many failed experiments that merely led to recrystallisation, but a search of the CSD,[19–22] using ConQuest, confirms that this is likely to be true (Figure 4.7).

The principal interaction between the zwitterions is a carboxylic acid-carboxylate charge-assisted hydrogen bond. Our objective was to test whether this interaction is more abundant, and thus presumably more favourable, than the interaction a zwitterion would have with a certain co-former. The first step was to search the CSD for all structures containing both a carboxylic acid- and a carboxylate group (whether on separate molecules or on the same molecule). Only organic molecules, for which the 3D coordinates of all atoms have been determined, were taken into account. A subsequent search within this subset allowed for the calculation of the number of times that an intermolecular CAHB forms between these two groups. This was followed by a search for other common interactions that the zwitterions could have with the co-formers that were used (Figure 4.7).

When both carboxylic acid and carboxylate functional groups are present in a crystal (as with the zwitterions, and 3622 other structures in the CSD), they form a CAHB 63.94% of the time. However, when viewing the structures not containing this interaction, it was clear that many could not form this intermolecular interaction as both functional groups were located on the same molecule, and were interacting with each other intramolecularly. When these structures are removed from the search, the propensity for the CAHB rises to 76.79%. When this result is compared to the propensity for other interactions to form (Figure 4.7), it is clear that the zwitterion-zwitterion interaction is more common than all of the other interactions – which would explain why it is dominant in our structures. It is, however, interesting to note that the synthon observed in our melamine salts is only 47.27% abundant (Figure 4.7 f). Here intramolecular interactions were not omitted as it is not a common occurrence. Such a CSD search should thus not be used to rule out the possibility of multi-component crystals forming, but as a tool to try and understand experimental results.

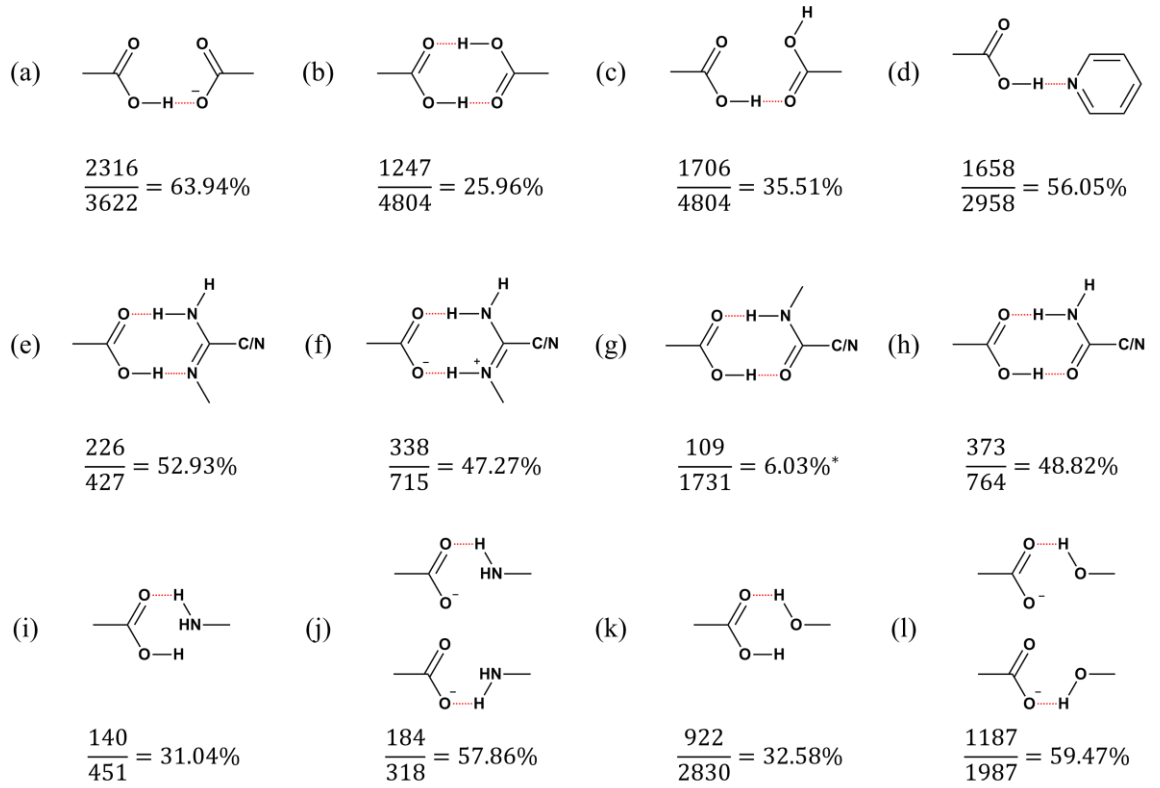

* This value is artificially low as many of the secondary amides form part of longer chains and peptides and so are often sterically hindered from interacting with the carboxylic acid group.

Figure 4.7 Possible interactions that the zwitterions could have with another zwitterion or with the co-formers that were used. Fractions and percentage values represent the number of times that the synthon is observed in the structure if both functional groups are present. The interacting groups are (a) a carboxylic acid and a carboxylate anion, (b) two carboxylic acid groups forming a symmetrical dimer, (c) two carboxylic acid groups forming a single hydrogen bond, (d) a carboxylic acid and pyridine or a pyridine derivative, (e) a carboxylic acid and a molecule containing an amine conjugated to an imine such as 2-aminopyridine, (f) a carboxylate anion and a conjugated amine-iminium group, (g) a carboxylic acid and a secondary amide, (h) a carboxylic acid and a primary amide, (i) a carboxylic acid and an amine, (j) a carboxylate anion and an amine, (k) a carboxylic acid and a hydroxyl group, and (l) a carboxylate anion and a hydroxyl group.

Of course, the values obtained are not perfectly accurate – the CSD is inherently biased, as not all materials diffract well enough to give structural data that can be solved. There could also be other factors inhibiting the interactions that were searched for, such as steric constraints. Furthermore, even though strong intermolecular interactions, such as the hydrogen bond, play an important role in determining crystal packing, it is not the only determining factor; many weaker interactions such as π-π interactions and van der Waals interactions could also have a significant effect. However, the information does give us a

good idea of the relative hydrogen-bond propensities, and therefore the likelihood of molecules to interact.

Another demonstration of the strength of the homomeric zwitterion-zwitterion interaction is the length of the hydrogen bonds between the zwitterions, compared to those observed in the melamine salts. The carboxylate-carboxylic acid CAHB formed between the zwitterions is roughly 2.5 Å long (Table 4.2), while the hydrogen bonds in the salts are longer and range from 2.73 to 2.81 Å (Table 4.3).

Table 4.2 Hydrogen bond geometries of the reported zwitterions and salt.

Structure	D–H···A	D–H /Å	H···A /Å	D···A /Å	D–H···A /°	Symmetry codes
1	O2–H2···O8	1.04 (3)	1.44 (3)	2.4760 (2)	178 (3)	x, y+1, z
2	O1–H1···O7	0.93 (2)	1.63 (2)	2.5593 (1)	175 (2)	x, y+1, z
2a	N1–H1···O11	1.06	1.51 (2)	2.5631 (2)	174 (2)	−x+2, −y, −z+1

Table 4.3 Hydrogen bond geometries of the reported melamine salts.

Structure	D–H···A	D–H /Å	H···A /Å	D···A /Å	D–H···A /°	Symmetry codes
1-Melamine	N27–H27B···O30	0.88	1.94	2.767 (3)	156.1	x−1, y, z
	N28–H28B···O29	0.88	1.97	2.765 (3)	150.5	x−1, y+1, z
	N20–H1···O2	0.84 (3)	1.93 (3)	2.733 (3)	158 (3)	
2-Melamine	N18–H18···O8	0.88 (2)	1.90 (2)	2.7692 (2)	172.9 (2)	x, y–1, z–1
	O27–H27B···O8	0.88 (3)	1.92 (3)	2.7464 (2)	156 (2)	–x+1, –y+2, –z+1
	O27–H27A···O2	0.89 (3)	1.90 (3)	2.7305 (2)	154 (3)	x, y−1, z−1
3-Melamine	N17–H17···O7	0.88 (3)	1.93 (3)	2.814 (4)	173 (3)	–x+2, y–1/2, –z+3/2
	O26–H26A···O1	1.07 (4)	1.68 (4)	2.736 (4)	171 (6)	
	N23–H23A···O2	0.88 (3)	1.85 (4)	2.731 (4)	175 (3)	
	N25–H25A···O8	0.91 (4)	1.86 (4)	2.774 (4)	176 (4)	–x+2, y–1/2, –z+3/2

4.4 Conclusion

Two new zwitterions have successfully been synthesised. The nicotinamide-derived zwitterion (**1**) is robust and easy to make under a variety of conditions. The other, zwitterion **2** containing an isonicotinamide moiety, has a salt by-product, **2a**. From previous work[11] we know that this is the kinetic product of the reaction, and so it is easy to obtain crystals of zwitterion **2** after the fast-forming salt is filtered off.

These two zwitterions, as well as another similar one, **3**, were subsequently utilised to form three new hydrated salts with melamine. These can be obtained from solution and *via* mechanochemistry – the latter proving to be a very fast and convenient technique for salt-

formation screening purposes. The three salts have been fully characterised and described, with emphasis on the intermolecular interactions that contribute to their formation. All three salts display charge-assisted hydrogen bonds between the carboxylate group of the zwitterion and the positively charged nitrogen atom in melamine. The extra amide functionality in **1** and **2** also plays an important role, as this group is utilised in hydrogen bonds to melamine.

Furthermore, we highlight the importance of mechanochemistry as a screening tool. LAG is fast and simple and was subsequently used in conjunction with PXRD, NMR and FTIR to identify six other potential salts of which crystal structures have not been obtained. The co-formers used (2-aminopyridine and 2,6-diaminopyridine) are very similar to melamine with regards to possible hydrogen bond formation, and thus it is not surprising that they could form salts with the zwitterions. Further work will need to be carried out to confirm their exact identity, either by using crystallisation methods that have not been attempted thus far, or by solving the crystal structures from the powder patterns.

When salt and co-crystal formation was attempted, a variety of co-formers were used, yet only three salts were crystallised per zwitterion. Could it be that the zwitterions interact so strongly with each other, that this inhibits the incorporation of other co-formers? A search of the Cambridge Structural Database was carried out to compare the likelihood of various hydrogen bonds and CAHBs to form. The carboxylic acid-carboxylate CAHB, such as that which forms between the zwitterions, occurs in 63.94% of structures that contain both of these functional groups. Compared to this, other interactions that the zwitterions could have with the co-formers were found to be less likely. Experimentally we observe that the zwitterion-zwitterion CAHB is not only abundant, but very strong. Hydrogen bond lengths in the zwitterions are around 2.5 Å, while the hydrogen bond lengths observed in the salts range from 2.73 to 2.81 Å.

The way in which these zwitterions form (or do not form) multi-component crystals, is thought-provoking and definitely creates a greater appreciation for the effect of the relative propensities of intermolecular interactions on the outcome of supramolecular syntheses.

4.5 Experimental

All PXRD, TGA, DSC, NMR, and FTIR data are available in the Supporting Information.

4.5.1 Synthesis and crystallisation

Zwitterion **1,** (Z)-2-(3-carbamoylpyridin-1-ium-1-yl)-3-carboxyacrylate**,** was made by combining acetylenedicarboxylic acid (ADC, 0.020 g, 0.175 mmol) with nicotinamide (0.021 g, 0.172 mmol) in a solvent mixture containing acetonitrile (2 ml) and water (0.5 ml). The mixture was stirred at 100 °C until the components had completely dissolved. The vial was capped and left on a shelf to crystallise at room temperature. Small, colourless plate-like crystals formed after 24 hours. If the solution is stirred any longer, the zwitterion starts to precipitates out as a fine white powder.

Zwitterion **2,** (Z)-3-carboxy-2-(4-carboxypyridin-1-ium-1-yl)acrylate**,** was made by combining acetylenedicarboxylic acid (ADC, 0.020 g, 0.175 mmol) with isonicotinamide (0.021 g, 0.172 mmol) in a solvent mixture containing water (3 ml) and THF (3 ml). The mixture was stirred for 5 minutes at 100 °C. The vial was capped and left on a shelf to crystallise at room temperature. Colourless plate-like crystals formed within 3 days.

The salt **2a**, containing the same components, was also obtained by stirring the reagents for 5 minutes, at 100 °C, but in a solvent mixture of 0.5 ml diethyl ether and 6 ml water. Colourless, needle-like crystals formed within a day. While neat grinding was unsuccessful, the salt could also be synthesised mechanochemically by grinding the reagents together for 10 minutes with a few drops of THF.

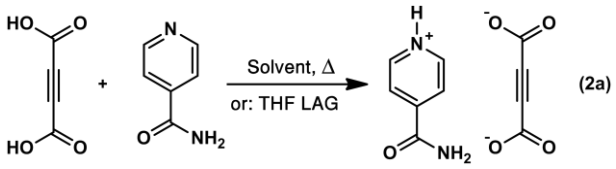

Scheme 4.3 General reaction scheme for the preparation of salt **2a** from acetylenedicarboxylic acid and isonicotinamide.

The salt of zwitterion **1** and melamine (**1-Melamine**) was made by combining zwitterion **1** (0.010 g, 0.042 mmol) with melamine (0.005 g, 0.040 mmol) in 3 ml water and stirring them together at 100 °C until the components had completely dissolved. The vial was then capped and left on a shelf to crystallise at room temperature. Small, colourless plate-like crystals

formed after 2 weeks. A powder of this salt can also be obtained by grinding the two components together for 10 minutes in a mortar and pestle (neat or with a few drops of water).

The salt of zwitterion **2** and melamine (**2-Melamine**) was made by combining zwitterion **2** (0.010 g, 0.042 mmol) with melamine (0.005 g, 0.040 mmol) and grinding them together for 10 minutes in a few drops of MeOH. The powder was then recrystallised from D_2O and a drop of pyridine. Colourless plate-like crystals were obtained within 2 days.

The salt of zwitterion **3** and melamine (**3-Melamine**) was made by combining zwitterion **3** (0.010 g, 0.042 mmol) with melamine (0.006 g, 0.048 mmol) and stirring these together for 30 minutes in 7 ml water at 100 °C. The vial was capped and left to crystallise on a shelf at room temperature. Colourless plate-like crystals formed after 2 months. This salt can also be obtained by grinding the two components for 10 minutes in a few drops of MeOH.

4.5.2 Methods of characterisation

All products obtained were crystalline, with most giving crystals large enough for single-crystal X-ray diffraction (SCXRD). Powder X-ray diffraction (PXRD) was used to confirm purity of the bulk material. Where single crystal data was not obtainable, Nuclear Magnetic Resonance (NMR) spectroscopy was used for identification. The thermal properties of all materials were investigated using Thermogravimetric Analysis (TGA) and Differential Scanning Calorimetry (DSC). FTIR was used to confirm that the material was a salt, rather than a co-crystal.

Powder X-ray diffraction (PXRD) patterns were collected on a Bruker D2 Phaser powder X-ray diffractometer equipped with a copper source producing radiation of wavelength 1.54183 Å. The instrument was operated at 30 kV voltage and 10 mA current. Samples were gently crushed and flattened onto a zero-background holder. Each scan was made up of 2260 steps of 0.5 seconds each (0.0161° step size) that ranged from $2\theta = 4$ to 40°.

Single-crystal X-ray Diffraction (SCXRD) for all compounds, except **3-Melamine**, was performed using a Bruker SMART Apex II diffractometer. The diffractometer makes use of MoKα radiation of wavelength 0.71073 Å produced using a microfocus sealed tube and a 0.5 mm MonoCap collimator. Frames were detected by a Bruker APEX SMART CCD

area-detector. An Oxford Cryosystems cryostat (Cryostream Plus 700 Controller) was used to keep the single crystals at 100 K throughout all data collections.

Single-crystal X-ray Diffraction (SCXRD) of **3-Melamine** was performed using a Bruker Apex II DUO Quasar CCD area-detector diffractometer. This dual source diffractometer was operated using MoKα radiation of wavelength 0.71073 Å produced by an Incoatec $I_{\mu S}$ microsource coupled with a multilayer mirror optics monochromator. An Oxford Cryogenics Cryostat (700 Series Cryostream Plus) was used to keep the single crystal at 100 K throughout the data collection.

Data were collected and reduced using the Bruker software package SAINT[23] in the ApexIII software. SADABS[24,25] was used for the absorption correction and correcting for other systematic errors. Finally, the structures were solved (SHELXS-13)[26] using direct methods and refined (SHELXL-16)[27] through the graphical user interface XSeed.[28,29] Hydrogen atoms on sp^2-hybridised carbon atoms were placed in calculated positions using riding models, while O-H and N-H hydrogen atoms were placed on maxima in the electron density difference maps. All images were created using POV-Ray.[30]

Thermogravimetric analysis (TGA) was performed using a TA Q500 instrument. Powdered samples (3-15 mg) were suspended in an open aluminium pan while being heated in a furnace at 10 °C min^{-1}. The sample was kept under the flow of nitrogen gas throughout (50 ml min^{-1}) to ensure that solvent vapours and decomposition materials were removed as they formed.

Differential Scanning Calorimetry (DSC) was performed using a TA Q20 instrument. Powdered samples (3-10 mg) were placed in a closed aluminium pan. The lid of the pan was punctured before closing. An empty reference pan was made in exactly the same way. Both pans were placed under a nitrogen flow of 50 ml min^{-1} and heated at 10 °C min^{-1} until just before decomposition.

Nuclear Magnetic Resonance (NMR) spectroscopy was performed using a 300 MHz Agilent spectrometer. Samples were dissolved in D_2O and filtered before analysis. Where needed, a few drops of pyridine were added to aid dissolution.

Fourier Transform Infrared spectroscopy (FTIR) was carried out using a Bruker Alpha spectrometer with Platinum ATR attachment. A background scan was acquired before each sample scan.

4.5.3 Details of the CSD search

To carry out a search of the CSD (version 5.38, May 2017),[19–22] the ConQuest software, version 1.19 (Build RC1, 2016), was used. Filters were applied in order to only search for organic molecules for which the 3D coordinates of all atoms have been determined.

4.6 Acknowledgements

Financial support from the Wilhelm Frank Scholarship Fund, the National Research Foundation of South Africa and Stellenbosch University is gratefully acknowledged. We also acknowledge the Central Analytical Facility at Stellenbosch University for use of their NMR instrument.

4.7 References

1 D. J. Berry and J. W. Steed, *Adv. Drug Deliv. Rev.*, 2017.

2 G. Kuminek, F. Cao, A. Bahia de Oliveira da Rocha, S. Gonçalves Cardoso and N. Rodríguez-Hornedo, *Adv. Drug Deliv. Rev.*, 2016, **101**, 143–166.

3 M. F. Arafa, S. A. El-Gizawy, M. A. Osman and G. M. El Maghraby, *J. Drug Deliv. Sci. Technol.*, 2017, **38**, 9–17.

4 F. Grifasi, M. R. Chierotti, K. Gaglioti, R. Gobetto, L. Maini, D. Braga, E. Dichiarante and M. Curzi, *Cryst. Growth Des.*, 2015, **15**, 1939–1948.

5 N. K. Duggirala, M. L. Perry, Ö. Almarsson and M. J. Zaworotko, *Chem. Commun.*, 2016, **52**, 640–655.

6 S. Hiendrawan, B. Veriansyah, E. Widjojokusumo, S. N. Soewandhi, S. Wikarsa and R. R. Tjandrawinata, *Int. J. Pharm.*, 2016, **497**, 106–113.

7 E. Grothe, H. Meekes, E. Vlieg, J. H. ter Horst and R. de Gelder, *Cryst. Growth Des.*, 2016, **16**, 3237–3243.

8 G. R. Desiraju, *CrystEngComm*, 2003, **5**, 466–467.

9 J. D. Dunitz, *CrystEngComm*, 2003, **5**, 506–506.

10 C. B. Aakeröy and D. J. Salmon, *CrystEngComm*, 2005, **72**, 439–448.

11 L. Loots, D. A. Haynes and T. le Roex, *New J. Chem.*, 2014, **38**, 2778–2786.

12 L. Loots, J. P. O'Connor, T. le Roex and D. A. Haynes, *Cryst. Growth Des.*, 2015, **15**, 5849–5857.

13 J. Lombard, L. Loots, D. A. Haynes and T. le Roex, *Manuscript in preparation*, 2017.

14 M. D. Ward, in *Molecular networks*, ed. M. W. Hosseini, Springer, Berlin, 2009, pp. 1–23.

15 G. R. Desiraju, *Angew. Chem. Int. Ed.*, 1995, **34**, 2311–2327.

16 G. R. Desiraju, *Acc. Chem. Res.*, 2002, **35**, 565–573.

17 L. Leiserowitz and F. Nader, *Acta Crystallogr. Sect. B Struct. Crystallogr. Cryst. Chem.*, 1977, **B33**, 2719–2733.

18 A. J. Cruz-Cabeza, *CrystEngComm*, 2012, **14**, 6362–6365.

19 C. F. Macrae, P. R. Edgington, P. McCabe, E. Pidcock, G. P. Shields, R. Taylor, M. Towler and J. van de Streek, *J. Appl. Crystallogr.*, 2006, **39**, 453–457.

20 C. F. Macrae, I. J. Bruno, J. A. Chisholm, P. R. Edgington, P. McCabe, E. Pidcock, L. Rodriguez-Monge, R. Taylor, J. van de Streek and P. A. Wood, *J. Appl. Crystallogr.*, 2008, **41**, 466–470.

21 R. Taylor and C. F. Macrae, *Acta Crystallogr. Sect. B Struct. Sci.*, 2001, **B57**, 815–827.

22 I. J. Bruno, J. C. Cole, P. R. Edgington, M. Kessler, C. F. Macrae, P. McCabe, J. Pearson and R. Taylor, *Acta Crystallogr. Sect. B Struct. Sci.*, 2002, **B58**, 389–397.

23 *SAINT Data Collection Software, version V7.99A*, Bruker AXS Inc., 2012, Madison, WI.

24 *SADABS, version 2012/1*, Bruker AXS Inc., 2012, Madison, WI.

25 R. H. Blessing, *Acta Crystallogr. Sect. A Found. Crystallogr.*, 1995, **51**, 33.

26 G. M. Sheldrick, *Acta Crystallogr. Sect. A Found. Crystallogr.*, 2008, **64**, 112.

27 G. M. Sheldrick, *Acta Crystallogr. Sect. C*, 2015, **71**, 3–8.

28 L. J. Barbour, *J. Supramol. Chem*, 2001, **1**, 189–191.

29 J. L. Atwood and L. J. Barbour, *Cryst. Growth Des.*, 2003, **3**, 3–8.

30 *POV-RayTM for Windows, version 3.6*, Persistence of Vision Raytracer Pty. Ltd., 2004, Williamstown, Australia.

4.8 Supplementary information

Synthesis and crystallisation

All chemicals and solvents were obtained from Sigma Aldrich South Africa and used without further purification.

*(Z)-2-(3-carbamoylpyridin-1-ium-1-yl)-3-carboxyacrylate (**1**):*

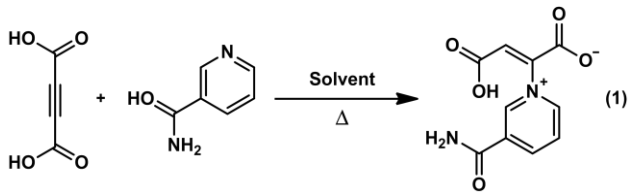

Figure S1 General reaction scheme for the preparation of the zwitterion (Z)-2-(3-carbamoylpyridin-1-ium-1-yl)-3-carboxyacrylate (**1**) from acetylenedicarboxylic acid and nicotinamide.

Zwitterion **1** was made by combining acetylenedicarboxylic acid (ADC, 0.020 g, 0.175 mmol) with nicotinamide (0.021 g, 0.172 mmol) in a solvent mixture containing acetonitrile (2 ml) and water (0.5 ml). The mixture was stirred at 100 °C until the components had completely dissolved. The vial was capped and left on a shelf for crystals to form at room temperature. Small, colourless plate-like crystals formed after 24 hours. When the solution was stirred any longer, the zwitterion started to form and would precipitate out as a fine white powder.

Various solvent mixtures were used when formation of this zwitterion was attempted: Combinations of methanol, ethanol, water, dimethylformamide and dimethylsulfoxide with each other as well as with acetone, acetonitrile, chloroform, dichloromethane, diethyl ether, 1,4-dioxane, tetrahydrofuran, toluene, cyclohexane, ethyl acetate and benzene (A total of 70 different combinations). All of these produced the zwitterion (whether a powder or crystals) and no salt was ever observed as with zwitterion **2**. Mechanochemisty was attempted, but was unsuccessful.

The salt of zwitterion **1** and melamine (**1-Melamine**) was crystallised by combining zwitterion **1** (0.010 g, 0.042 mmol) with melamine (0.05 g, 0.040 mmol) in 3 ml water and stirring them together at 100 °C until the components had completely dissolved. The vial was capped and left on a shelf for crystals to form at room temperature. Small, colourless plate-like crystals formed after 2 weeks. A powder of this salt can also be obtained after grinding the two

components together for 10 minutes with a mortar and pestle (neat or with a few drops of MeOH, EtOH or water).

Two more new materials (which are suspected to be salts) can also be formed when zwitterion **1** is combined with 2-aminopyridine or 2,6-diaminopyridine (**1-AP** and **1-DAP**). These are formed by grinding the zwitterion and coformer together, with a few drops of methanol, for 10 minutes using a mortar and pestle. Single crystals have not been obtained, but we suspect that they are salts based on PXRD, NMR, and IR data.

Various other co-formers were also combined with **1**, but no other multi-component crystals were formed. The co-formers used included: urea, isonicotinamide, nicotinamide, uracil, terephthalic acid, DABCO, 2-aminopyrimidine, thymine, pyrogallol, 2,2'-biphenol, isoquinoline, pyridine, 4-methylphenol, 2,3-dihydroxynapthalene, napthalene, phloroglucinol dihydrate, N-phenyl-2-napthylamine, pamoic acid, hydroquinone, piperazine, pyrazinecarboxylic acid, 4-phenylpyridine, 4-hydroxybenzaldehyde, α,α'-dibromo-o-xylene, and 2-amino-benzonitrile. We also attempted to co-crystallise the zwitterions with each other.

*(Z)-3-carboxy-2-(4-carboxypyridin-1-ium-1-yl)acrylate (**2**):*

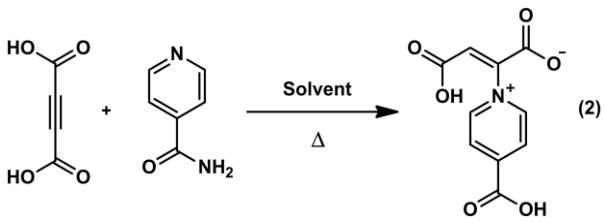

Figure S2 General reaction scheme for the preparation of the zwitterion (Z)-3-carboxy-2-(4-carboxypyridin-1-ium-1-yl)acrylate (**2**) from acetylenedicarboxylic acid and isonicotinamide.

Zwitterion **2** was made by combining acetylenedicarboxylic acid (ADC, 0.020 g, 0.175 mmol) with isonicotinamide (0.021 g, 0.172 mmol) in a solvent mixture containing water (3 ml) and THF (3 ml). The mixture was stirred for 5 minutes at 100 °C after which the vial was capped and left on a shelf to crystallise at room temperature. Colourless plate-like crystals formed within 3 days.

A salt, **2a**, containing the same components was also obtained by stirring the reagents for 5 minutes, at 100 °C, in a solvent mixture of 0.5 ml diethyl ether and 6 ml water. Colourless, needle-like crystals formed within a day. While neat grinding was unsuccessful, the salt could

also be formed mechanochemically by grinding the reagents together for 10 minutes with a few drops of THF.

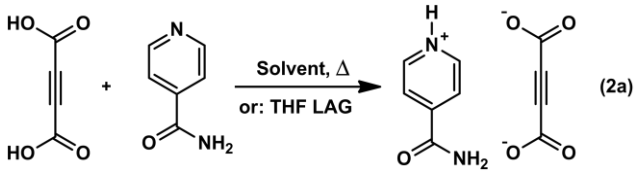

Figure S3 General reaction scheme for the preparation of salt **2a** from acetylenedicarboxylic acid and isonicotinamide.

The salt of zwitterion **2** and melamine (**2-Melamine**) was formed by combining zwitterion **2** (0.010 g, 0.042 mmol) with melamine (0.05 g, 0.040 mmol) and grinding them together for 10 minutes with a few drops of MeOH. The powder was then recrystallised from D_2O and a drop of pyridine. Colourless plate-like crystals were obtained in the refrigerator within 2 days.

Zwitterion **2** was combined with the same co-formers as **1**. As was seen with the previous zwitterion, two more new materials (which are suspected to be salts) can also be formed when zwitterion **2** is combined with 2-aminopyridine or 2,6-diaminopyridine (**2-AP** and **2-DAP**). These are formed by grinding the zwitterion and co-former together with a few drops of methanol for 10 minutes using a mortar and pestle. Single crystals have not been obtained, but we suspect that they are salts based on PXRD, NMR, and IR data.

*(Z)-3-carboxy-2-(4-cyanopyridin-1-ium-1-yl)acrylate **(3)**:*

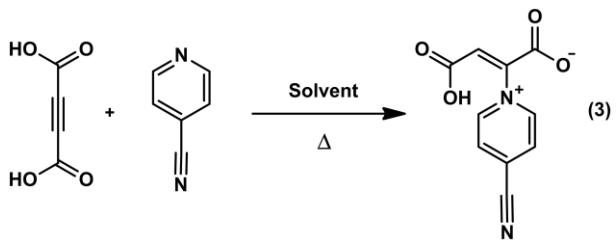

Figure S4 General reaction scheme for the preparation of the zwitterion (Z)-3-carboxy-2-(4-cyanopyridin-1-ium-1-yl)acrylate **(3)** from acetylenedicarboxylic acid and 4-cyanopyridine.

The synthesis of zwitterion **3** and its polymorphic behaviour is discussed at length in our previous paper on polymorphic zwitterions.[1]

The salt of zwitterion **3** and melamine (**3-Melamine**) was crystallised by combining zwitterion **3** (0.010 g, 0.042 mmol) with melamine (0.006 g, 0.048 mmol) and stirring these

together for 30 minutes in 7 ml water at 100 °C. The vial was capped and left to crystallise on a shelf at room temperature. Colourless plate-like crystals formed after 2 months. This salt can also be obtained by grinding the two components for 10 minutes with a few drops of MeOH.

Two more new materials (which are suspected to be salts) can again be formed when zwitterion **3** is combined with 2-aminopyridine or 2,6-diaminopyridine (**3-AP** and **3-DAP**). These are formed by grinding the zwitterion and co-former together for 10 minutes in a mortar and pestle with a few drops of MeOH. Single crystals have not been obtained, but we suspect that they are salts based on PXRD, NMR, and IR data.

Powder X-Ray Diffraction patterns

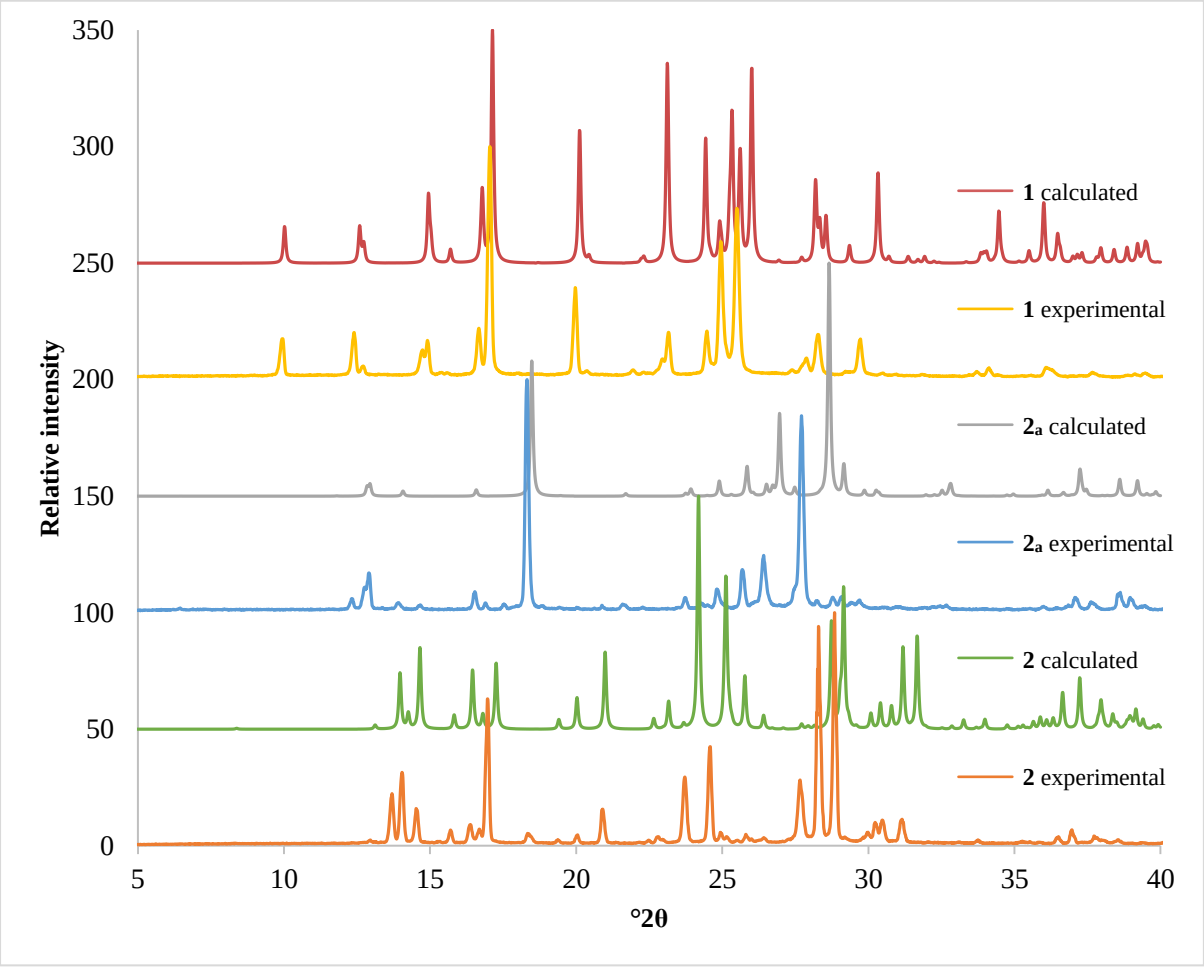

Figure S5 Comparison of the experimental and calculated powder patterns of the two zwitterions as well as the salt, **2a**. The slight shift in angle between the calculated and experimental patterns is due to the difference in temperature (powder pattern at room temperature; crystal structure at 100 K).

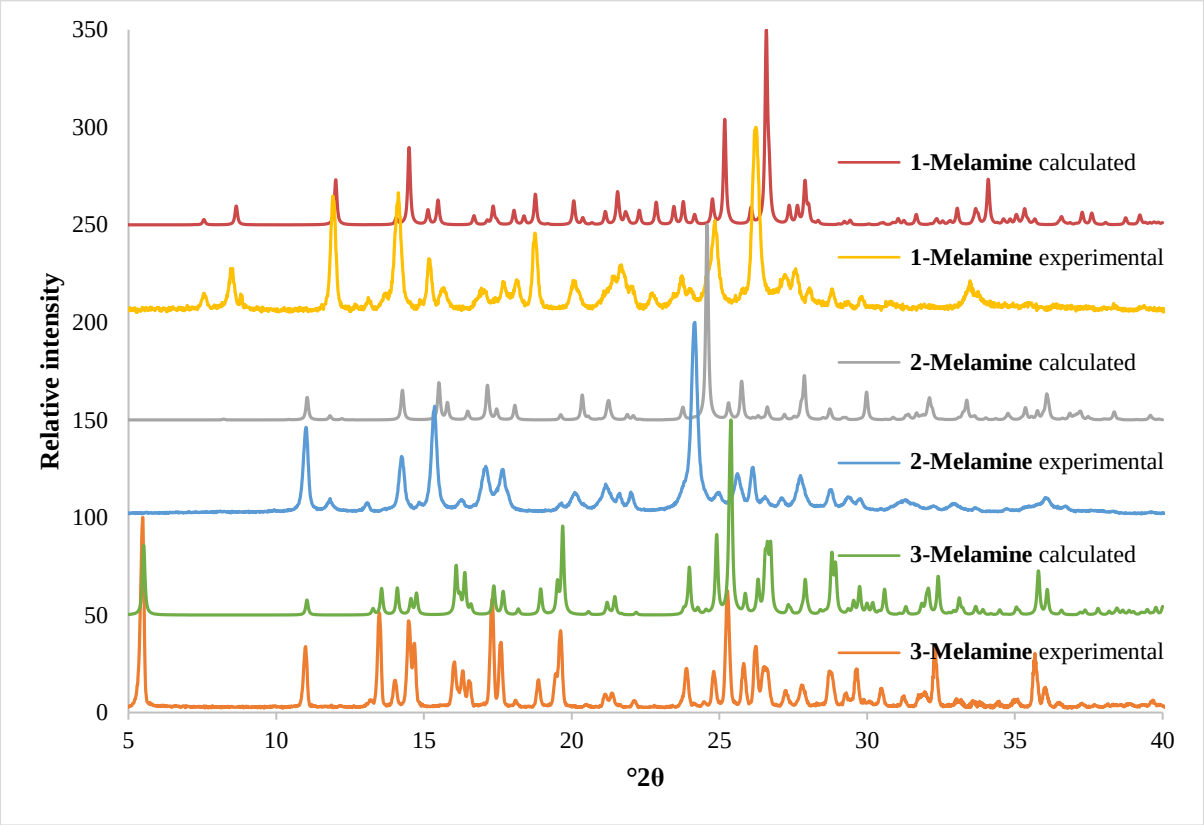

Figure S6 Comparison of the experimental and calculated powder patterns of the three melamine salts. The slight shift in angle between the calculated and experimental patterns is due to the difference in temperature.

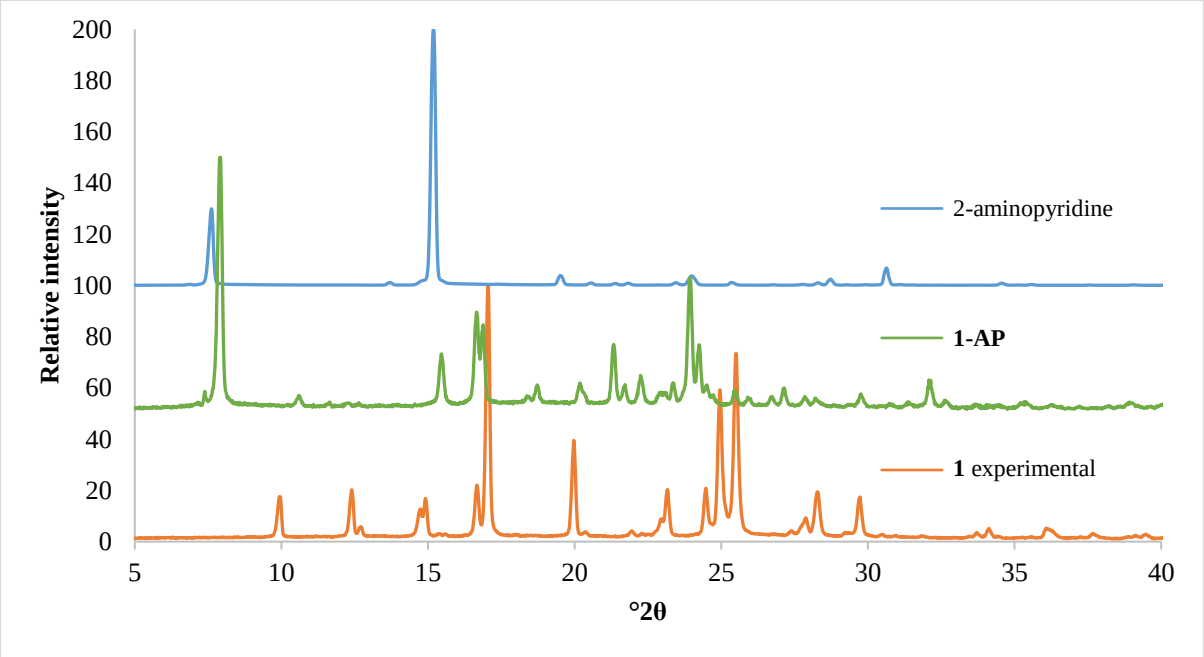

Figure S7 Comparison of the collected powder patterns of the starting materials (zwitterion **1** and 2-aminopyridine) and the product obtained after LAG (**1-AP**).

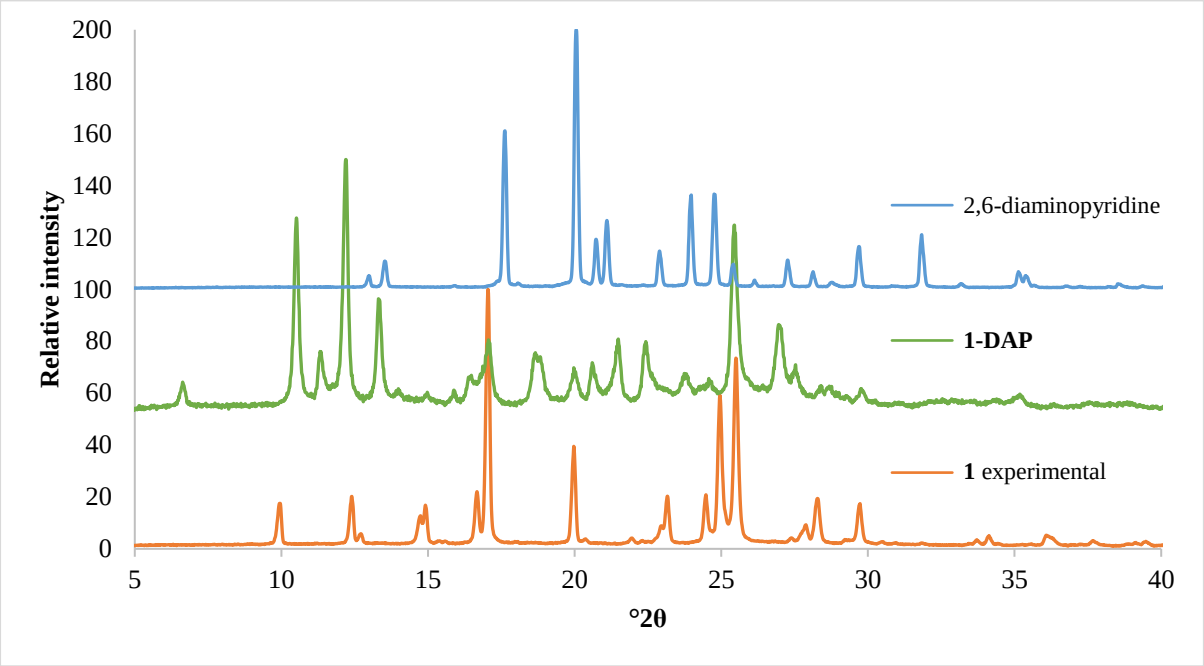

Figure S8 Comparison of the powder patterns of the starting materials (zwitterion **1** and 2,6-diaminopyridine) and the product obtained after LAG (**1-DAP**).

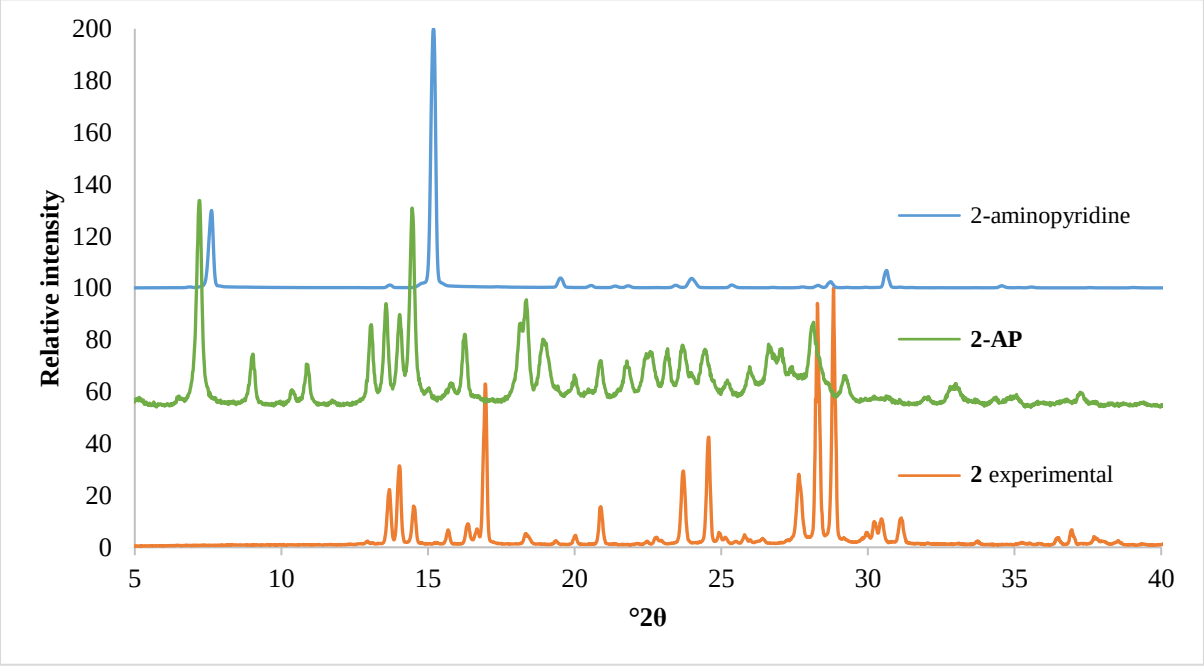

Figure S9 Comparison of the powder patterns of the starting materials (zwitterion **2** and 2-amino-pyridine) and the product obtained after LAG (**2-AP**).

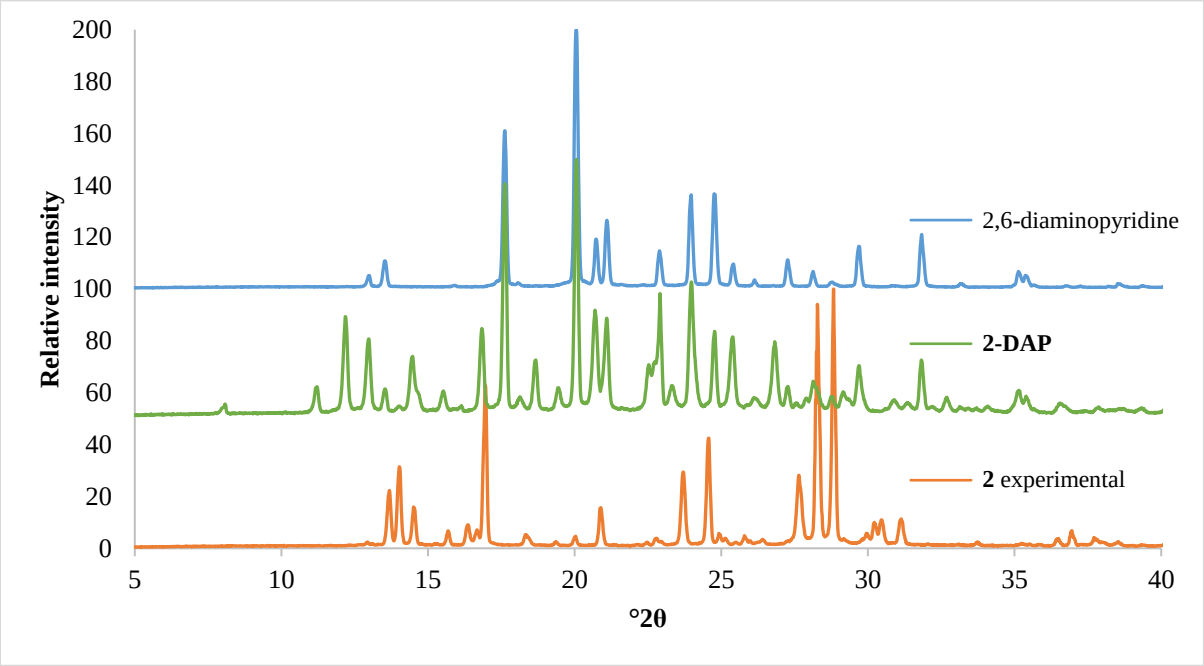

Figure S10 Comparison of the powder patterns of the starting materials (zwitterion **2** and 2,6-diamino-pyridine) and the product obtained after LAG (**2-DAP**). Peaks of the starting materials are still visible in **2-DAP**, but new peaks have also formed.

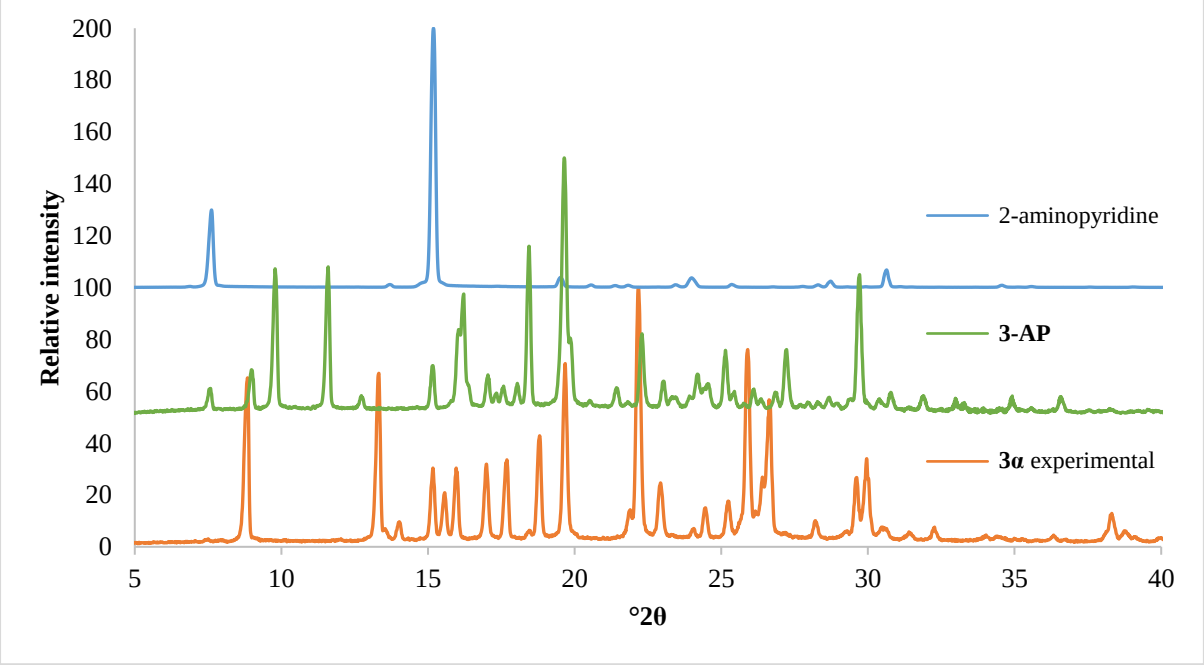

Figure S11 Comparison of the powder patterns of the starting materials (zwitterion **3α** and 2-aminopyridine) and the product obtained after LAG (**3-AP**). Some peaks of the starting materials are still visible in **3-AP**, but new peaks have also formed.

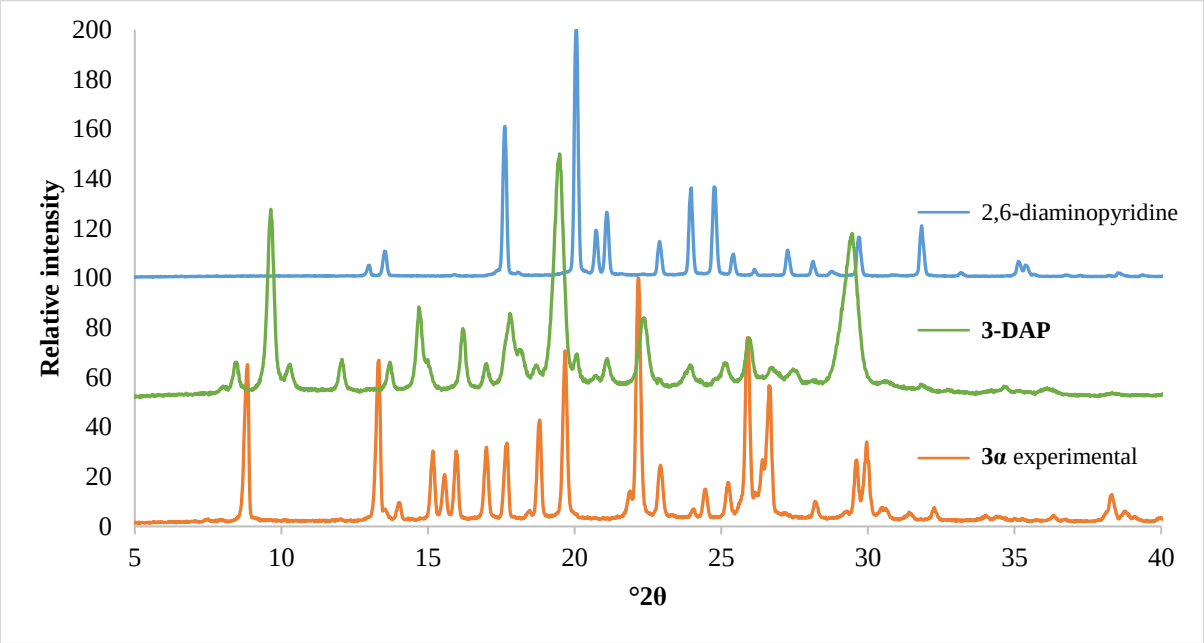

Figure S12 Comparison between the collected powder patterns of the starting materials (zwitterion **3α** and 2,6-diaminopyridine) and the product obtained after LAG (**3-DAP**). An unknown pattern is obtained.

Thermal analysis (TGA and DSC)

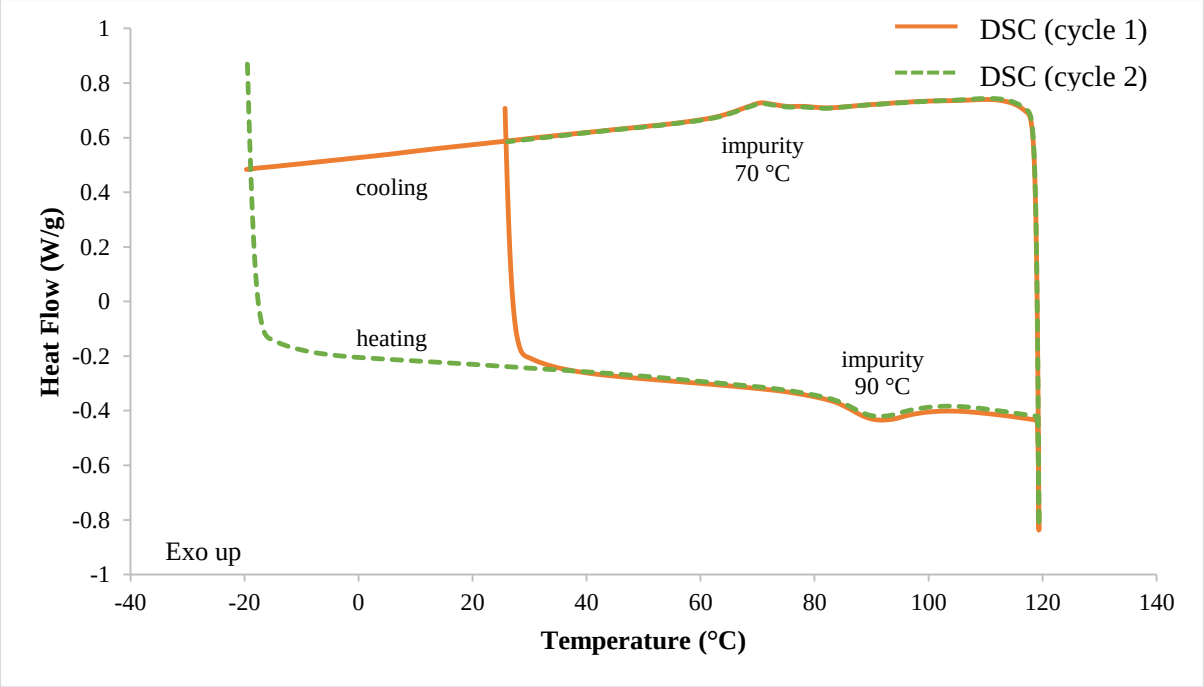

Figure S13 DSC trace for the starting material ADC used as an example. There is an impurity in the instrument which causes the small exo- and endotherms during heating (90 °C) and cooling (70 °C). This impurity can be seen in all the following DSC curves and can be ignored (The higher the mass of the sample tested, the smaller the impurity peaks).

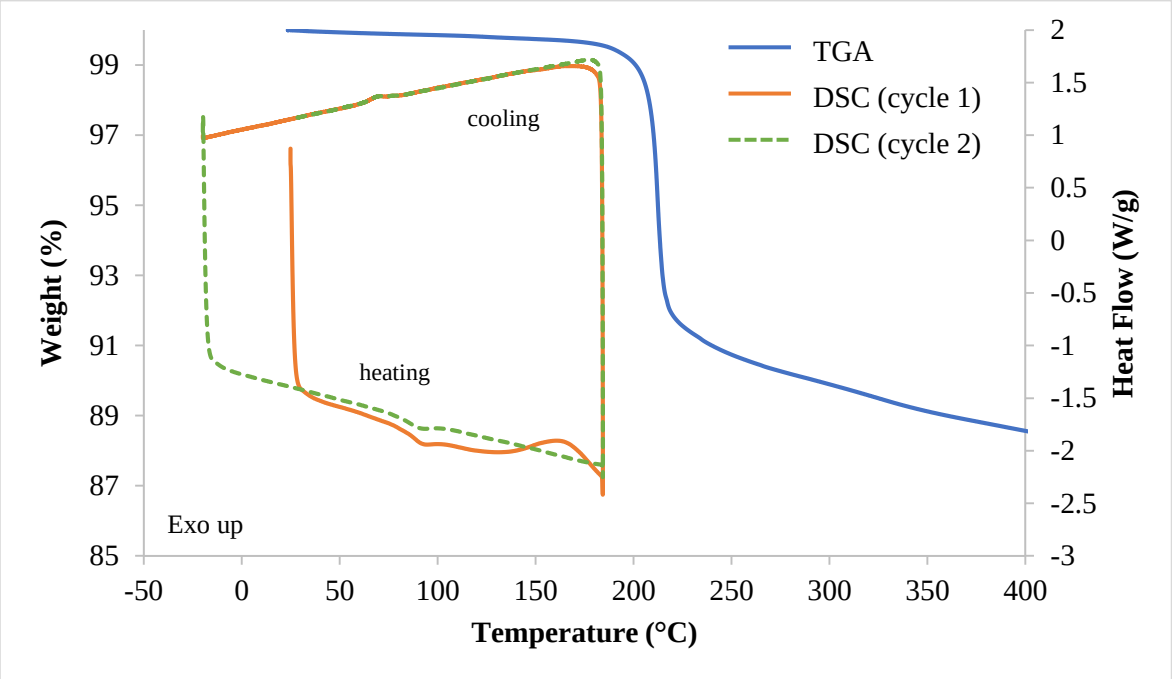

Figure S14 Thermal analysis results for zwitterion **1**. TGA trace shown in blue and DSC traces in orange (cycle 1) and green dashes (cycle 2). The small exo- and endotherms in the DSC are due to an impurity present in the instrument.

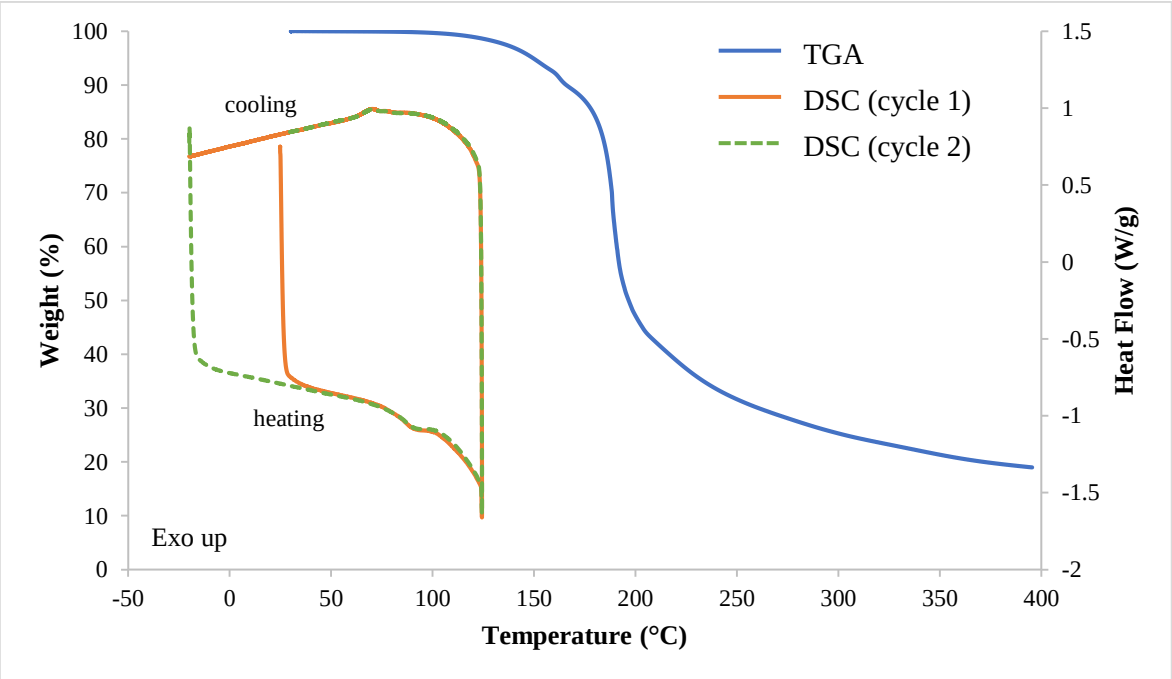

Figure S15 Thermal analysis results for zwitterion **2**. TGA trace shown in blue and DSC traces in orange (cycle 1) and green dashes (cycle 2). The small exo- and endotherms in the DSC are due to an impurity present in the instrument. The sloping baseline in the DSC trace is caused by water molecules slowly coming out of the hydrate crystals. This can also be seen in the TGA trace where there is a slow decrease in mass before degradation.

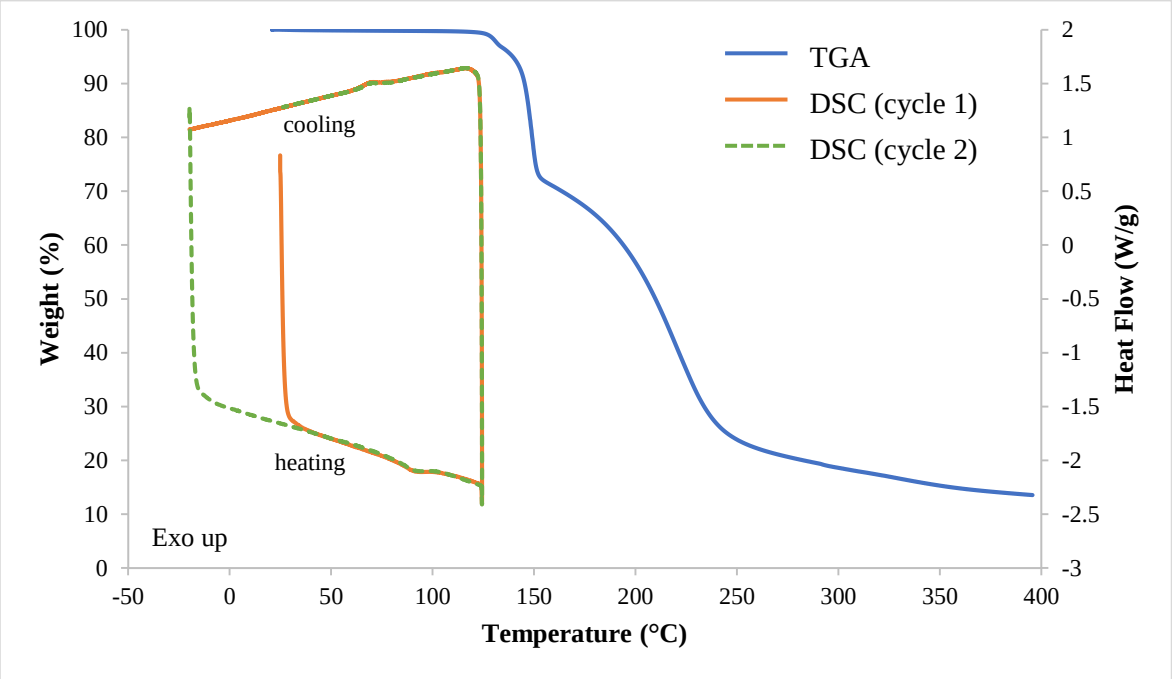

Figure S16 Thermal analysis results for the salt **2a**. TGA trace shown in blue and DSC traces in orange (cycle 1) and green dashes (cycle 2). The small exo- and endotherms in the DSC are due to an impurity present in the instrument. TGA shows a two-step degradation profile.

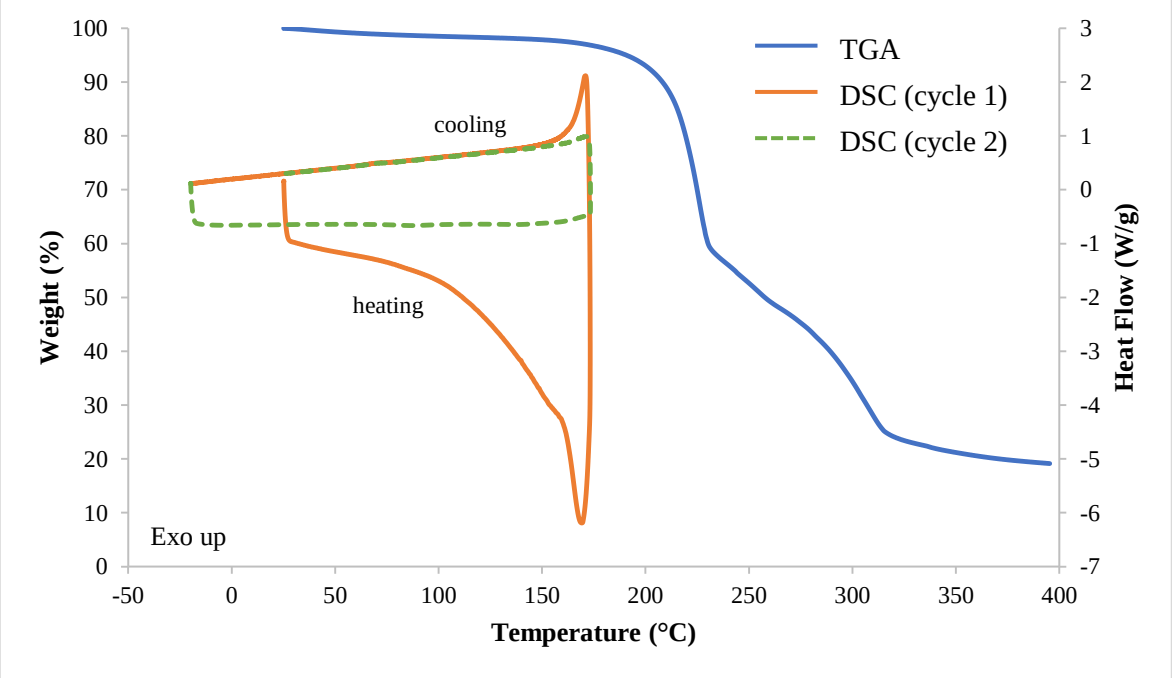

Figure S17 Thermal analysis results for the salt **1-Melamie**. TGA trace shown in blue and DSC traces in orange (cycle 1) and green dashes (cycle 2). The sloping baseline in the DSC trace is caused by water molecules slowly coming out of the hydrate crystals.

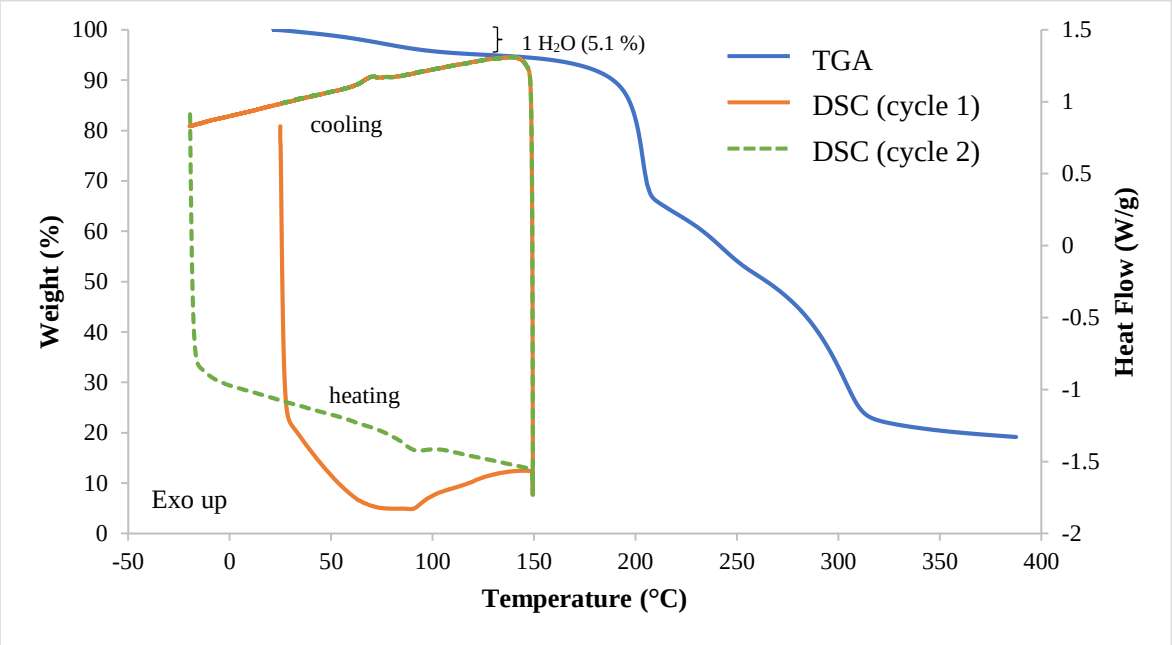

Figure S18 Thermal analysis results for salt **2-Melamine**. TGA trace shown in blue and DSC traces in orange (cycle 1) and green dashes (cycle 2). The broad endotherm in the first DSC cycle is caused by water molecules coming out of the crystals. This mass loss can also be seen in the TGA trace as a loss of 5.1% that corresponds to the mass of one water molecule (4.8%).

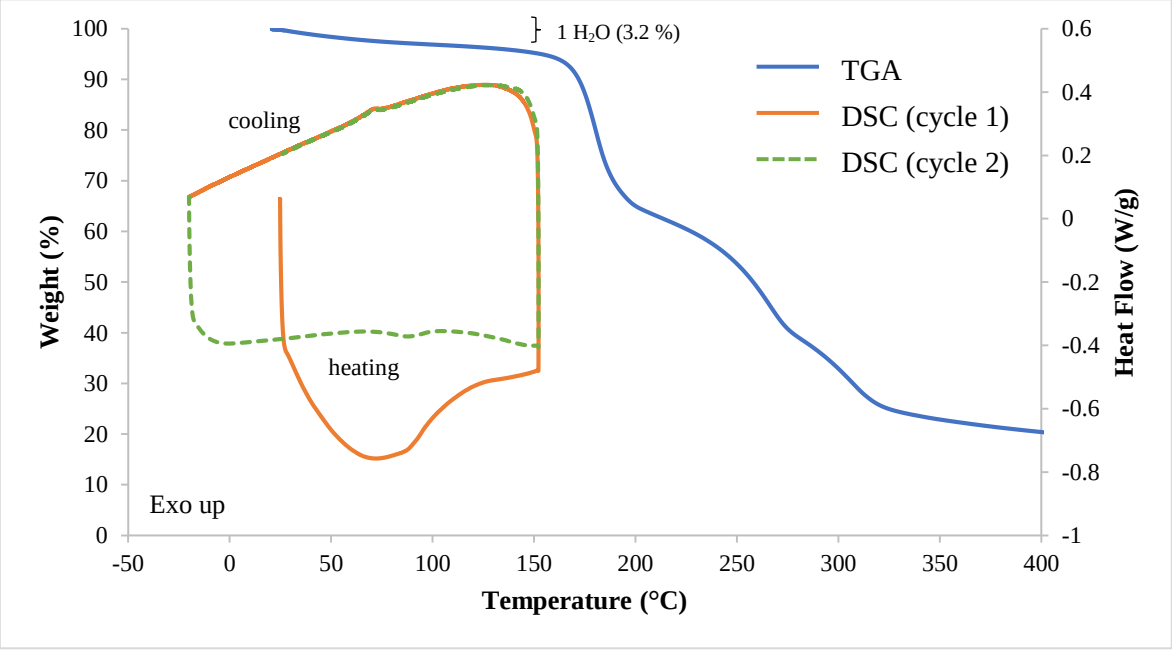

Figure S19 Thermal analysis results for salt **3-Melamine**. TGA trace shown in blue and DSC traces in orange (cycle 1) and green dashes (cycle 2). The small exo- and endotherms in the DSC are due to an impurity present in the instrument. The broad endotherm in the first DSC cycle is caused by water molecules coming out of the crystals. This mass loss can also be seen in the TGA trace as a loss of 3.2% (some may have evaporated at room temperature) that corresponds to the mass of one water molecule (calculated as 5.0%).

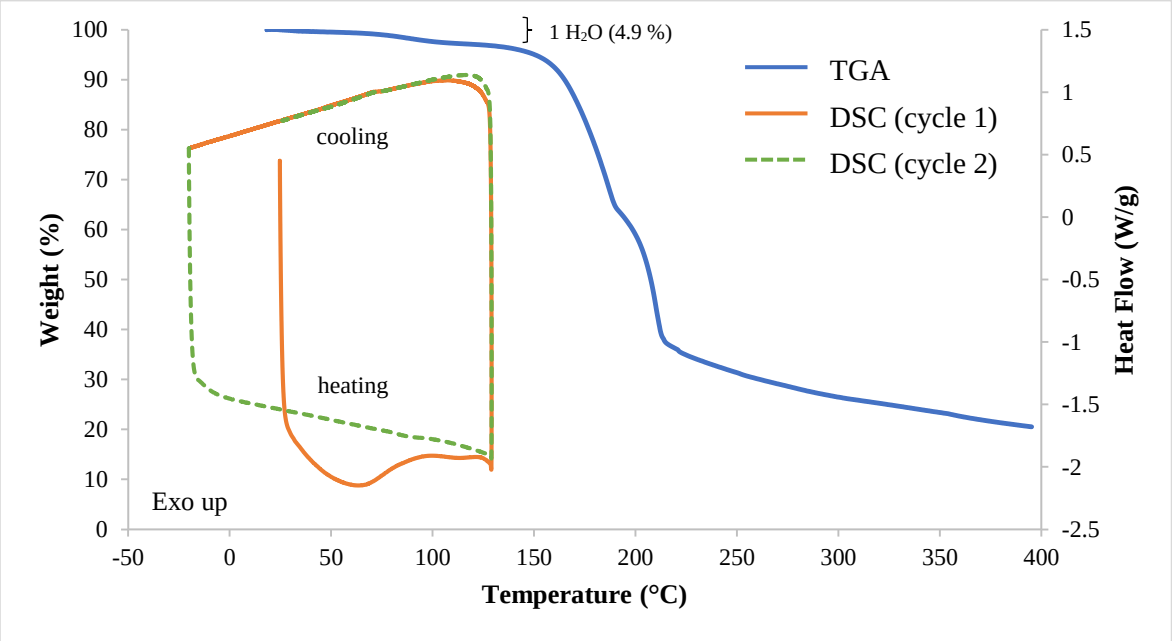

Figure S20 Thermal analysis results for the suspected salt **1-AP**. TGA trace shown in blue and DSC traces in orange (cycle 1) and green dashes (cycle 2). The endotherm in the first DSC cycle is possibly caused by solvent loss as it is not seen in the second cycle. This mass loss can also be seen in the TGA trace as a loss of 4.9% that corresponds to the mass of one water molecule (calculated as 5.2%).

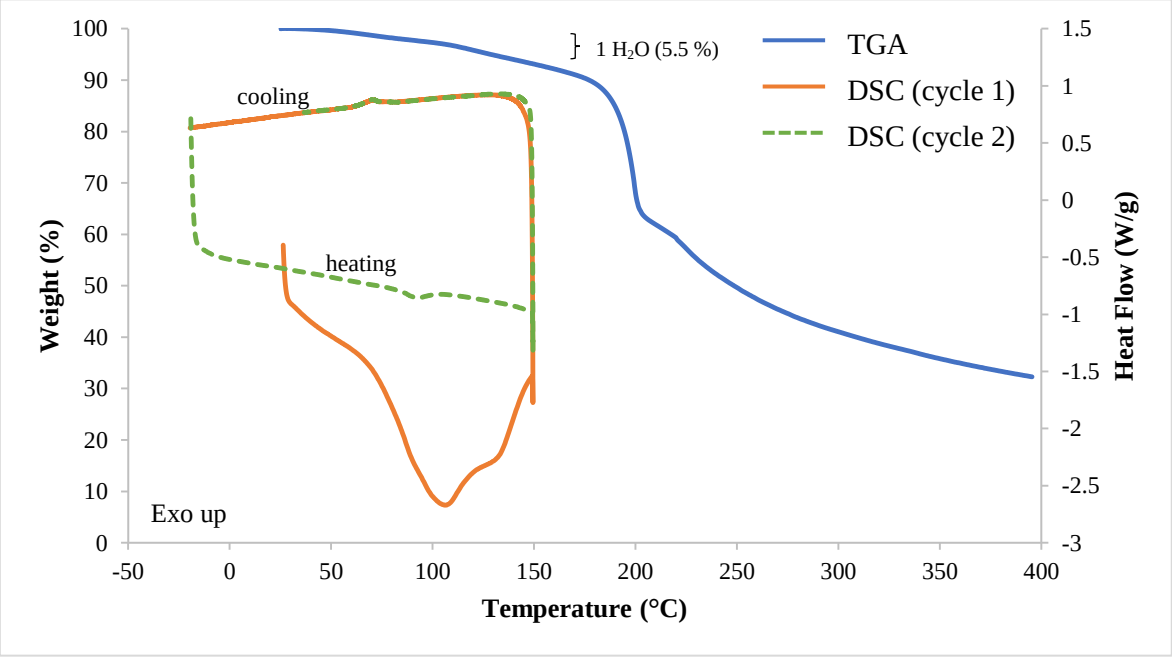

Figure S21 Thermal analysis results for the suspected salt **1-DAP**. TGA trace shown in blue and DSC traces in orange (cycle 1) and green dashes (cycle 2). The small exo- and endotherms in the DSC are due to an impurity present in the instrument. The broad endotherm in the first DSC cycle is due to slow solvent evaporation and is therefore absent in the second cycle. The TGA trace also shows a corresponding mass loss of 5.5%, which could indicate that this is a hydrated product (water calculated as 5.1%.).

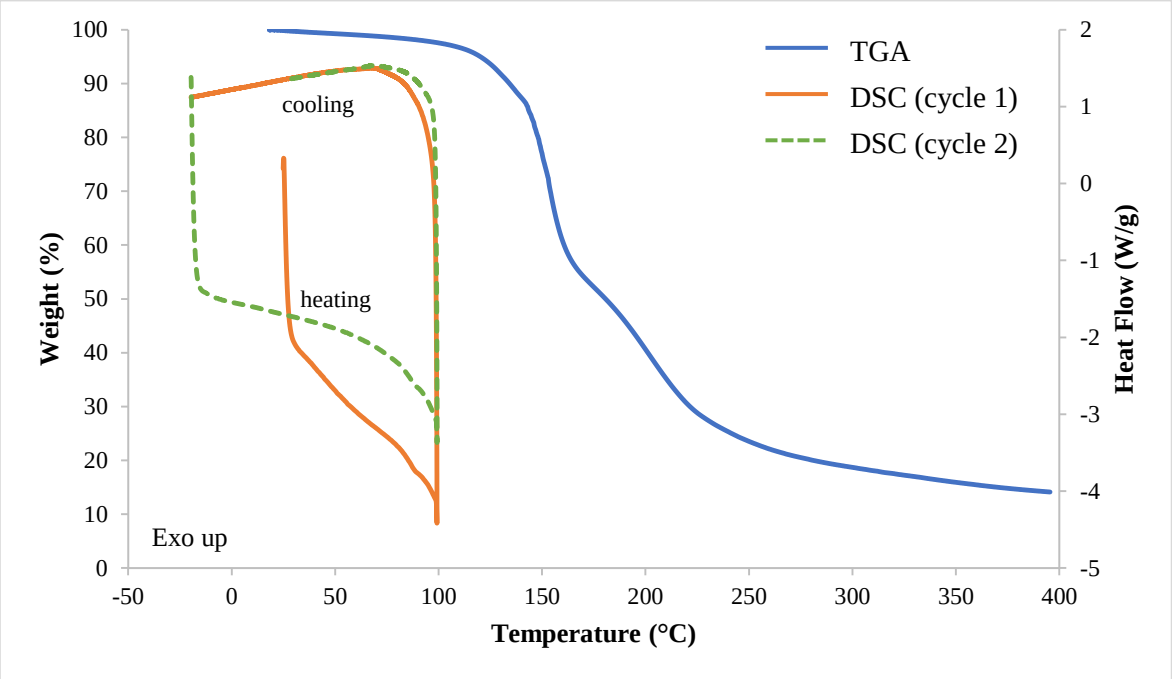

Figure S22 Thermal analysis results for the suspected salt **2-AP**. TGA trace shown in blue and DSC traces in orange (cycle 1) and green dashes (cycle 2).

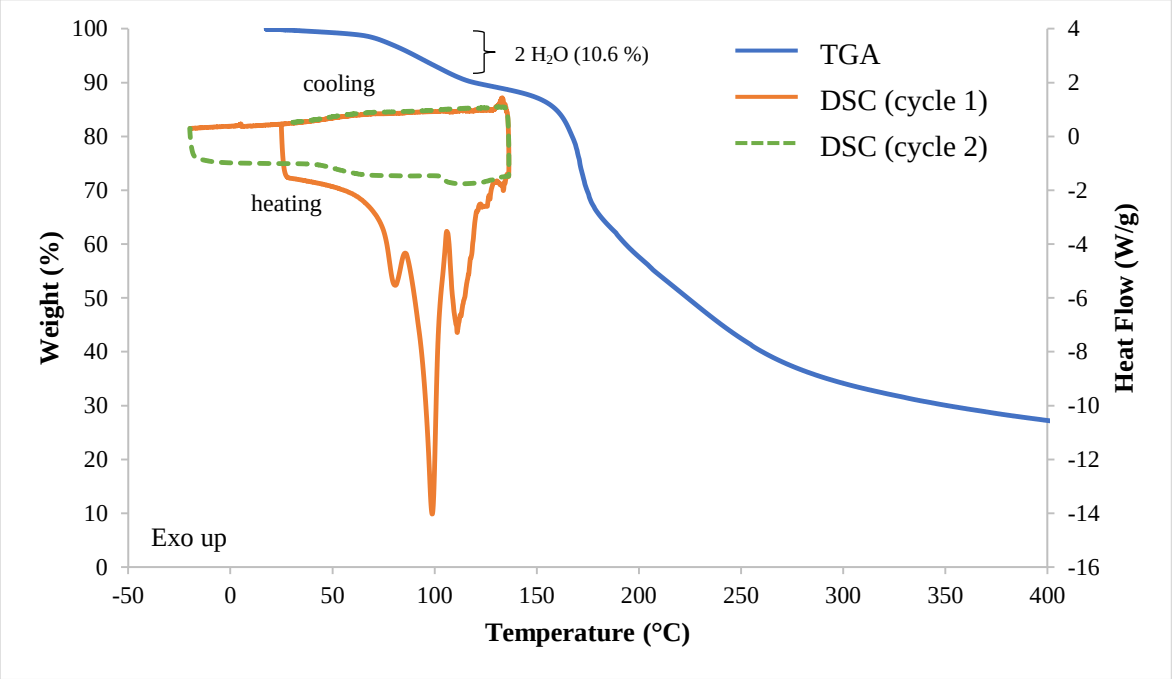

Figure S23 Thermal analysis results for the suspected salt **2-DAP**. TGA trace shown in blue and DSC traces in orange (cycle 1) and green dashes (cycle 2). The large endotherms in the first DSC cycle is due to solvent evaporation and is therefore absent in the second cycle. The TGA trace also shows a corresponding mass loss of 10.6%, which could indicate that this is a hydrated product (two water molecules calculated as 9.4%).

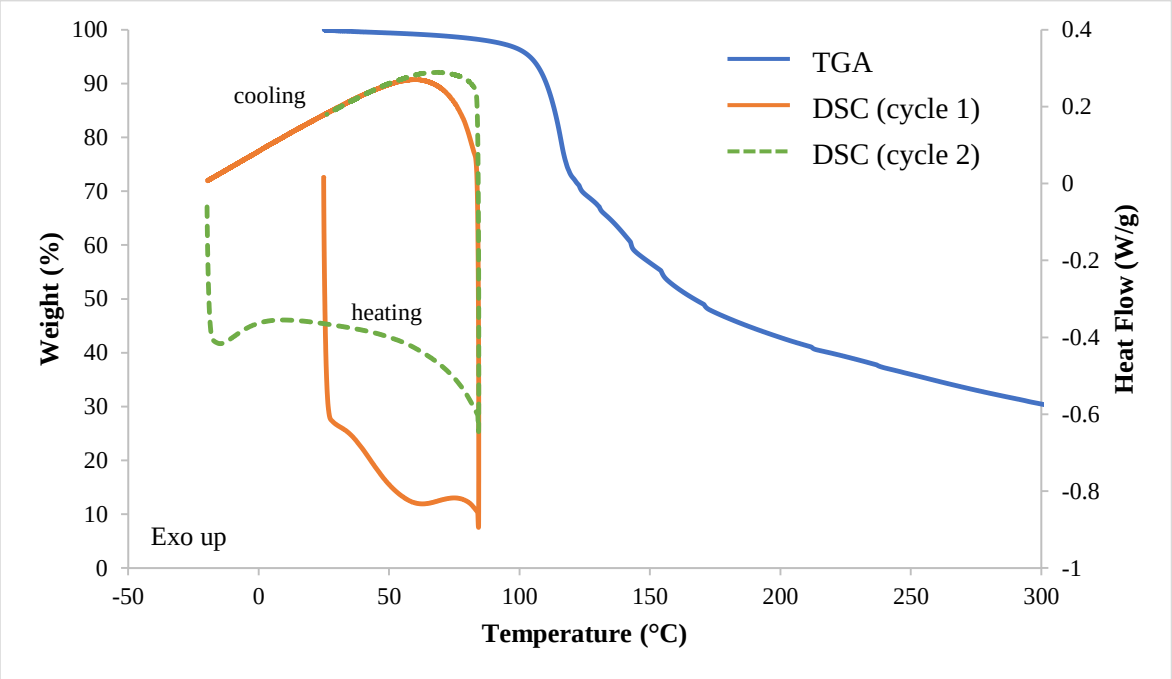

Figure S24 Thermal analysis results for the suspected salt **3-AP**. TGA trace shown in blue and DSC traces in orange (cycle 1) and green dashes (cycle 2).

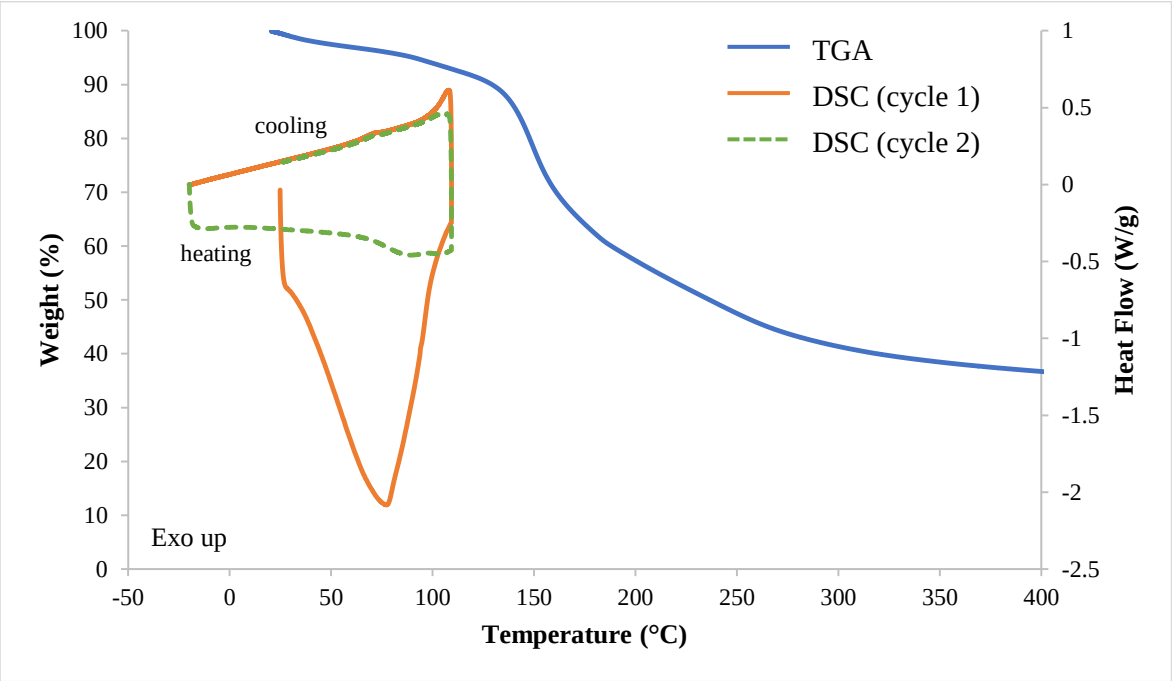

Figure S25 Thermal analysis results for the suspected salt **3-DAP**. TGA trace shown in blue and DSC traces in orange (cycle 1) and green dashes (cycle 2). The endotherm in the first DSC cycle indicates a possible mass loss. The TGA trace shows a small amount of gradual mass loss which is most likely water molecules being lost.

NMR

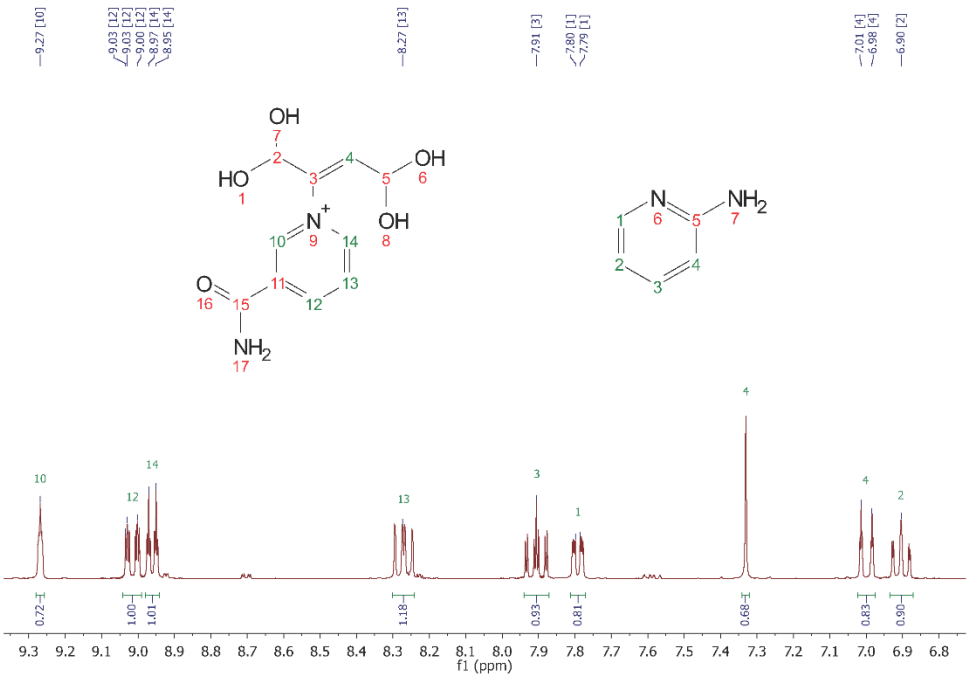

Figure S26 ^{1}H NMR spectrum (300MHz) of **1-AP** showing that both starting materials are present in the product. Peaks are referenced to the deuterium oxide peak at 4.79 ppm (not shown).

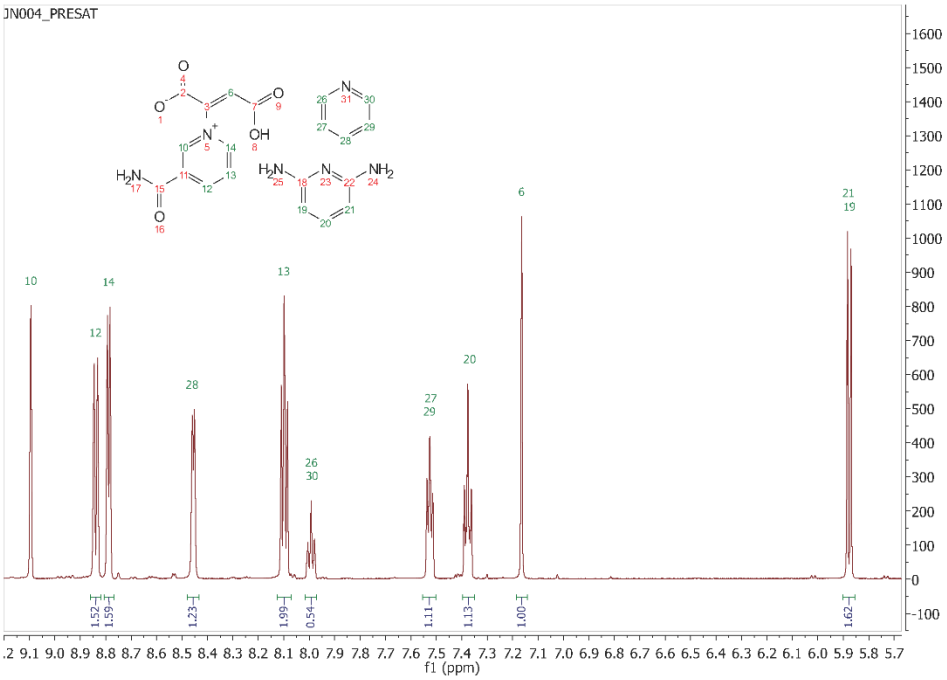

Figure S27 ^{1}H NMR spectrum (300MHz) of **1-DAP** showing that both starting materials are present in the product. A drop of pyridine was added to aid with dissolution of the sample. Peaks are referenced to the deuterium oxide peak at 4.79 ppm (not shown).

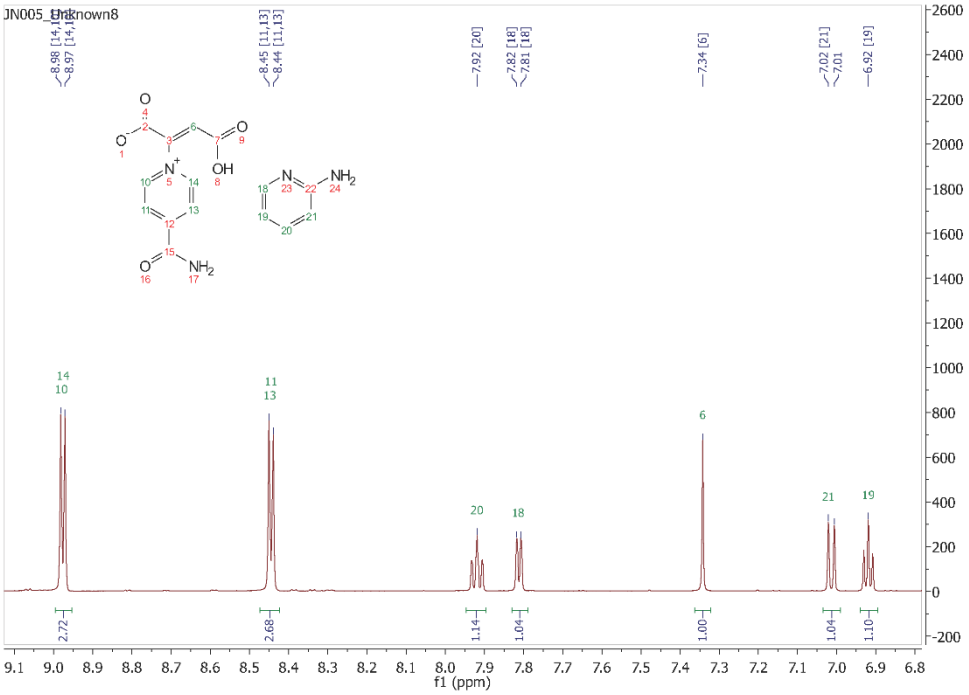

Figure S28 ^{1}H NMR spectrum (300MHz) of **2-AP** showing that both starting materials are present in the product. Peaks are referenced to the deuterium oxide peak at 4.79 ppm (not shown).

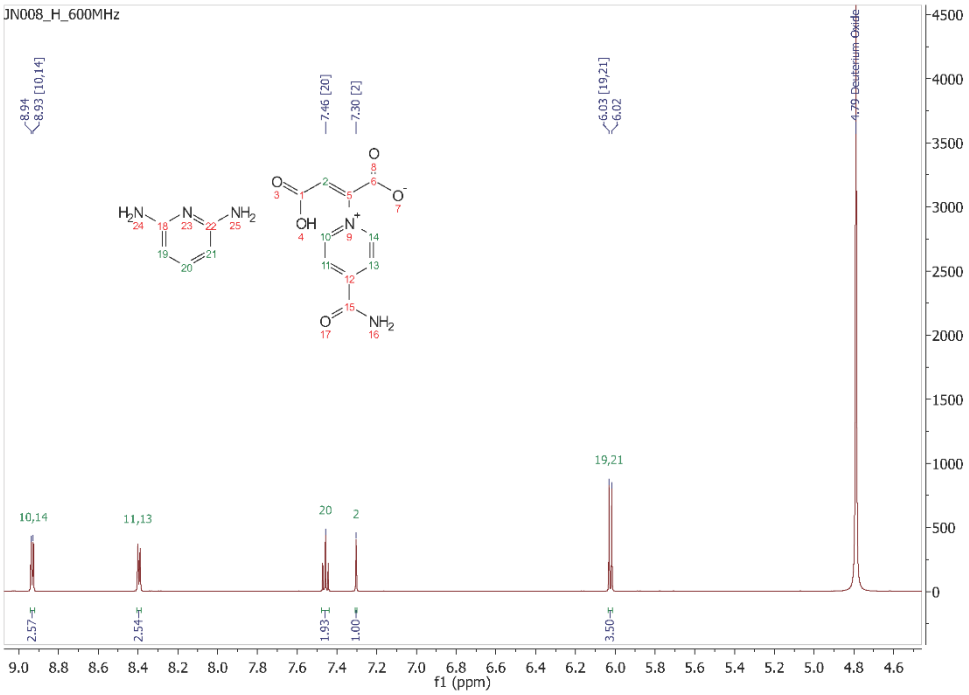

Figure S29 ^{1}H NMR spectrum (300MHz) of **2-DAP** showing that both starting materials are present in the product.

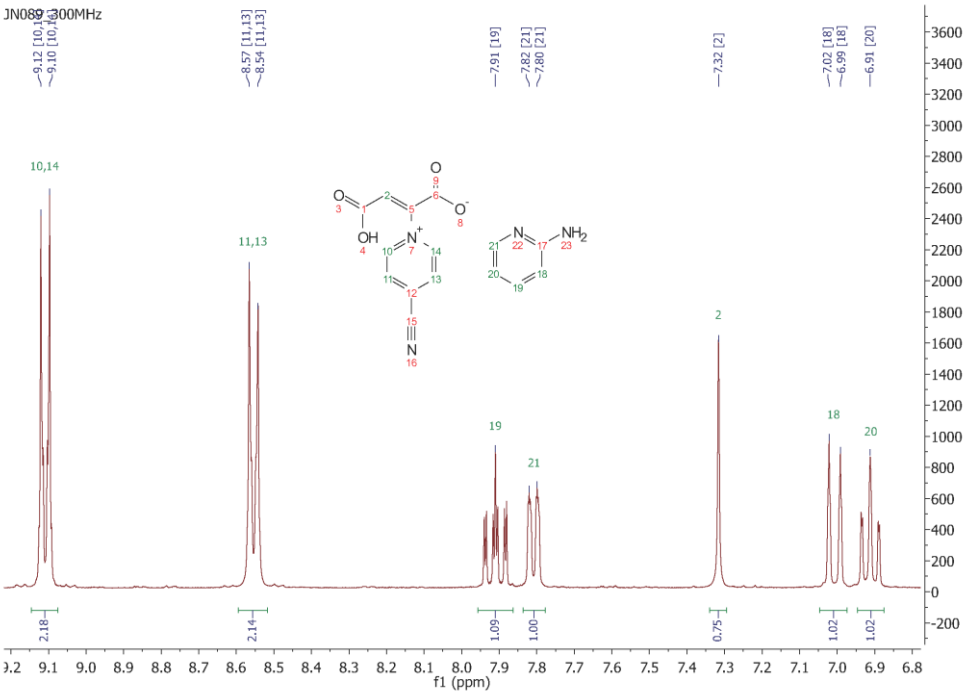

Figure S30 ^{1}H NMR spectrum (300MHz) of **3-AP** showing that both starting materials are present in the product.

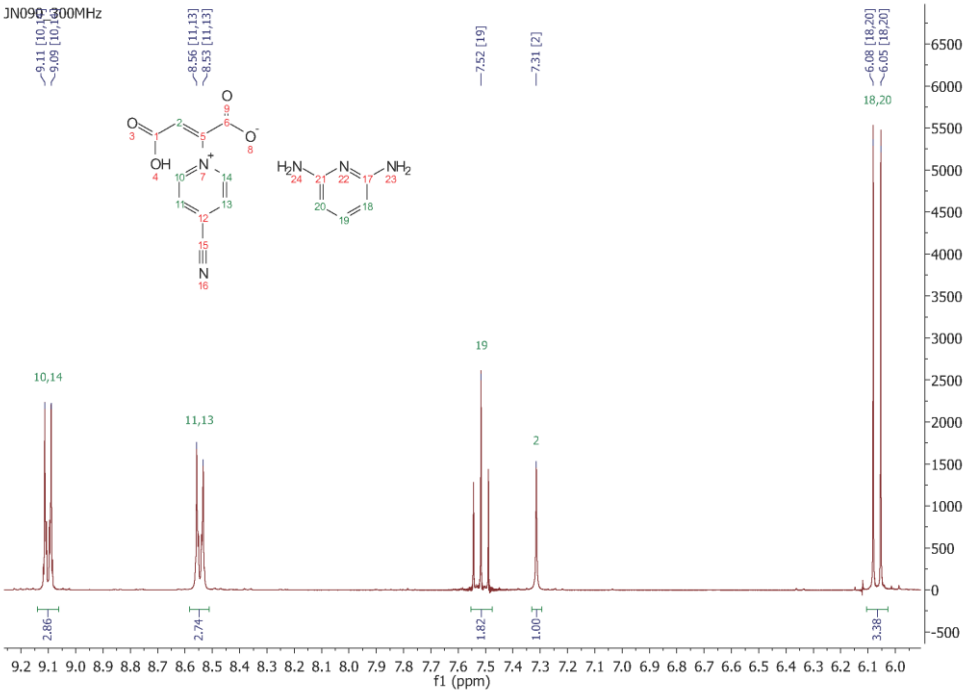

Figure S31 ^{1}H NMR spectrum (300MHz) of **3-DAP** showing that both starting materials are present in the product.

FTIR

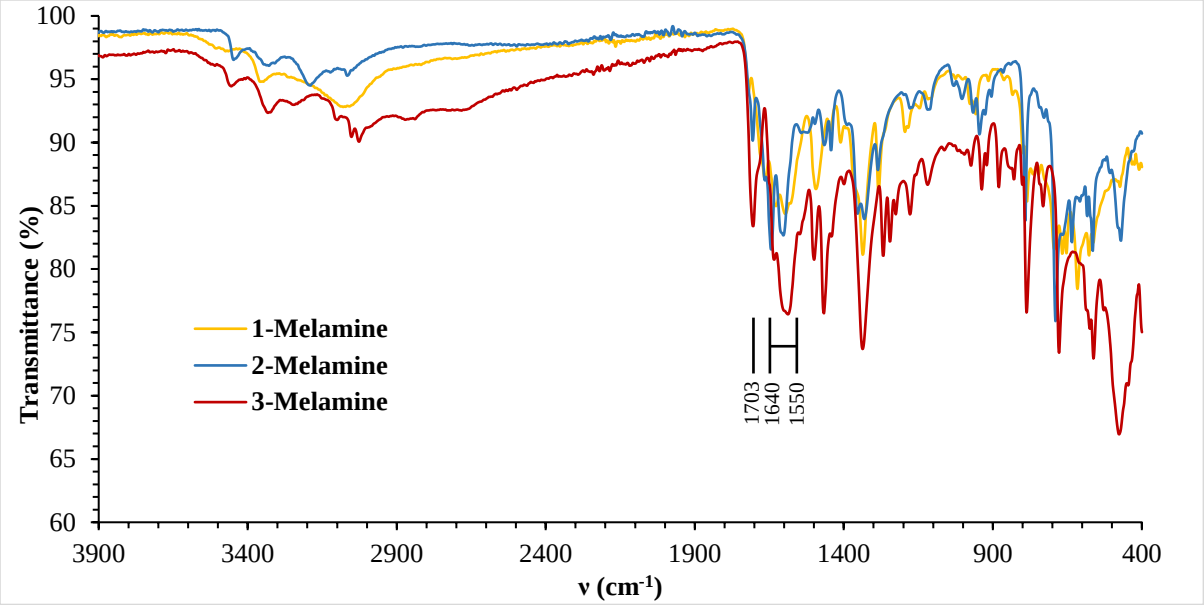

Figure S32 FTIR spectra for the three melamine salts, **1-Melamine**, **2-Melamine**, and **3-Melamine**. The region from 1550-1640 cm^{-1} represents the carboxylate C=O stretching frequencies. The weaker peaks at 1703 cm^{-1} indicate that the hydrogen atom is slightly disordered between the nitrogen and oxygen atom to give the materials a slight co-crystal character, although they are still predominantly salts.

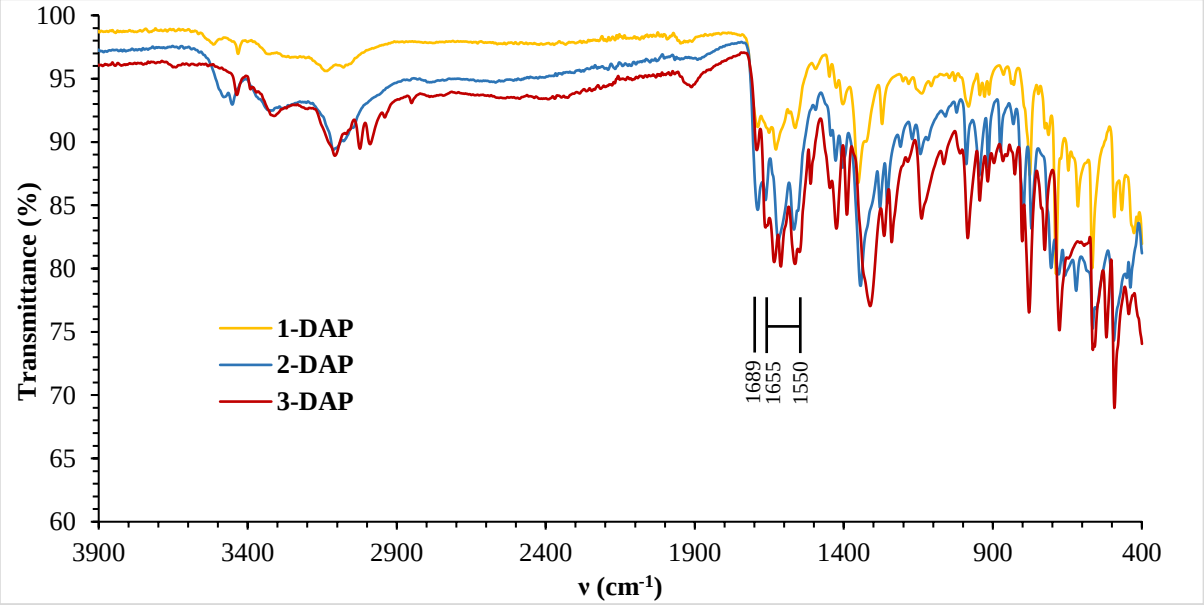

Figure S33 FTIR spectra for the three suspected 2,6-diaminopyridine salts, **1-DAP**, **2-DAP**, and **3-DAP**. The region from 1550-1655 cm^{-1} represents the carboxylate C=O stretching frequencies. The weaker peaks at 1689 cm^{-1} indicate that the hydrogen atom is slightly disordered between the nitrogen and oxygen atom to give the materials a slight co-crystal character, although they are still predominantly salts.

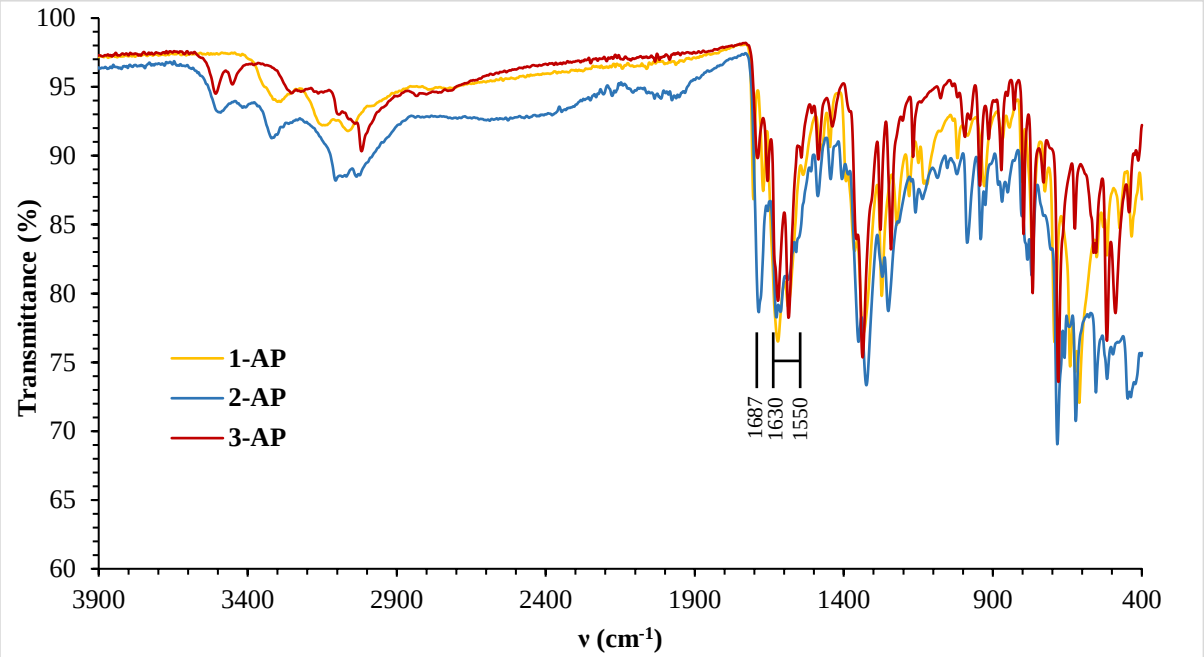

Figure S34 FTIR spectra for the three suspected 2-aminopyridine salts, **1-AP**, **2-AP**, and **3-AP**. The region from 1550-1630 cm^{-1} represents the carboxylate C=O stretching frequencies. The weaker peaks at 1687 cm^{-1} indicate that the hydrogen atom is slightly disordered between the nitrogen and oxygen atom to give the materials a slight co-crystal character, although they are still predominantly salts.

References

1 J. Lombard, D. A. Haynes and T. le Roex, *Cryst. Growth Des.*, 2017, acs.cgd.7b01271.

CHAPTER 5

SELECTIVITY BEHAVIOUR OF AN ISOSTRUCTURAL SERIES OF FRAMEWORKS

5.1 Introduction

Host-guest compounds are multicomponent supramolecular compounds in which one molecule, the guest, is smaller than the other (the host) and therefore is positioned inside a cavity or channel, either within the host molecule itself or within a framework formed by the host molecules.[1,2] The host molecules often interact with one another *via* intermolecular interactions, forming a framework with openings in which the guest molecules are located.[3] The guest can then bind to the host through intermolecular interactions (hydrogen bonds, van der Waals interactions, π-π interactions, etc.)[4] or simply fill the cavities formed due to shape complementarity.[5] Most often, the host framework is unstable without the guest and can only form in a process referred to as 'guest-induced host assembly'.[6] In cases where the guest is a solvent molecule, these compounds are also called solvates.

Host-guest compounds can display interesting properties such as porosity and selectivity. Porosity occurs when the host's stability, and therefore structure, is independent of the guest, and the guest can therefore be removed or exchanged for various others, i.e. it is a stable, permeable structure.[7] It is also useful if the host can selectively encapsulate one solvent above others from a mixture.[8] Selective hosts have potential applications in many industrial processes in which mixtures of products or by-products are obtained. If a particular framework is selective for one compound over others, selective enclathration provides an effective method for separation.[9] This is also applicable for removal of impurities or toxins.[10]

Recently, we discovered that a specific pamoate-phenanthrolinium host (Scheme 5.1)[11] can include four different, but similar in size, solvent molecules. The selectivity of this host for these solvents has subsequently been investigated. Solvent competition experiments were carried out by crystallising the host from various two-component solvent mixtures

containing calculated ratios of each solvent. Experiments were also repeated mechanochemically (specifically in a mortar and pestle) as, to our knowledge, selectivity has not yet been demonstrated in this way. In these experiments, solvent mixtures containing calculated ratios of two solvents were made up before stoichiometric quantities of the host components were ground together with a few drops of this solvent mixture.

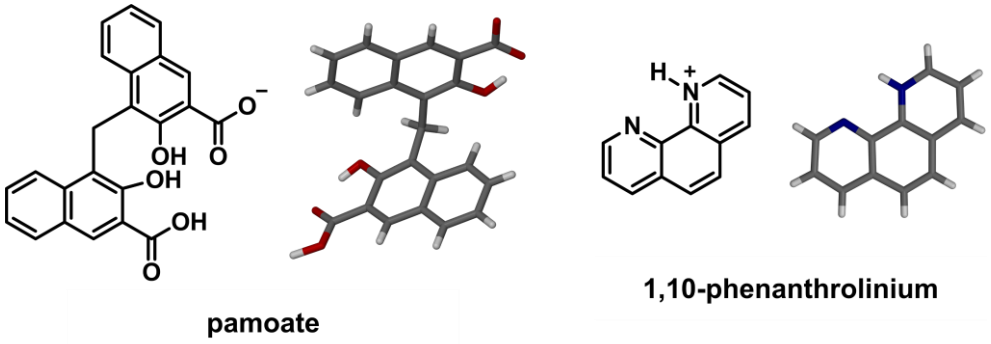

Scheme 5.1 The two components comprising the host framework, namely the pamoate and 1,10-phenanthrolinium ions.

5.2 Results

5.2.1 The isostructural solvates

A two-component organic host, the pamoate salt of 1,10-phenanthroline, was found to form four isostructural solvates. This means that the structure of the host framework is virtually independent of the solvent included, and solvates can therefore be superimposed, as their packing is nearly identical.[12] The solvents included are tetrahydrofuran (THF), dimethylformamide (DMF), dimethylacetamide (DMA), and dimethyl sulfoxide (DMSO). The DMF solvate has previously been reported in the literature (refcode: QEXJEJ)[13], while the others were obtained in our group. Crystallographic data are included in Table 5.1. These solvates can be made by dissolution of a 1:1 molar ratio of the host components in the solvent that is to be included, and can also be made mechanochemically by liquid assisted grinding, using a few drops of the relevant solvent.

Table 5.1 Crystallographic data for the solvates.

Structure	**DMA solvate**	**DMF solvate***	**DMSO solvate****	**THF solvate****
Chemical formula	$C_{39}H_{32}N_2O_7$	$C_{38}H_{31}N_3O_7$	$C_{37}H_{30}N_2O_7S$	$C_{39}H_{32}N_2O_7$
Formula weight /g mol^{-1}	655.68	641.66	646.69	640.66
Crystal system	Triclinic	Triclinic	Triclinic	Triclinic
Space group	$P\bar{1}$	$P\bar{1}$	$P\bar{1}$	$P\bar{1}$
a /Å	11.035(2)	10.699(2)	10.5540(2)	10.653(3)
b /Å	11.907(2)	11.630(2)	11.3682(2)	11.153(3)
c /Å	13.273(3)	13.421(2)	13.7388(2)	13.566(4)
α /°	81.380(2)	82.162(5)	84.165(1)	85.062(4)
β /°	70.064(2)	72.106(5)	74.550(1)	74.512(3)
γ /°	71.719(2)	72.058(5)	72.852(1)	72.396(3)
Calculated density /g cm^{-3}	1.400	1.411	1.415	1.437
Volume /Å^3	1555.0(5)	1510.4(5)	1517.71(5)	1480.6(7)
Z	2	2	2	2
Temperature /K	100(2)	100(2)	100(2)	108(2)
Independent reflections	8339	7485	7684	7068
R_{int}	0.0637	0.0974	0.0311	0.0289
R_1 [I > 2σ(I)]	0.0498	0.0503	0.0459	0.0681

* Although the structure of the DMF solvate has been published previously, data were recollected at 100 K for comparative purposes.

** Data collected by Francis Prins and Helene Wahl.

The hosts are isostructural, which means that the interactions between the components are essentially the same for all of the solvates. Most notably, the pamoate ions form very strong hydrogen bonds to each other, forming chains throughout the structure (Figure 5.1 a). Furthermore, there are π-π interactions between the pamoate and phenanthrolinium ions (Figure 5.1 b). Lastly, the phenanthrolinium ions are hydrogen bonded to the solvent molecules *via* the protonated nitrogen atom that interacts with an oxygen atom in the solvent molecule (Figure 5.2). In each case the solvent molecules are positioned in discrete pockets within the structure (two molecules per pocket), and the ASU consists of one anion, one cation, and one solvent molecule.

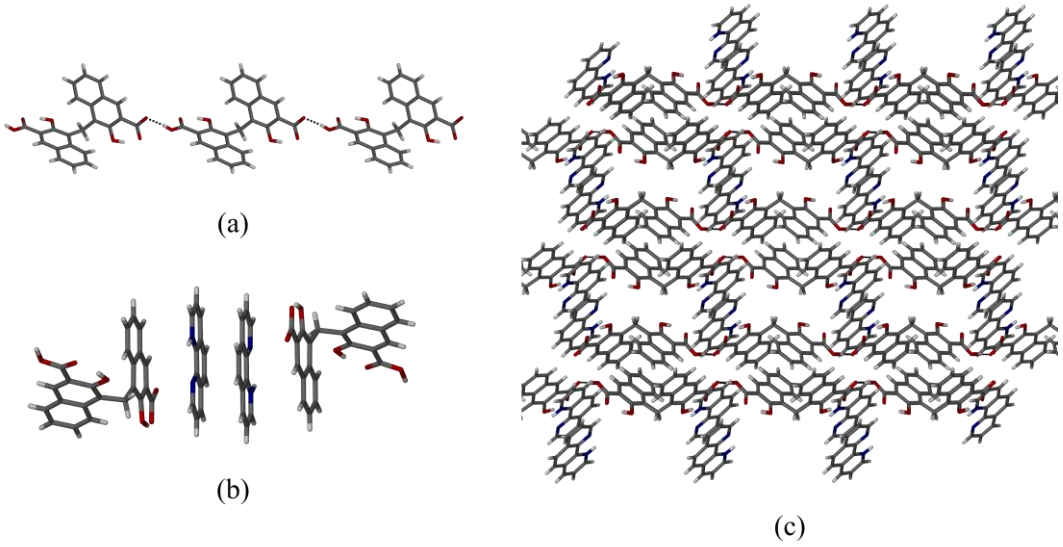

Figure 5.1 (a) The hydrogen-bonded chain of pamoate ions viewed down the *b*-axis. (b) The π-π interactions present in the host framework, viewed down [011]. (c) The host framework viewed without any solvent molecules (viewed down the *a*-axis). The host framework of the DMA solvate is used here as a representation of the isostructural series.

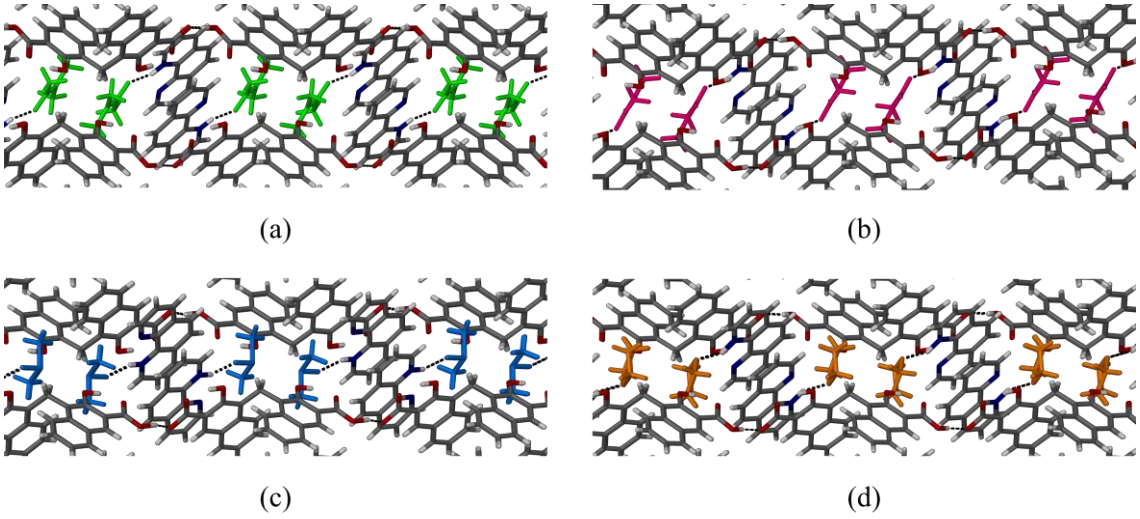

Figure 5.2 Comparison of the solvates as viewed down the *a*-axis to show the solvent pockets present in each structure. (a) The DMA solvate, (b) the DMF solvate, (c) the DMSO solvate, and (d) the THF solvate are shown. The DMSO molecules are disordered, but only the major component of the disorder is shown. The N^{+}–H···O hydrogen bond between the phenanthrolinium ions and the solvent molecule can be seen in each case.

The crystallisation conditions for the solvates had previously been established, however, they were crystallised once more to obtain the accurate NMR data that were needed for subsequent selectivity studies.

The DMA solvate was obtained by combining pamoic acid (53 mg, 0.14 mmol) with 1,10-phenanthroline hydrate (27 mg, 0.15 mmol) in 6 ml DMA at 80 °C, and stirring until the components dissolved. The vial was capped and left on a shelf for crystallisation to occur. Clear, yellow crystals formed within a week. δ_H (300 MHz, DMSO-d_6) 1.95 (3H, s), 2.78 (3H, s), 2.93 (3H, s), 4.80 (2H, s), 7.21 (2H, J = 7.9 Hz, J = 6.9 Hz, J = 0.8 Hz, ddd), 7.36 (2H, J = 8.3 Hz, J = 6.8 Hz, J = 1.4 Hz, ddd), 7.85 (4H, m), 8.04 (2H, s), 8.13 (2H, J = 8.8 Hz, d), 8.46 (2H, s), 8.58 (2H, J = 8.1 Hz, J = 1.7 Hz, dd), 9.13 (2H, J = 4.4 Hz, J = 1.75, dd).

The DMF solvate was obtained by combining pamoic acid (53 mg, 0.14 mmol) with 1,10-phenanthroline hydrate (27 mg, 0.15 mmol) in 3 ml DMF at 80 °C, and stirring until the components dissolved. The vial was capped and left on a shelf for crystallisation to occur. Clear, yellow crystals formed within 1 to 2 days. δ_H (300 MHz, DMSO-d_6) 2.72 (3H, s), 2.88 (3H, s), 4.79 (2H, s), 7.21 (2H, J = 7.9 Hz, J = 6.9 Hz, J = 0.8 Hz, ddd), 7.36 (2H, J = 8.3 Hz, J = 6.8 Hz, J = 1.4 Hz, ddd), 7.84 (4H, m), 7.95 (1H, s), 8.05 (2H, s), 8.13 (2H, J = 8.8 Hz, d), 8.46 (2H, s), 8.59 (2H, J = 8.1 Hz, J = 1.7 Hz, dd), 9.14 (2H, J = 4.4 Hz, J = 1.8 Hz, dd).

The DMSO solvate was obtained by combining pamoic acid (53 mg, 0.14 mmol) with 1,10-phenanthroline hydrate (27 mg, 0.15 mmol) in 4 ml DMF at 65 °C, and stirring until the components dissolved. The vial was capped and left on a shelf for crystallisation to occur. Clear, yellow crystals formed within a week. δ_H (300 MHz, DMSO-d_6) 2.54 (6H, s), 4.79 (2H, s), 7.21 (2H, J = 7.9 Hz, J = 6.8 Hz, J = 0.8 Hz, ddd), 7.37 (2H, J = 8.3 Hz, J = 6.8 Hz, J = 1.4 Hz, ddd), 7.86 (4H, m), 8.05 (2H, s), 8.13 (2H, J = 8.1 Hz, d), 8.46 (2H, s), 8.58 (2H, J = 8.2 Hz, J = 1.8 Hz, dd), 9.14 (2H, J = 4.4 Hz, J = 1.8 Hz, dd).

The THF solvate was obtained by combining pamoic acid (53 mg, 0.14 mmol) with 1,10-phenanthroline hydrate (27 mg, 0.15 mmol) in 8 ml THF and 0.5 ml water at 65 °C, and stirring until the components dissolved. The vial was capped and left on a shelf for crystallisation to occur. Clear, yellow crystals formed within a week. δ_H (300 MHz,

DMSO-d_6) 1.74 (4H*, m), 3.59 (4H*, m), 4.79 (2H, s), 7.21 (2H, J = 7.9 Hz, J = 6.8 Hz, J = 0.8 Hz, ddd), 7.37 (2H, J = 8.3 Hz, J = 6.8 Hz, J = 1.4 Hz, ddd), 7.86 (4H, m), 8.04 (2H, s), 8.13 (2H, J = 8.1 Hz, d), 8.46 (2H, s), 8.58 (2H, J = 8.2 Hz, J = 1.7 Hz, dd), 9.13 (2H, J = 4.3 Hz, J = 1.7 Hz, dd).

5.2.2 Competition experiments

The aim of our experiments was to determine whether the phenanthrolinium pamoate host demonstrates selectivity for any particular solvent. This was carried out by crystallising the host framework from solvent mixtures containing various mole ratios of DMA:DMF, DMA:DMSO, and DMF:DMSO, to determine whether one solvent is preferentially encapsulated. Mixtures containing THF gave irregular results because the THF solvate is not 100% occupied by THF molecules. THF also evaporates from the NMR tubes, so results were not consistent. Crystals usually formed within a few days, depending on whether the vials were left at room temperature, or in the refrigerator (4 °C). The same experiments were also repeated mechanochemically, and while the solution and mechanochemical results are similar, they do not show exactly the same selectivity. NMR analysis was used to determine the ratio of solvents that were included in the crystals. The ratios were calculated from the solvent peak intensities of at least three repeated experiments of each solvent ratio used.

5.2.2.1 Solution method

Pamoic acid (106 mg, 0.273 mmol) and 1,10-phenanthroline hydrate (54 mg, 0.272 mmol) were dissolved in a specific solvent mixture by stirring and gently heating – keeping the caps partially on to prevent evaporation. Vials were capped and left on a shelf, or in the refrigerator, for crystallisation to occur. Crystallisation times depended on the ratio of solvents used and on the crystallisation environment. Crystallisations carried out in the refrigerator occurred within 1-3 days, while room temperature crystallisations occurred more slowly. In each case, a small amount (13 mg) of the crystalline product was patted dry using filter paper, crushed, and dissolved in 0.6 ml DMSO-d_6 before analysis *via* ^{1}H NMR

* These peaks represent the eight hydrogen atoms of THF, however the integrals do not add up to this total as the THF solvate is not fully occupied by solvent molecules.

(300 MHz). The relative intensities of the solvent peaks were used to determine the ratio of the included solvents.

5.2.2.2 Mechanochemical method

Pamoic acid (53 mg, 0.137 mmol) was combined with 1,10-phenanthroline hydrate (27 mg, 0.136 mmol) and ground together with a mortar and pestle for 10 minutes while adding a few drops of the solvent mixture. A small amount (13 mg) of the crystalline product was dissolved in 0.6 ml DMSO-d_6 and analysed *via* ^{1}H NMR (300 MHz). The relative intensities of solvent peaks were used to determine the ratio of the included solvents.

5.2.2.3 Selectivity results

The DMA:DMF and DMF:DMSO selectivity experiments that were carried out at room temperature took longer than seven days to crystallise, therefore these results were omitted, as external factors such as solvent evaporation would start to have an effect. On the other hand, for the DMA:DMSO selectivity experiments, crystals grown in the refrigerator and at room temperature gave indistinguishable results, and thus these results were all combined.

DMA:DMF selectivity experiments indicate that the host preferentially includes DMA over DMF when crystals are grown from solution, or when the compound is formed mechanochemically, except at very low mole fractions of DMA where there is no notable selectivity observed (Figure 5.2). The DMA:DMSO selectivity experiments (both in solution and mechanochemically) indicate that the host selectively includes DMSO when the solution contains mostly DMSO. When the crystallisations are carried out in solution, the host also shows selectivity for DMA when the solution contains mostly DMA. However, when experiments are carried out mechanochemically, the host shows no notable selectivity at higher concentrations of DMA (Figure 5.3). The DMSO:DMF selectivity experiments indicate that the host preferentially includes DMSO over DMF, more so when the solvates were formed mechanochemically than in solution (Figure 5.4).

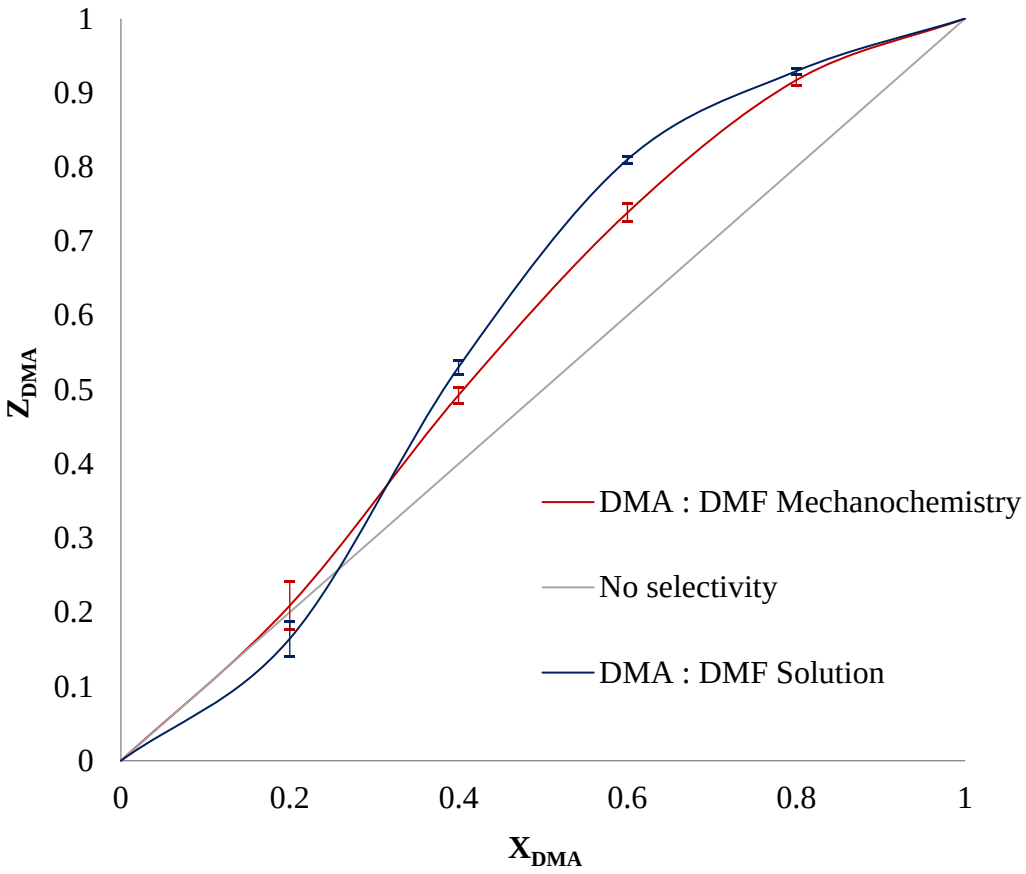

Figure 5.2 DMA:DMF selectivity plot for crystallisations performed in the refrigerator (blue) and mechanochemically (red). X_{DMA} represents the mole fraction of DMA in the solvent mixture and Z_{DMA} is the measured mole fraction of DMA in the crystals. Error bars indicate the standard deviation of at least three repeated experiments. There is a definite selectivity towards DMA over DMF in both the solution and mechanochemical experiments.

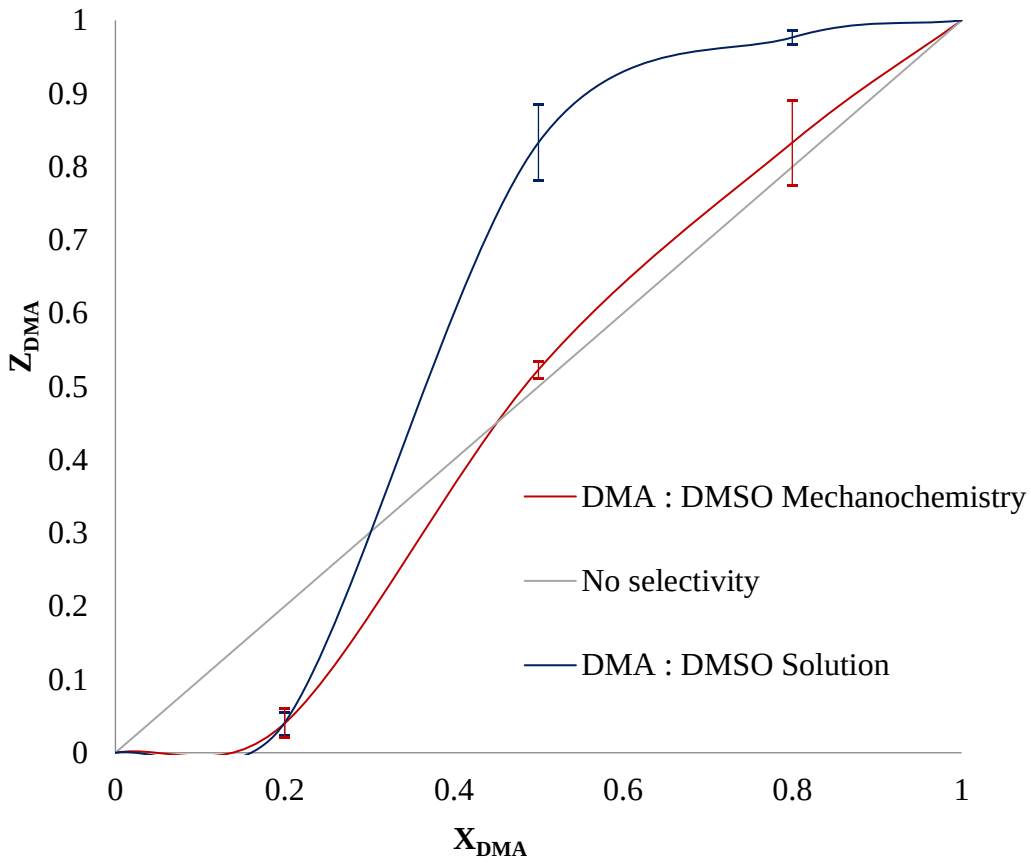

Figure 5.3 DMA:DMSO selectivity plot for crystallisations performed in the refrigerator and at room temperature (blue) as well as mechanochemically (red). X_{DMA} represents the mole fraction of DMA in the solvent mixture and Z_{DMA} is the measured mole fraction of DMA in the crystals. Error bars indicate the standard deviation of at least three repeated experiments. For both sets of experiments the host shows selectivity towards DMSO when the solution contains mostly DMSO. When the crystallisations are carried out in solution, the host also shows selectivity for DMA when the solution contains mostly DMA. However, when experiments are carried out mechanochemically, the host shows no selectivity at higher concentrations of DMA

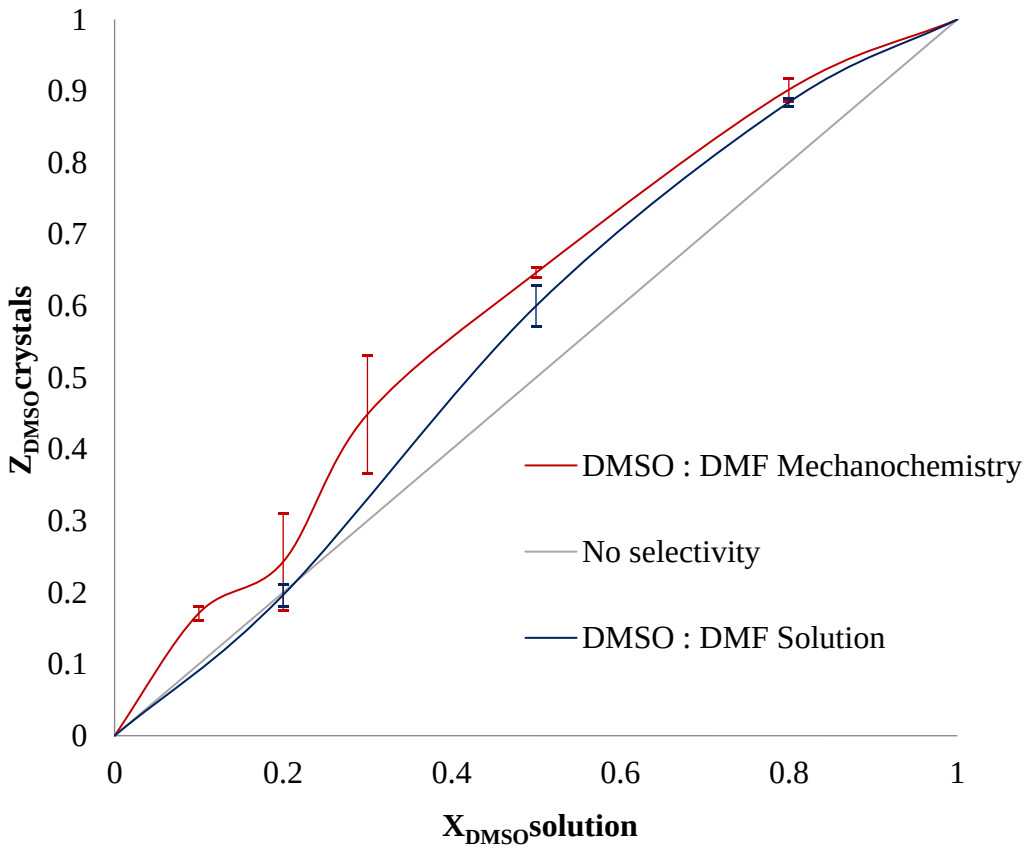

Figure 5.4 DMSO:DMF selectivity plot for crystallisations performed in the refrigerator (blue) and mechanochemically (red). X_{DMSO} represents the mole fraction of DMSO in the solvent mixture and Z_{DMSO} is the measured mole fraction of DMSO in the crystals. Error bars indicate the standard deviation of at least three repeated experiments. There is a selectivity for DMSO over DMF, more so when the solvates were formed mechanochemically.

5.2.3 Structural comparisons

In order to rationalise the selectivity observed in the competition experiments, an investigation of the relevant intermolecular interactions in the structures was carried out. The N^+–H···O hydrogen bond between the phenanthrolinium ions and the solvent molecules can give us information about the interaction between the host and guest. The hydrogen-bond lengths between host and guest are 2.662(2), 2.609(2) and 2.589(3) Å for the DMF, DMA, and DMSO solvates respectively (Table 5.2). Although all three hydrogen bonds are strong, and the difference between them not very large, the DMF solvate has the longest, and therefore possibly the weakest,[14] hydrogen bond between host and guest.

The corresponding interaction energy between the phenanthrolinium ion and the solvent molecule was calculated in each case using the program CrystalExplorer 17.5.[15] The Tonto computational chemistry package was used for wavefunction calculations,[16] which makes use of the B3LYP/6-31G(d,p) level of theory. For the DMF solvate the interaction energy was calculated to be -16.6 kJ mol^{-1}, while for the DMA and DMSO solvates the interaction has an energy of -20.6 and -19.6 kJ mol^{-1} respectively (Table 5.2). The interaction with DMF is thus less favourable than that with DMA and DMSO, both of which have similar interaction energies with the host.

Table 5.2 Summary of the hydrogen bond length and interaction energy between the host and guest in the solvates, as well as the calculated densities of the solvates.

	DMF solvate	**DMA solvate**	**DMSO solvate**
N^+–H···O hydrogen bond length (Å)	2.662(2)	2.609(2)	2.589(3)
Host-guest interaction energy (kJ mol^{-1})	-16.6	-20.6	-19.6
Density (g cm^{-3})	1.411	1.400	1.415

5.3 Discussion and Conclusion

The ability of a 1,10-phenanthrolinium pamoate host to preferentially include one solvent above others in a mixture, has been demonstrated. The host preferentially includes DMA above DMF for all ratios of DMA:DMF except at very low concentrations of DMA where there is no significant selectivity. This is true whether the solvates are obtained from

solution, or obtained mechanochemically. When exposed to mixtures of DMSO and DMF, the host framework shows a slight but definite preference for DMSO above DMF – more so when the solvates are obtained *via* mechanochemical methods. When exposed to mixtures of DMA and DMSO, the preference of the host is not as clear-cut: when crystal are obtained from solution, the host displays concentration dependant selectivity i.e. the host is selective for DMA at high concentrations of DMA, and selective for DMSO at high concentrations of DMSO. When the competition experiments are carried out by mechanochemistry the selectivity shown by the host is less pronounced, as the host is only selective for DMSO at high concentrations of DMSO, and shows no selectivity at high concentrations of DMA.

The reason behind this selectivity has been investigated. The solvent molecules (DMA, DMF, and DMSO) are similar in size, and are included into the host to produce solvates of similar densities (1.400, 1.411, and 1.415 g cm^{-3} respectively). The selectivity must then stem from the strength and nature of the host-guest interactions.

A study of the intermolecular interactions (specifically between the positively charged nitrogen atom of the phenanthrolinium ion and an oxygen atom in the solvent molecule) was carried out. The hydrogen bond between the phenanthrolinium ion and DMF is slightly longer than the equivalent hydrogen bonds in the other two solvates. The interaction energy between the two interacting molecules in the DMF solvate is also weaker than the others. These two observations could explain why DMA and DMSO are selectively included above DMF. The DMA and DMSO solvates are also shown to be very similar with respect to their host-guest interactions, which explains why a clear preference between the two was not observed. The slightly different solution and mechanochemistry results could potentially be caused by a difference in temperature (heating for dissolution *vs* frictional heating), or by the effect of large amounts *vs* small amounts of solvent (more solvent-solvent and solvent-host interactions in solution).

To our knowledge, this is the first time mechanochemistry has been used to demonstrate selectivity. As the mechanochemical results differ slightly from those in solution, it would be interesting to see how the results of other competition experiments previously reported in the literature, might be altered by using this method. Additionally this may aid in determining the reason behind the difference in selectivity.

5.4 References

1 D. Cram, *Science*, 1988, **240**, 760–767.

2 J. Dowden, J. D. Kilburn and P. Wright, *Contemp. Org. Synth.*, 1995, **2**, 289–314.

3 W. Yan, X. Yu, T. Yan, D. Wu, E. Ning, Y. Qi, Y.-F. Han and Q. Li, *Chem. Commun.*, 2017, **53**, 3677–3680.

4 M. Lohse, K. Nowosinski, N. L. Traulsen, A. J. Achazi, L. K. S. von Krbek, B. Paulus, C. A. Schalley and S. Hecht, *Chem. Commun.*, 2015, **51**, 9777–9780.

5 I. Neogi, A. Bajpai, G. Savitha and J. N. Moorthy, *Cryst. Growth Des.*, 2015, **15**, 2129–2136.

6 E. Weber, in *Encyclopedia of Supramolecular Chemistry*, eds. J. L. Atwood and J. W. Steed, Marcel Dekker, Inc., New York, 2004, pp. 261–273.

7 L. J. Barbour, *Chem. Commun.*, 2006, 1163–1168.

8 L. R. Nassimbeni, *Acc. Chem. Res.*, 2003, **36**, 631–637.

9 P. Li, Y. He, J. Guang, L. Weng, J. C. G. Zhao, S. Xiang and B. Chen, *J. Am. Chem. Soc.*, 2014, **136**, 547–549.

10 C. García-Simón, M. Garcia-Borràs, L. Gómez, T. Parella, S. Osuna, J. Juanhuix, I. Imaz, D. Maspoch, M. Costas and X. Ribas, *Nat. Commun.*, 2014, **5**, 5557–5566.

11 H. Wahl, PhD thesis, Stellenbosch University, 2014.

12 M. Caira, in *Encyclopedia of supramolecular chemistry*, eds. J. L. Atwood and J. W. Steed, Marcel Dekker, Inc., New York, 2004, pp. 767–770.

13 T.-M. Shang, Q.-F. Zhou and J.-H. Sun, *Acta Crystallogr. Sect. E Struct. Reports Online*, 2007, **63**, o506–o508.

14 M. L. Huggins, *J. Am. Chem. Soc.*, 1953, **75**, 4126–4133.

15 M. J. Turner, S. K. McKinnon, D. J. Wolff, P. R. Grimwood, D. Spackman, D. Jayatilaka and M. A. Spackman, *CrystalExplorer17(2017)*, University of Western Australia. http://hirshfeldsurface.net.

16 Tonto, A Fortran Based Object-Oriented System for Quantum Chemistry and Crystallography, D. Jayatilaka and D. J. Grimwood, *Computational Science - ICCS* 2003, **4**, 142-151.

CHAPTER 6

SUMMARY AND CONCLUDING REMARKS

An investigation into the solid-state forms that materials can adopt is a worthwhile endeavour, as the form obtained after synthesis is not always the one that is most useful. Without further examination, one could think something is not of value. However, further investigation could reveal polymorphs or multi-component crystals with improved properties for the intended application. In this study, polymorphism and the formation of multi-component crystals was investigated, as well as the effect thereof on the structure and properties of certain zwitterionic organic molecules. Furthermore, the structure-property relationships of another organic host have also been studied by investigating the selectivity of the host for different guests, and correlating these results with the solid-state structures. Here follows a short summary of the results obtained:

- Four zwitterions were successfully synthesised by reacting acetylenedicarboxylic acid with nicotinamide, isonicotinamide, 4-cyanopyridine, and pyridine.
- Two of the zwitterions have salt by-products that can also form. These are the kinetic products of the zwitterion-formation reactions.
- Chapter 3 describes the polymorphic behaviour of the known 4-cyanopyridine (**1**) and pyridine (**2**) zwitterions. The first exists as two forms, while the latter has three different polymorphs. The solid-state behaviour of all forms was investigated, as well as the relationships between them. We report on the factors influencing which polymorph forms as well as the structural changes that occur.
- Chapter 4 reports on the two new nicotinamide (**1**) and isonicotinamide (**2**) zwitterions. The solid-state behaviour of these zwitterions was investigated, as well as their ability (and inability) to form multi-component crystals. Zwitterions **1** and **2** (as well as the 4-cyanopyridine zwitterion discussed in the previous chapter) form salts with melamine, as well as suspected salts with 2-aminopyridine and 2,6-diaminopyridine. Salts are compared with regards to their intermolecular interactions.

- Chapter 5 describes an isostructural series of solvates formed by the 1,10-phenanthrolinium-pamoate host, namely a DMA, DMF, DMSO, and THF solvate. The selectivity of this host, for these particular solvents, has been demonstrated when it crystallises from solution, as well as when the solvates are formed mechanochemically. The host shows selective encapsulation of DMA and DMSO above DMF, using both these methods. This selectivity has been rationalised by a comparison of the structures.

6.1 Obstacles

Throughout a research project, results (or the lack thereof) are heavily influenced by the problems that are encountered – whether these can be overcome or not. It is thus important to discuss these obstacles if a clear picture of the work is to be obtained.

The majority of the problems experienced during this project were caused by solubility. The first instance where this was problematic was during initial synthesis of the zwitterions. The acetylenedicarboxylic acid starting material is not very soluble, so this reduced the number of solvents and solvent mixtures that could practically be used during synthesis. To dissolve the starting materials, the solvent mixtures had to contain either methanol, ethanol, water, DMF, or DMSO. The last three of these have very high boiling points, which meant that it took a very long time for crystals to grow from these solutions, as crystals were grown *via* slow evaporation of the solvent.

An even bigger problem was the insolubility of the zwitterions themselves. None of the zwitterions dissolve in any common laboratory solvent – dissolution has only been achieved in water near boiling point. In addition, once the zwitterion is dissolved, it remains in solution until almost all the water has evaporated and the zwitterion precipitates out as a fine powder. This is quite unusual. Recrystallisation and co-crystallisation experiments were therefore very challenging, especially since most organic co-formers are highly soluble in water and therefore in discord with the zwitterions. The addition of a weak base, such as pyridine, could be used to aid dissolution of the zwitterions in water so that lower temperatures could be used, but in those cases the zwitterion remained in solution even longer, with no formation of crystals at all.

This may be one of the practical reasons why more multi-component crystals were not discovered (Chapter 4). The salts that were discovered were first observed from LAG screening experiments, of which only three could be crystallised. There are a total of six other salts that we suspect were also formed, but which could not be crystallised as single crystals. In addition, because the powders of these suspected salts were obtained from grinding experiments, they were slightly amorphous. Such materials do not produce well resolved powder X-ray diffraction data, which would be needed for structure solution from powder data.

Nevertheless, a smooth ride does not leave much room for learning, and it is through the challenges that we learn most about the nature and behaviour of molecules, and are forced to discover the usefulness of new techniques, such as mechanochemistry.

6.2 Mechanochemistry

Mechanochemistry was used throughout this project as it is a simple and fast technique that can be used to obtain a product within a few minutes. Unfortunately, the zwitterions could not be made in this way as more energy (heat) is needed to form this thermodynamic product. It would be interesting and useful to see if the synthesis would be successful if the vessel could somehow be heated during grinding. On the other hand, the salts can easily be made *via* grinding. Liquid-assisted grinding also proved to be a very effective screening tool when attempting to form multi-component crystals, especially since it is not affected as much as the solution methods are by the insoluble nature of the zwitterion. Not only that, it is significantly faster than waiting for the zwitterion to dissolve and then waiting up to a few weeks for the product to form, if ever. All salts can quickly be obtained *via* LAG. In the case of the three melamine salts, these powders can then be recrystallised to obtain single crystals, as the salts have improved solubility compared to the zwitterions. Unfortunately, crystals could not be obtained for the combinations of zwitterions with 2-aminopyridine and 2,6-diaminopyridine.

The four isostructural solvates formed by the phanthrolinium-pamoate host can also easily be formed mechanochemically. Additionally, mechanochemistry is shown to be very useful for selectively encapsulating solvents – to our knowledge, this has not been reported before. The selectivity results obtained, after grinding the host components in solvent mixtures, are not exactly the same as those obtained when crystals are formed from solution. We do not

yet fully understand why the results differ, but it should become clear as more selectivity studies are carried out in this way. Furthermore, it would be interesting to compare these selectivity results with those that could be obtained if experiments were performed in a mechanical mill.

6.3 Temperature

The reaction initially used to synthesise the zwitterions is straightforward, but in most cases temperature dependent. Mild to high reaction temperatures are needed for the covalent bond to form between the pyridine moiety and the carboxylate backbone. When lower reaction temperatures are used, or solutions are left to crystallise in the refrigerator, a salt of the two reaction components often forms – this is the kinetic product of the reaction. In some instances, the salt can even start to form at room temperature as it forms significantly faster than the zwitterion. However, if the salt is removed after a few hours by filtration, the zwitterion will proceed to form (unless the vial is left in the refrigerator, in which case the salt will form again). For this reason, it has also not been possible to synthesise the zwitterions mechanochemically as we do not have the instrumentation to heat while grinding. It should be noted that some zwitterions have no such salt by-product, and will therefore crystallise even in the refrigerator. In these cases, mechanochemical synthesis was found to leave the starting materials unaffected.

It is not clear why some zwitterions do not have a matching kinetic product. It could be that the packing of a salt would be too unfavourable, but this is unlikely due to the small size of the components and their complementary functional groups. You might think that this is due to zwitterion formation being more favourable in these cases, but why then can they not form mechanochemically? It seems most likely that the lack of salt formation is due to the pH of the solution not promoting proton transfer, but what about mechanochemical salt formation? An in-depth study regarding the thermodynamic *vs* kinetic relationship between the zwitterion and salt has not yet been carried out.

In the case of the phenanthroline-pamoate solvates, crystallisation does not seem to be temperature dependant. The solution selectivity experiments were often crystallised both at room temperature and in the refrigerator, with minimal deviation in the results. However, the difference between the mechanochemistry and solution results could possibly be linked to temperature. The solution experiments were heated for dissolution, while the only heat

present in the mechanochemical experiments was the localised frictional heating caused by the grinding process. It is not clear how or why this would affect the outcome of selectivity studies, but as it is a significant experimental difference, we suspect it could have an effect.

6.4 Guest inclusion

During the initial zwitterion synthesis, various solvents and solvent mixtures were used to test the effect thereof on the polymorphic behaviour of the zwitterions. However, we also performed these extensive tests to see whether certain solvent molecules could be included into the structures – which could lead to studies in solvent selectivity and porosity. Although similar zwitterions have shown such inclusion behaviour,[1] none of the zwitterions in this study crystallise as solvates, and only the isonicotinamide zwitterion crystallises as a hydrate.

When these zwitterions crystallise they form very strong hydrogen bonds and charge-assisted hydrogen bonds with each other. In each case, the carboxylate backbones of the zwitterions hydrogen bond to one another to form chains of zwitterions. In some instances, these hydrogen bonds are so strong that they seem to mimic covalent bonds – forming polymer-like strings. While we did not necessarily expect to break these strong chains, the idea was that solvent molecules could occupy the space between them. The nicotinamide and isonicotinamide zwitterions were chosen for this study because of their additional amide functionalities. We thought that these amide groups could interact with each other, to keep the zwitterion chains further apart and thus leaving space for solvent molecules, or possibly interact with solvent molecules. Unfortunately, instead of keeping the framework open, these interactions only serve to hold the chains of each ladder even more tightly together to form close-packed structures. It seems as though the interactions between the zwitterions themselves are merely stronger than any possible interaction they could have with solvent molecules.

Of course, shape complementarity also plays an important role in solvate formation and it is possible that there is simply no stable way for the zwitterions and solvent molecules to interlock closely enough. Solvent molecules are often located in pockets or channels within a host framework; in the case of these zwitterions, they may just be too small to form a supporting framework. Previous zwitterions that showed solvent inclusion had longer pyridyl groups between which solvent molecules are positioned.

On the other hand, the phenanthrolinium-pamoate host framework is more inclined to include solvent molecules, and can even do so selectively. The molecules comprising the host are both larger than the zwitterions, so it makes sense that such a framework could include guest molecules. This host can include four different solvents, namely DMA, DMF, DMSO and THF. The solvent molecules are located in pockets within the framework and are hydrogen bonded to the host (specifically the phenanthrolinium ion) *via* the oxygen atom in the solvent. As the guest molecules are all very similar, the host is able to retain its geometry irrespective of the guest. When the host is crystallised from mixtures of DMA, DMF and DMSO, it preferentially includes DMA and DMSO above DMF. We suspect that this selectivity is due to the weaker host-guest interaction between the host and DMF compared to the DMA- and DMSO solvate host-guest interactions.

6.5 Polymorphism and multi-component crystals

Chapter 3 describes the polymorphic nature of two zwitterions (Figure 6.1). We are able to control which form is obtained, and have studied the relationships between them by examining experimental data, as well as carrying out some supportive calculations. The zwitterion derived from 4-cyanopyridine (**1**) exists as a pair of conformational polymorphs. The first, **1α**, is the kinetic polymorph that forms quickly, and is less stable than **1β**. The second polymorph, **1β**, forms more slowly and is stabilised due to additional weak π-π interactions between overlapping aromatic rings. On the other hand, zwitterion **2**, derived from pyridine, exists as three distinct forms, **2α**, **2β** and **2γ**. In this case the polymorphs do not differ greatly with respect to stability – although they are characterised by a slight change in conformation, they are not conformers. Even though zwitterion **2** is not solvated, the conformation of each polymorph is determined by the solvents used during crystallisation (possibly due to some sort of templating effect).

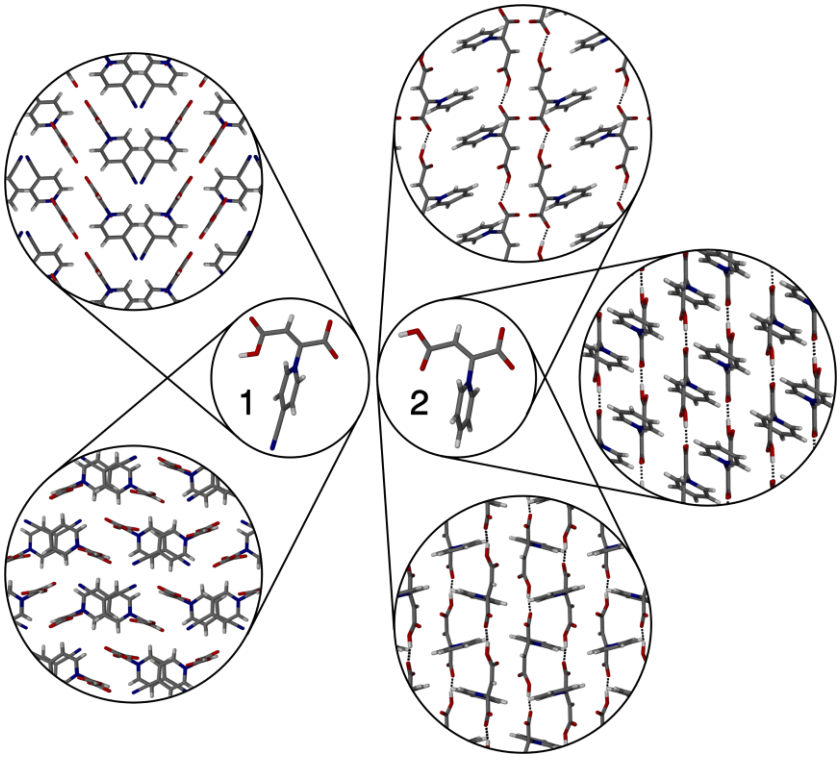

Figure 6.1 Summary showing the packing diagrams of the different solid-state forms that each zwitterion can adopt.

For both of these zwitterions one would expect it to be possible to interconvert between the different polymorphs. However, these polymorphs could not be interconverted, either by changing the temperature, immersing/stirring them in different solvents/out in air or by grinding them (with or without added solvents). This is unusual, but is probably due to the zwitterion ladders being very closely interlocked. Major shifts in the crystal structure and hydrogen bonding would need to occur if one form were to change to another. Unfortunately we were not able to test the effects that a change in pressure could have, so such experiments will still need to be carried out along with further tests regarding humidity and a change in room temperature. Furthermore, there are calculations that could still be carried out in order to evaluate and compare the different forms. For example, when looking at zwitterion **2**, we see that the major difference between the polymorphs is the angle of the ring with respect to the carboxylic acid backbone. A potential energy scan could be carried out by varying this angle and measuring the lattice energy of the system in 5° increments in order to see if there is a rotational barrier that is preventing interconversion between the different forms. By optimising the crystal structure at each point, we could also determine if changing the angle would force the forms to interconvert.

Chapter 4 describes the formation of two new zwitterions, neither of which is polymorphic. The zwitterion derived from nicotinamide (**1**) is robust and can be made under a variety of conditions without the risk of a salt by-product forming. On the other hand, zwitterion **2**, derived from isonicotinamide, is more variable and is often plagued by a salt by-product (although this can easily be removed by filtration).

Both of these zwitterions (as well as zwitterion **1** from Chapter 3) form salts with melamine (Figure 6.2). These salts were characterised and compared with respect to their intermolecular interactions. All three salts have a charge-assisted hydrogen bond between the carboxylate group of the zwitterion and a positively charged nitrogen atom on the melamine. The two zwitterions containing amide functionalities also have hydrogen bonding between the amide group and melamine. Through mechanochemistry screening tests it was possible to identify six other potential salts, formed by the combination of each of these zwitterions with either 2-aminopyridine or 2,6-diaminopyridine. Crystal structures have not been obtained for these, but they have been identified based on NMR and PXRD data, and IR data established that they are salts. What is important to note about all of these salts is that they are more soluble than the zwitterions themselves.

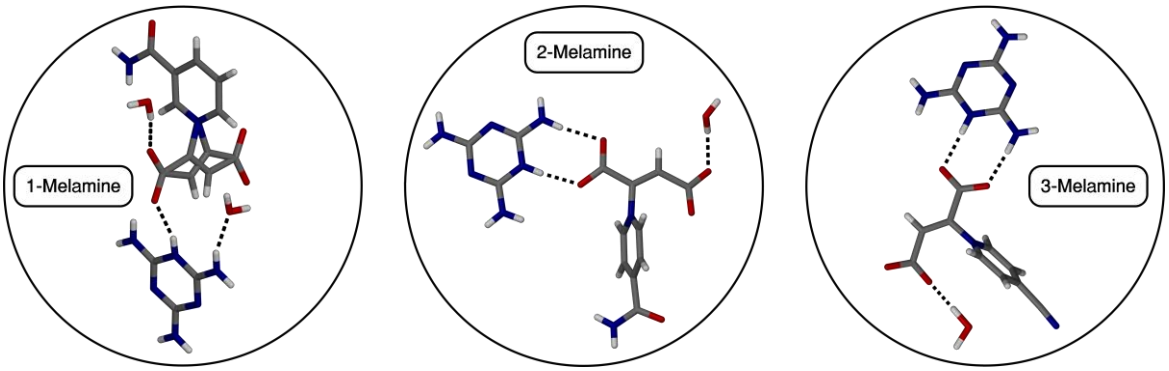

Figure 6.2 Summary showing some of the hydrogen- and charge-assisted hydrogen bonds in the three melamine salts.

The important question is, why did we not form more of these multi-component crystals? By carrying out a search of the CSD we determined that the carboxylate-carboxylic acid synthon holding the zwitterions together is more likely to be formed than any interaction the zwitterions could have with co-formers through these groups. However, the melamine salts show one of these weaker interactions, which means that this test should not be used to rule out the possibility of salt or co-crystals, it simply shows that it will be difficult to find them, and indeed it was – extensive screening tests had to be carried out to find these.

Originally one of our aims for the nicotinamide and isonicotinamide zwitterions was to form multi-component crystals *via* interaction with the amide functional group, as we already suspected that the zwitterion chains would probably not break (we see these chains in every zwitterion structure). It is still unclear why this did not happen and why more co-formers did not interact with this amide group – could the solubility issue overrule all else? If this is the case, why then could salts not be formed between different zwitterions with similar solubilities and functional groups? Or could the charged nature of the zwitterions deter neutral molecules from interacting with them?

It is clear that multi-component crystals formed by these zwitterions are not common, but they do exist. Extensive screening tests seem to be the only answer, luckily this is not very difficult to do mechanochemically. The zwitterions could still be combined with other simple molecules, drug molecules, or even other zwitterions, such as amino acids. Further attempts could also be made to obtain crystals of the six suspected salts with 2-aminopyridine and 2,6-diaminopyridine. Although many techniques have already been attempted, new methods are always being developed and could possibly be used to obtain single crystals. As we know what the constituents of these materials are, and their ratios with respect to each other, solving their crystal structures from powder data should be possible for someone skilled in this technique. The instrumentation available to us was not sufficiently sensitive for this application, but some other institutions are better set up for this type of structure solution, so it could be investigated in the future.

One other experiment that can be carried out would be to use the improved solubility of the salts to our advantage. Practically the co-crystallisations were hindered by the insolubility of our zwitterions, but the salts are much more soluble. If we dissolve one of the salts, what we have in solution is dissolved zwitterion. Of course, the co-former is also still in solution, but if we add another co-former it could be possible for a new salt to form. It could even be possible to obtain mixed salts with more than one co-former.

In fact, this is exactly what salts, co-crystals, and polymorphs are all about – improving the properties of compounds to make them more useful.

Overall, the molecules investigated all show very interesting behaviour with regard to polymorphism, multi-component crystal formation, and selective guest inclusion. Solvent selectivity has also been demonstrated with mechanochemistry, something which has not

been seen before. Studies like these are crucial for understanding how organic molecules interact, and assemble to form crystals, as well as the balance of conditions and properties that need to be taken into account during crystallisation, such as temperature and solubility. This critical knowledge will ultimately lead to the deliberate design of new functional materials.

6.6 References

1 L. Loots, J. P. O'Connor, T. le Roex and D. A. Haynes, *Cryst. Growth Des.*, 2015, **15**, 5849–5857.

APPENDICES

- Appendix A can be found at the back of this thesis and contains supplementary studies carried out during the course of this project.
- Appendix B is provided on the appended CD, and contains the following supplementary data:
    - .res files (structure visualisation)
    - .CIF files (crystallographic data files containing info regarding atomic coordinates and therefore bond lengths and -angles)
    - CheckCIF files (contains information regarding the quality of data)
    - NMR data for the solvates in chapter 5
- Appendix C is provided on the appended CD. This contains the poster presenting parts of this work, as well as the manuscript submitted to *Crystal Growth and Design*.

APPENDIX A

OTHER EXPERIMENTS AND ZWITTERIONS

A.1 Isoquinoline zwitterion

Another zwitterion, (Z)-2-(3-carboxy-1,1-dihydroxyprop-2-en-1-ide-2-yl)isoquinolin-2-ium, was also investigated. It was previously reported in the group (refcode: BIXMAY),[1] but had not been studied extensively. The same methodology was followed as is described in Chapter 2 – our aim was to obtain polymorphs, solvates, co-crystals, or salts.

The zwitterion was synthesised and crystallised in the following manner: 2 ml methanol and 1 ml water was added to isoquinoline (0.023 g, 0.178 mmol) and stirring was started. ADC (0.020 g, 0.175 mmol) was added and stirring was continued for 10 min at 60 °C. The vial was capped and left on a shelf for crystallisation to occur *via* slow evaporation of the solvent. Clear, colourless plate-like crystals formed after 7 days. No additional solid-state forms were obtained.

Further experiments were carried out where each of the reagents were, in turn, used in excess. The synthesis was also carried out at room temperature and 100 °C, but these changes had no effect. However, when the crystallisation vial was left in the refrigerator, a previously unreported salt, similar to those obtained for some of the other zwitterions, was formed (Figure A1). This salt can also be formed mechanochemically *via* neat grinding.

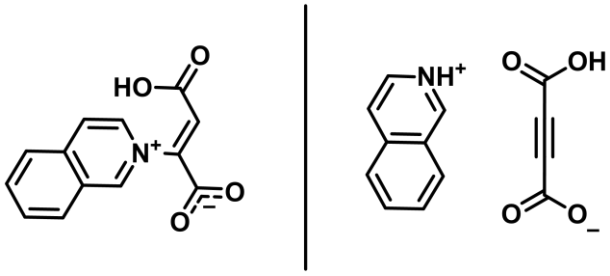

Figure A1 The isoquinoline zwitterion (left) and the corresponding salt (right).

The salt crystallises in the monoclinic space group, *Cc*, and has one protonated isoquinoline cation and one ADC anion per ASU (Figure A2). A charge-assisted hydrogen bond is formed between the two charged atoms.

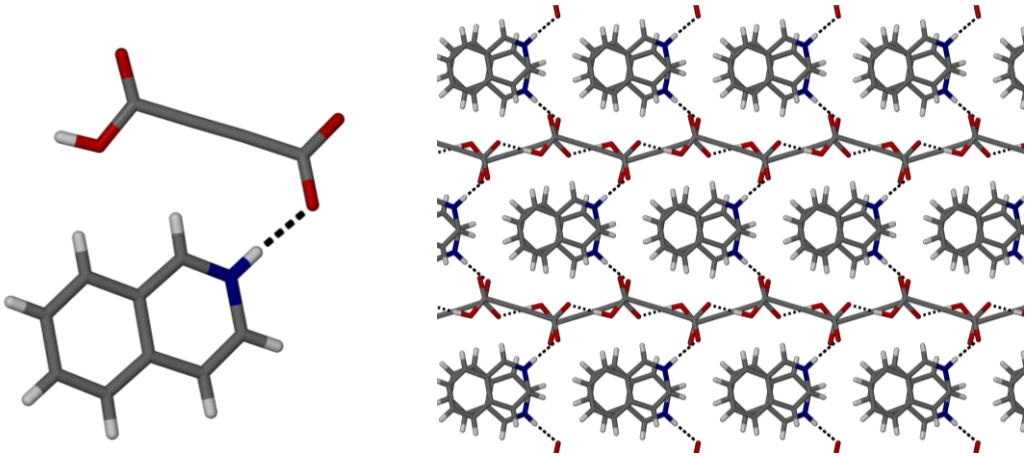

Figure A2 Asymmetric unit of the ADC-isoquinoline salt, viewed down the *c*-axis, as well as the packing diagram, viewed down the *c*-axis.

A.2 Unsuccessful zwitterion syntheses

The synthesis of two other, previously unpublished zwitterions was also attempted (Figure A3). The same methodology was followed as is described in Chapter 2, however in each case only the salts of the two starting materials formed.

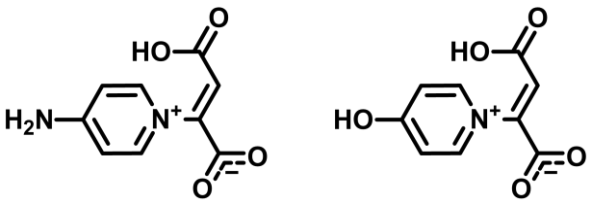

Figure A3 Zwitterions of which the synthesis was attempted, but not successful.

A.3 Metal complexes

Throughout the project all zwitterions were also combined with various metal salts (Table A1) by dissolving them together, in water, as well as in water/pyridine mixtures. The reason behind this choice of solvents is that the zwitterions are highly insoluble and this was the only way in which we could achieve dissolution. Unfortunately, this only led to precipitation or recrystallisation of the zwitterion, with the metal salt remaining in solution.

Subsequently, *in situ* crystallisation of metal complexes was attempted by combining each of the metal salts in Table 1 with ADC and the pyridine derivative in a 2:1:1 mole ratio. This was carried out by stirring the three components in water at 100 °C, for 10 minutes. These crystallisations only lead to formation of the zwitterion, or some combination of the metal and one of the zwitterion components (Figure A4). No zwitterion-metal complexes were formed.

Table A1 List of metal salts used in an attempt to form metal complexes.

Halogen salts	**Nitrate salts**	**Acetate salts**
$CrCl_3 \cdot 4H_2O$	$Mn(NO_3)_2 \cdot 4H_2O$	$Co(CH_3CO_2)_2 \cdot 4H_2O$
$FeCl_3$	$Ni(NO_3)_2 \cdot 6H_2O$	$Ni(CH_3CO_2)_2 \cdot 4H_2O$
$CoCl_2$	$Cd(NO_3)_2 \cdot 4H_2O$	$Cu(CH_3CO_2)_2 \cdot 4H_2O$
$FeCl_2 \cdot 4H_2O$	$Co(NO_3)_2 \cdot 6H_2O$	$Cd(CH_3CO_2)_2 \cdot 4H_2O$
$NiBr_2 \cdot H_2O$	$Zn(NO_3)_2 \cdot 6H_2O$	$Mn(CH_3CO_2)_2 \cdot 4H_2O$
$CdBr_2 \cdot 4H_2O$	$Cu(NO_3)_2$	$Zn(CH_3CO_2)_2 \cdot 2H_2O$
$CuCl$		
$CuCl_2 \cdot 2H_2O$	·	
$ZnCl_2$		

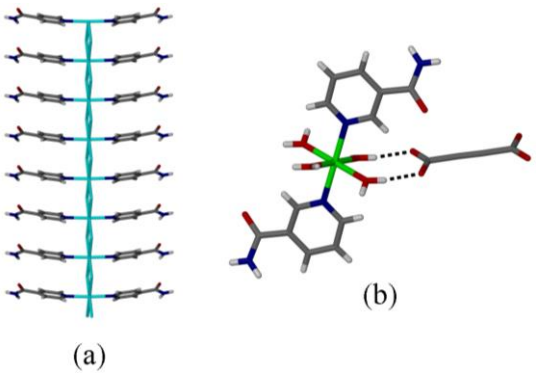

Figure A4 (a) A metal complex formed containing cadmium and isonicotinamide. (b) A metal complex formed containing nickel, ADC, nicotinamide and water.

References

1 L. Loots, D. A. Haynes and T. le Roex, *New J. Chem.*, 2014, **38**, 2778–2786.